Structural Framework and Target Generation in the Proterozoic Mt Isa region, Queensland, through analysis of Potential Field Multiscale Wavelets ("Worms").

November 2002

F. C. Murphy
pmd*CRC*
School of Earth Sciences
James Cook University

Table of Contents

List of Figures

List of Appendices

List of Maps

	Scale
Map 1: MIM_ Aeromagnetic Worms_MAX _Z (>600m)	1:500,000
Map 2: MIM_ Aeromagnetic Worms_EFVD _ Z (>600m)	1:500,000
Map 3: MIM_ Gravity Worms_MAX _ Z	1:500,000
Map 4: MIM_ Gravity Worms_EFVD _ Z	1:500,000
Map 5: pmd*CRC Gravity Worms MAX_ Z	1:1,000,000
Map 6: pmd*CRC Gravity Worms EFVD_ Z	1:1,000,000
Map 7: Magnetic Worm Lines, Depth Migrated	1:500,000
Map 8: Gravity Worm Lines, Depth Migrated	1:500,000
Map 9: Magnetic Edge Penetration Image	1:500,000
Map 10: Magnetic and Gravity Edge Intersection Image	1:500,000

Executive Summary

This project seeks to derive a structural framework in the Mt Isa region, by apply an interpretation methodology to the analysis of multiscale wavelet edges (worms) of potential field data in order to establish what correlations, if any, might exist between the worms and known mineralization that may be used in a predictive way to target ore systems of interest. The basis for this analysis comes from the perceived spatial relationship of the Barramundi Worm to Giant Ore deposits in the region, and from relationships derived between worms and deep tapping crustal scale structures (in other districts).

Worming is an edge detection technique that provides critical 3D information on the shape and relative depth extent of the edges (eg. faults, shears, intrusive contacts). The analysis of worms is based on numeric distributions of two inter-related variables, Z being the level of upward continuation, and W being the "amplitude" of the worm feature. A focus of the interpretation developed here is to enable the projection of these 3D data sets into a 2D exploration environment, and a methodology has been developed which attempts to minimise subjective interpretation.

There is a good correlation between worm edges (Z) and mapped geology which gives confidence to their interpretation undercover. A proximity test of the major 14 deposits in the district is used as a training set in the analysis of the worms. This indicates that, within 2km of each deposit, there exist deeply penetrative (>10,000m upward continued) edges and associated intersections along these edges. This relationship is interpreted as indicating that such regions are more permissive to ore localization. Quantitative analysis of the aeromagnetic worm interpretation was undertaken that generated a number of potential targets, results currently confidential to MIM (to Jan 2004).

The spatial distribution of W values provides an added dimension to the worms. While the aeromagnetic interpretation of this variable is currently confidential to MIM, the W values from gravity data are evaluated with respect to known mineralization. This highlights the Century area on the Lawn Hill platform as being regionally anomalous.

The integration of W and Z spatial patterns provides a useful first order area selection filter. Much of this integrated analysis needs to be undertaken using a second order filter of host rock potential and depth of burial, in order to effectively rank the regions of interest.

1. Introduction

This report concerns the interpretation of multiscale wavelet edges ("worms") derived from potential field data in the Mt Isa region (Fig. 1), with particular reference to the Eastern Succession. The objective is to derive a structural framework from the worms that allows an evaluation of the degree to which penetrative structures and intrusions exert control on existing ore body locations and, if so correlated, to form a basis for target area selection on a regional scale. It seeks to do this through integration and mapping of worm data sets, with respect to mapped or inferred geological features, and determining their spatial relationship to mineralisation.

This research contributes to the pmd*CRC I2/I3 project on "Total Systems Analysis of the Mt Isa Eastern Succession" (representing Module 1: Structural Framework), and to the I1 project on "Mt Isa Western Succession 3D architecture and ore systems". It seeks to build on the existing high level understanding of the region, as documented in the North West Queensland Mineral Province Report (NWQMPR 2000). This latter report represents a cornerstone in prospectivity analysis, and derives from the integration of a range of geological and geophysical data, mostly undertaken at 1:250,000 scale. The current work by the pmd*CRC incorporates new processing ("FracWorming") of similar geophysical data sets as those in NWQMPR (2000), and represents a more detailed scale of regional data integration, against the backdrop of Geoscience Australia's 1:100,000 digital solid geology map coverage (Fig. 1).

The concept that penetrative crustal scale structures provide a control on ore body location is not new (eg. O'Driscoll 1990), and is implicit in assessments of the deposit types contained in this region (eg. NWQMPR 2000, Large *et al*. 2002, Haynes 2002). It is critically demonstrated in the North Australian Proterozoic region by the spatial association of the deep "Barramundi Worm" (derived from gravity data) and "Giant Ore Deposits" proximal to it (Hobbs *et al.* 2000; Fig. 2). Initial assessments of such relationships using the Australian gravity field (Archibald *et al.* 2001) suggest a closer correlation of coarse scale worms with Pb Zn deposits than with Cu Au systems. This lends weight to the hypothesis that penetrative faults, and particularly fault intersections along them, may provide a first order control on the localization of ore systems. Such regions are, 'a priori', more permissive for ore localisation, through the ability to tap deep source regions for metal and/or magmatic fluids and thermal gradients, and to create volumes of high fracture density that can facilitate hydrothermal fluid flow. A second order filter, once such regions have been identified, is the existence or preservation of suitable host rocks. The objective of this analysis is to identify the more permissive regions (the first order filter).

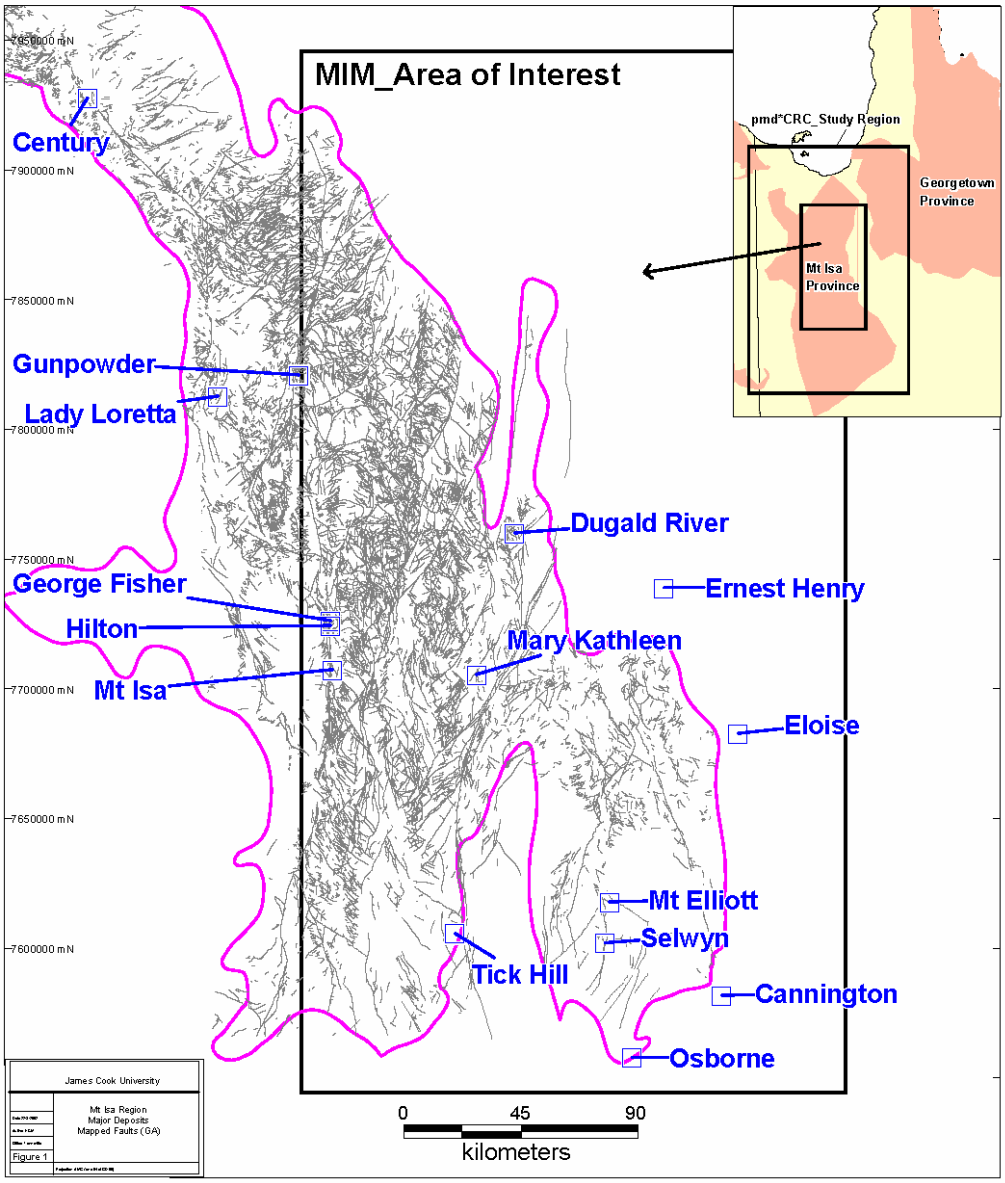

Figure 1: Regional location map of Proterozoic study area.

The power of the multiscale wavelet method of upward continuation lies in reducing the ambiguity in interpretation of potential field data by providing critical shape and depth information on edges in the data (Archibald *et al.* 1999, 2001). It is particularly useful for mapping faults and intrusive contacts (Fig. 3). The role that faults and intrusives have in the localization of IOCG and SHMS deposits in the district can then be addressed. Attributes of the worms are examined in the context of: a) the level of upward continuation (Z), being an indirect measure of relative penetration depth, b) the interpreted intersections of worm sheets, and c) other spatial features of the wavelets (e.g. W value). These attributes are evaluated using mapped geology where possible, to derive confidence in the interpretation, and become critical in the undercover environment.

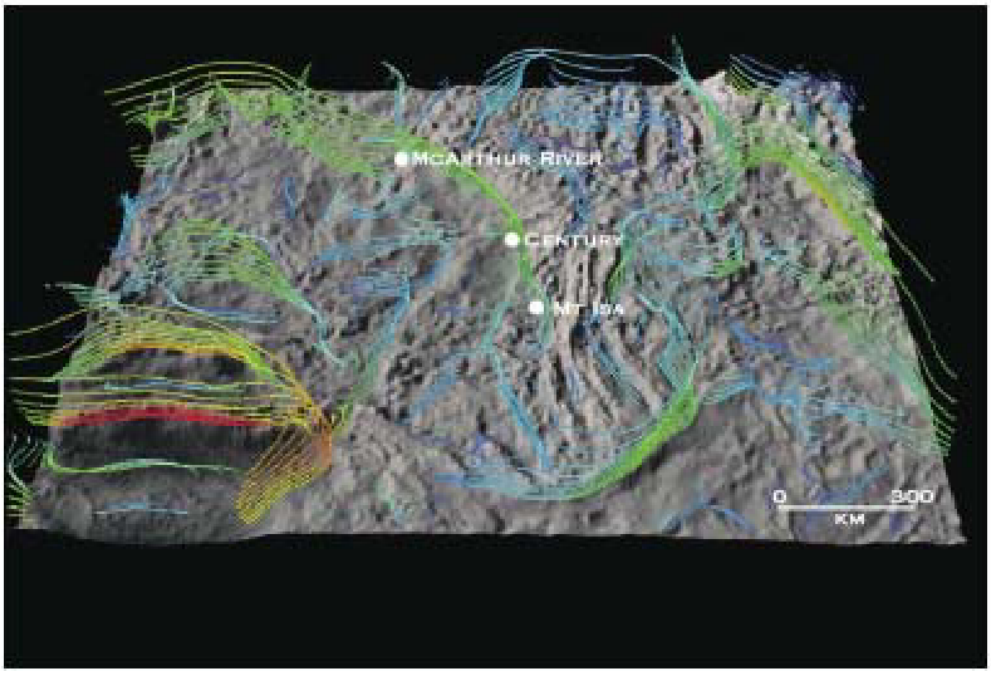

Figure 2: Oblique view of North Australian Gravity with upward continued worms to 220km. Major deposits spatially related to Barramundi Worm (Hobbs et al. 2000)

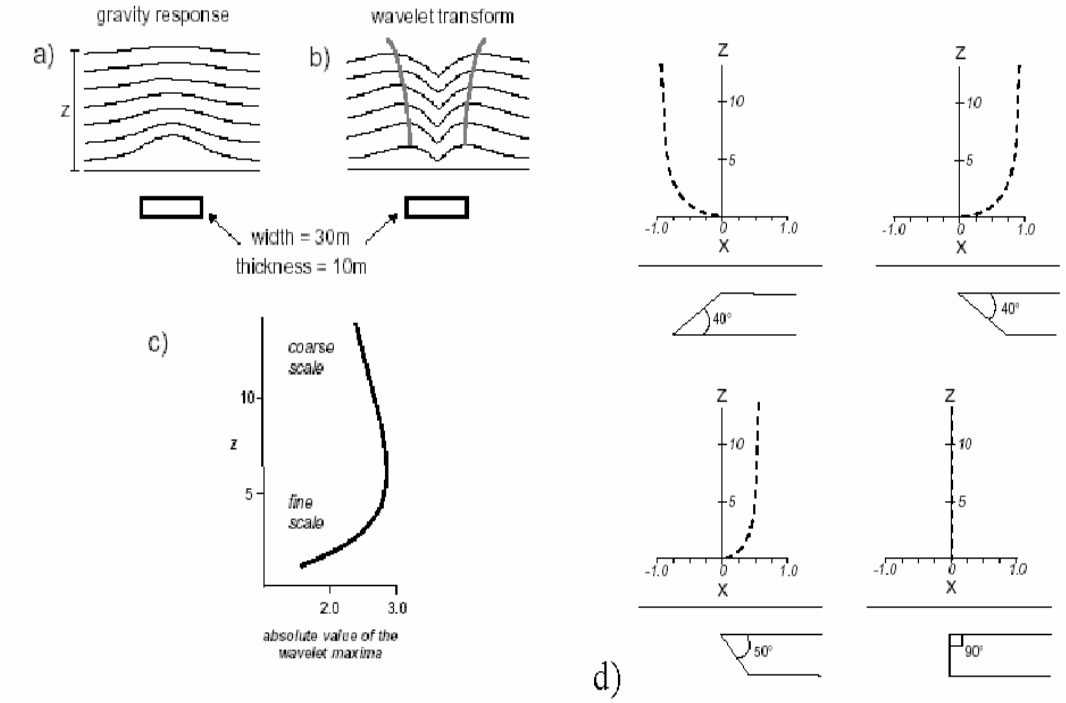

Figure 3: Synthetic models and their wavelet transformations for a) gravity source with increasing levels of upward continuation; b) Wavelet Transform of response; c) variation in Wavelet Maxima with increasing Z; d) models of Z migration in relation to direction of variably inclined edges (Archibald et al. 1999).

A methodology for migrating 3D worm data (Z values) into a 2D image of their near surface expression was developed by the author as a targeting tool in the Irish mineral

province. A key aspect to the analysis is the up-dip projection of worm sheets into an "exploration" environment, where their geological context can be evaluated. The Irish case study indicated that intersections of crustal scale structures have a strong control on ore body location. This resulted in delineation of 11 target regions (of which 4 contain existing ore systems), and became the basis for Pasminco's area selection in the region – potentially, a cost effective, focused program. Based on this type of analysis, MIM is seeking to apply similar techniques in the Isa region, one that is far more complex than the Irish setting and more than twice the size. Key aspects of this interpretation remain confidential to MIM.

Naturally, further work is needed to refine and test the interpretations contained here. In particular, the context of the edge features that are mapped have not been integrated or evaluated comprehensively with respect to their geological or seismic expression. A further limitation, through the reduction of the 3D data sets into a 2D framework, is that this has been done without recourse to a 3D viewing platform. As such, it is considered a first pass assessment, and is an avenue for future research into the 3D architecture of the region and its ore systems.

2. Data Inputs and Processing

Multiscale wavelet data was supplied by Fractal Geoscience who processed ("FracWormed") the three sets of regional potential field data used in this analysis (Fig. 1). The first, more detailed coverage is the MIM aeromagnetic data (Fig. 4). The second is ground gravity provided to the pmd*CRC by industry partners (BHP- Billiton, Placer) and government (QDNRM, GA) organisations. This data was selected for analysis as it has a more regional coverage and contains significant additional data to a third data set – being MIM's gravity worm data (Fig. 5). Together, these data sets cover a region of interest across the entire Mt Isa region, eastwards towards the Georgetown block, and northwards to the Gulf of Carpentaria (Fig. 1).

Fractal Geoscience outlined the processing and provided a preliminary interpretation of the data to MIM (House 2002). The multiscale wavelets from each data set were supplied to the pmd*CRC as ascii point files, comprising Easting, Northing, Z and W values. The Z value is a measure of the level of upward continuation (in meters) of detected edges or gradients. The worming technique (Fig. 3) involves the use of upward continuations to separate the potential field data into high frequency / short wavelength responses (near surface) and low frequency / long wavelength responses (possibly deeper sources). The W value is derived from the amplitude (or contrast) in the gradient at a particular Z value. Fractal's processing generated up to 32 levels of Z ranges for individual data sets. The MIM aeromagnetic data was gridded to 200m and upward continued to approximately 30km, the MIM gravity data gridded at 500m was upward continued to approximately 30km, while the pmd*CRC gravity data was gridded at 500m and upward continued to 60km. Two types of worms are produced for each upward continuation level. The "MAX" worms are the standard maximum horizontal gradient points derived from the either the magnetic or gravity fields. The "EFVD" worms are maximum horizontal gradient points derived from the enhanced first vertical derivative of either the gravity or magnetic fields. The EFVD worms provide additional spatial resolution at low levels of upward continuation and combined with the MAX worms can help determine approximate depth to source (House 2002).

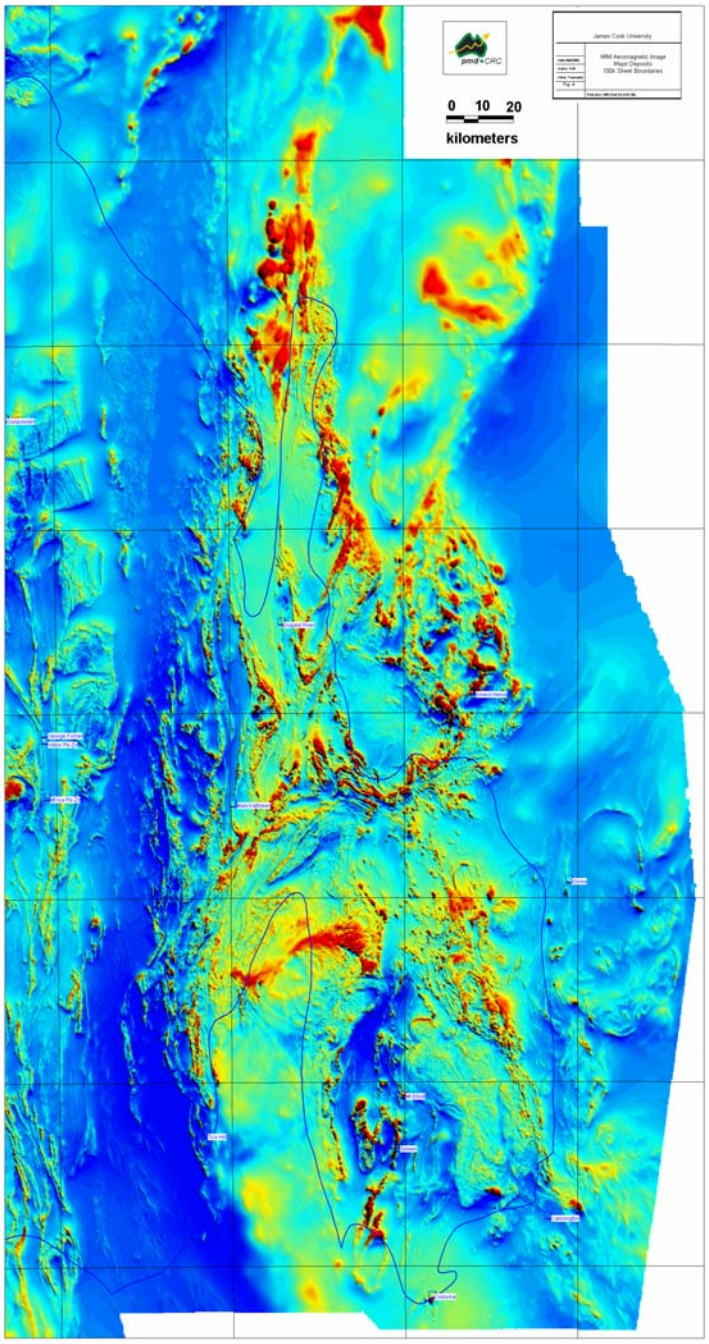

Figure 4: MIM Aeromagnetic Data, TMI Image, with Major Deposit locations.

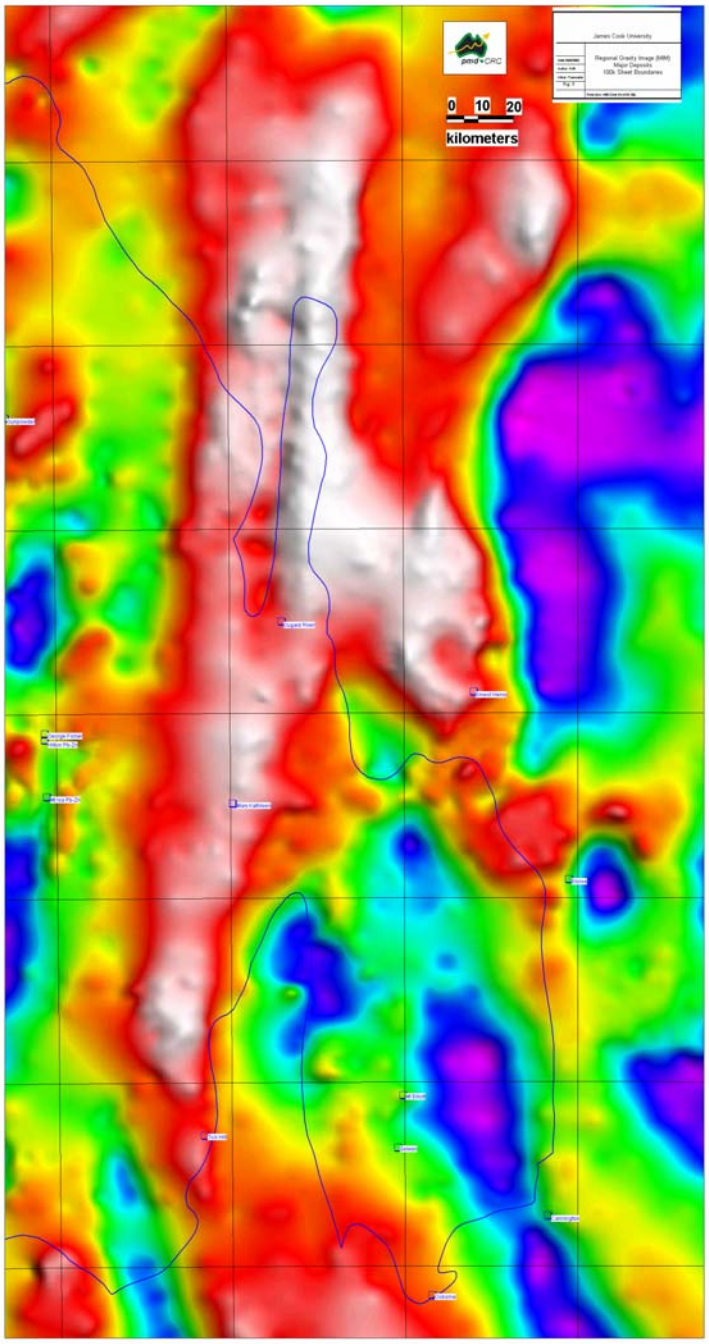

Figure 5: Gravity Data, TMI Image, with Major Deposit locations.

3. Interpretation

Initial inspection of the EFVD and MAX data was performed in Datadesk from which a series of "cutoffs" in the numeric distributions for Z and W were determined. The combination of three data sets, each with two levels of processing and associated two derived values, results in 12 outputs to be considered (Appendix 1).

A key objective of the interpretation is to derive a 2D near surface representation of the 3D worm sheets (Z values). As a rule of thumb, the apparent depth of penetration of an edge equates to approximately half the equivalent level of upward migration. The interpretation has involved a methodology to map the near surface expression of worm sheets and to attribute such features with their apparent depth dimensions. Three routes to this end product have been explored in the context of reliability, repeatability and time/cost effectiveness: a manual or visual method (as in the original Irish case study), a semi-automated method (outlined in Appendix 2), and an automated routine (under development). For the magnetic data, the derived edge architecture is representative of features that are projected onto a 200-500m level of upward continuation, whereas the gravity interpretation is projected to 1000-2000m. Faults derived from the 1:100,000 GA digital geology were used as a backdrop to the interpretation. An updated fault file was initially created which attempts to create more linkages of faults than are shown in the original GA data (Fig. 1). There are two streams to the interpretation, involving Z and W respectively.

3.1 Z Distributions

- A series of "dot" maps are plotted at 1:500,000 and 1:1,000,000 scale to illustrate the worms, their relationship to the mapped fault architecture, and locations of the major deposits. (Maps 1-6). Examples of these are shown here for the Mag_MAX and Grav_MAX data (Fig. 6 & 7)
- The structural architecture derived through the up-dip projection of the Z data is shown as a series of line interpretations for the aeromagnetics (Map 7; Fig. 8) and gravity (Map 8; Fig. 9). Individual lines are colour coded by the apparent level of upward continuation. The rectilinear fracture network derived in the interpretation is similar to other natural fracture systems seen at a range of scales. It is characterized by reasonably consistent, regionally extensive trends.
- In their geological context, where mapped faults and intrusive edges are known to exist, the spatial distribution of edges, particularly those that migrate to significant upward continuations, show a good correlation. The edge detection method appears to be remarkably sensitive to relatively minor mapped structures within the Proterozoic outcrop, and gives confidence that the worms are reflecting real features in the under cover environment.
- Many of the "deep" (high Z) worms shown in the magnetics (Fig. 6; Maps 1 & 2) outline large strike length features that include:
    - An upward continued edge to 30km is associated with the Cloncurry Fault. This feature has a strike length of >200km, though with significant dip direction changes along it. A field trip in the Cloncurry district attempted to validate this "giant worm" structure on the ground. The up-dip projection of the worm sheet was found to correlate with outcropping mylonites that were previously un-recognized as such –

the implication being that the Cloncurry Fault, as mapped in the area of the Fullarton Gorge, is misplaced by several kilometers.

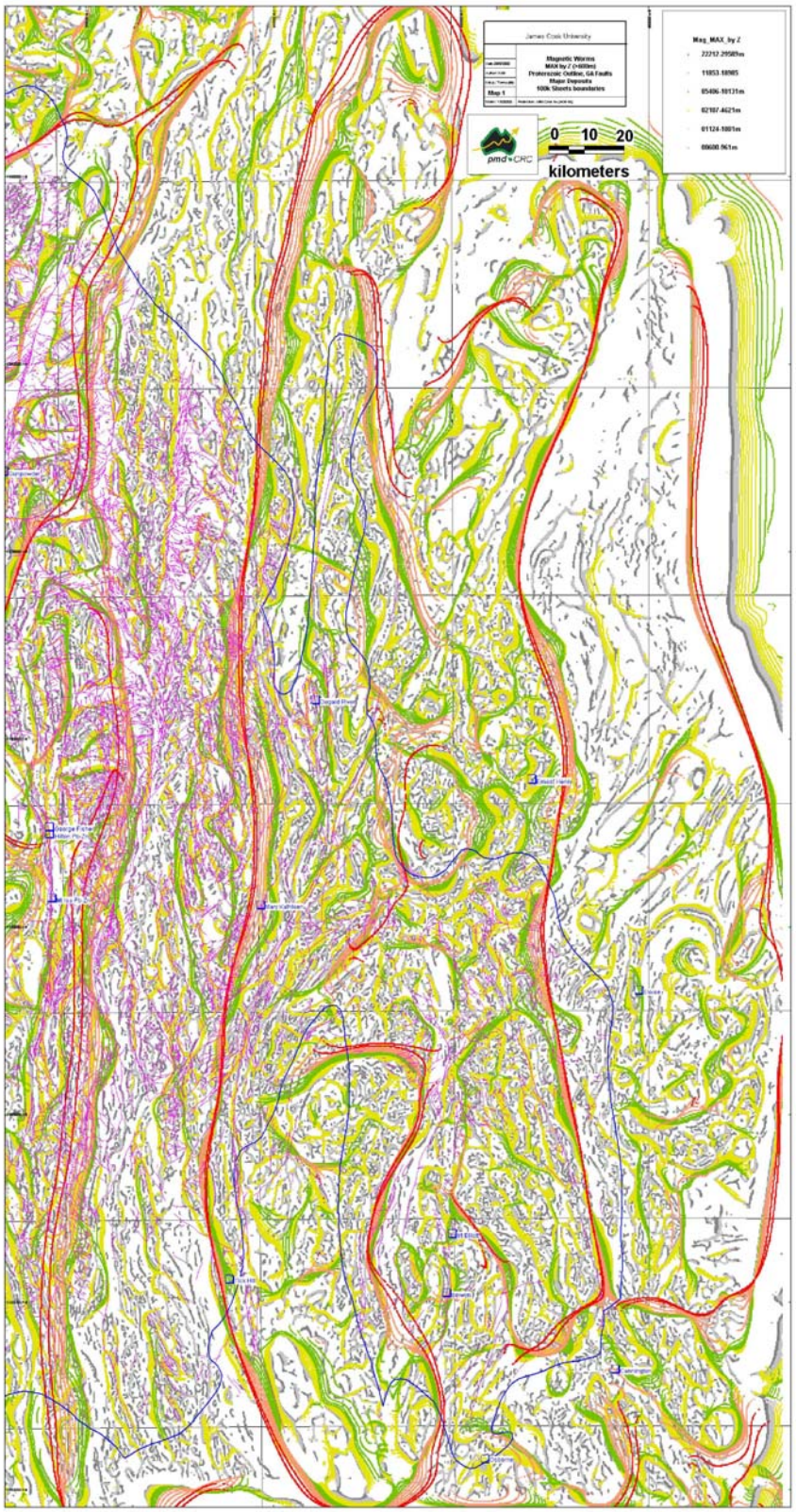

Figure 6: Aeromagnetic Worm Dot Map, MAX by Z.

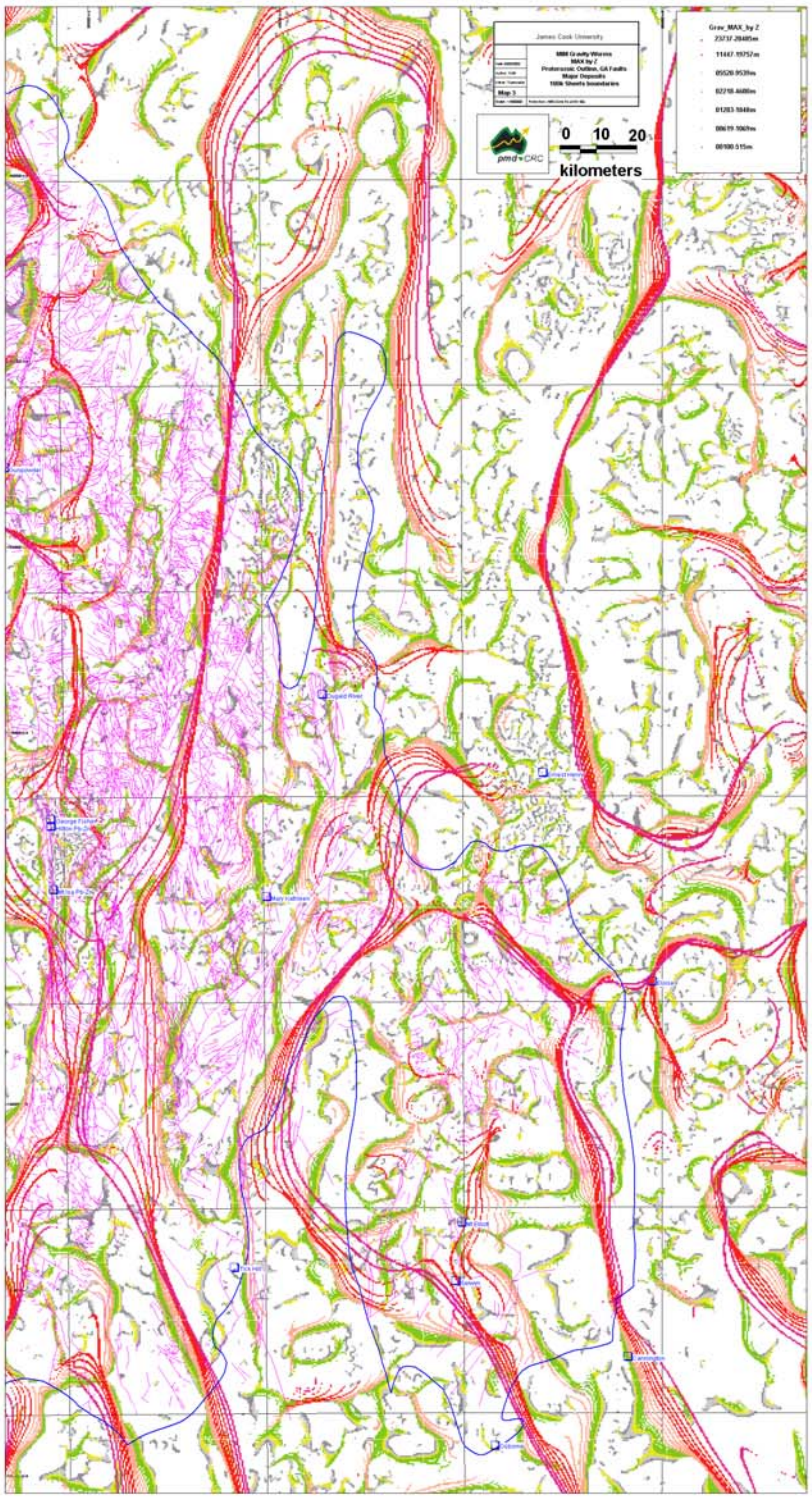

Figure 7: Gravity Worm Dot Map, MAX by Z.

- A major magnetic feature through the central part of the region, similar in dimensions to the "Cloncurry worm", with Tick Hill and Mary Kathleen spatially related to it. This largely mirrors the boundary of the Quamby-Malbon subprovince and the Wonga subprovince in the southern part of the Isa block but departs significantly from this boundary further north.
- The boundary western boundary of the Kalkadoon-Ewan Province and the Leichardt River subprovince is defined by a major deep seated worm for most of its strike length (Fig. A1, A3)
- Curvilinear edges and closures in places are related to granitoids, such as the Sybella and parts of the Williams Suite (Fig. A1, A3)

- The "deep" (high Z) worms shown in the gravity (Fig. 7; Maps 3 to 6) also outline large strike length features, and numerous geological – mainly structural - correlations are apparent.

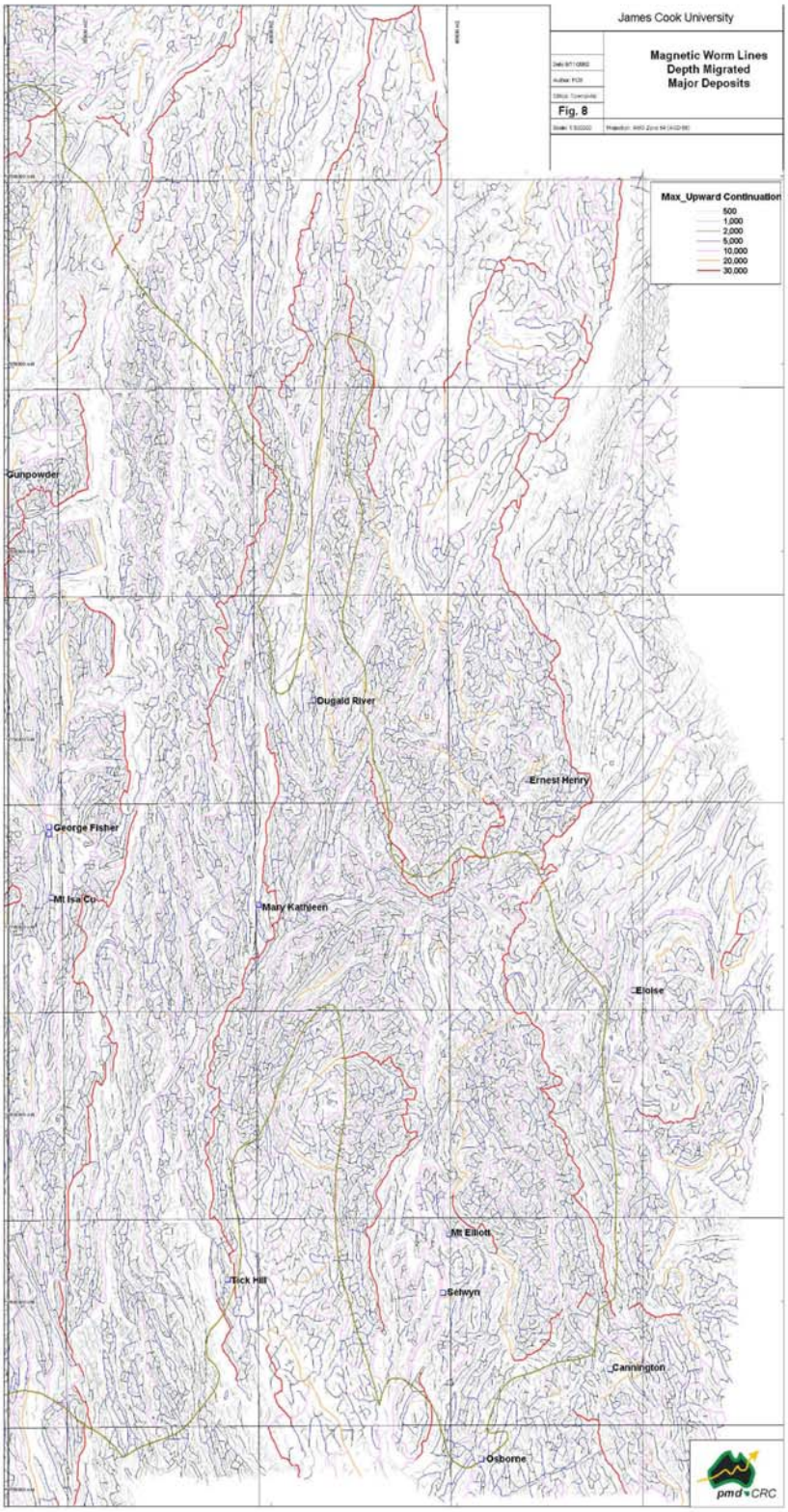

Figure 8: Depth migrated aeromagnetic edges

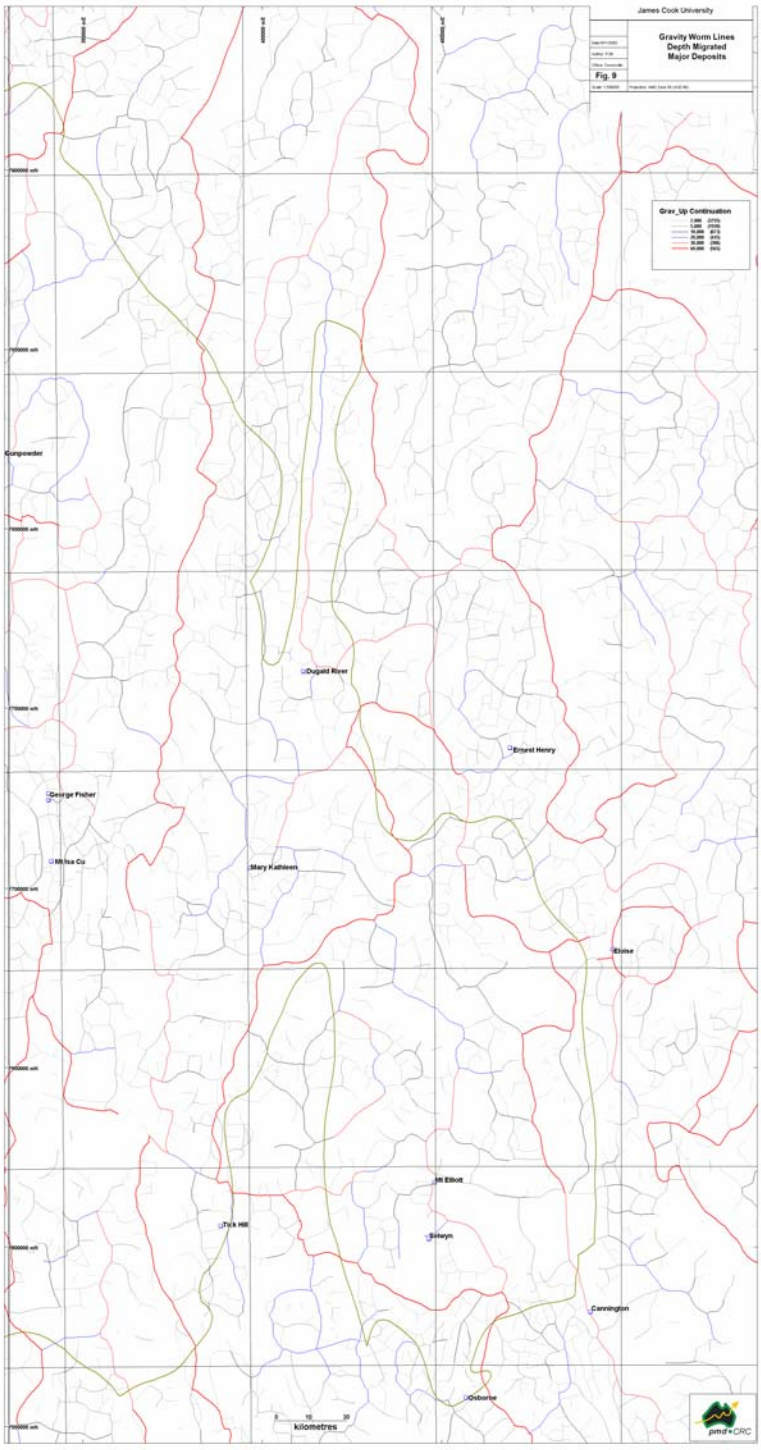

Figure 9: Depth migrated gravity edges

3.1.2 Deposit Analysis

The interpretation of the structural framework from magnetics and gravity was undertaken, in the first instance, without reference to ore body location. The two related questions to be addressed here are – what is the spatial relationship of worms to existing mineralization, and are there any criteria that derive from this that may provide a vector to areas where new mineralization might be found?

If the concept of proximity to deeply penetrative structures and intersections along them has a bearing on ore body location, then this may be evaluated in a semi-quantitative way against the structural framework, as it exists today (derived from interpretation of Z ranges). Given that apparent penetration depths are an approximation of the level of upward continuation, one may seek to integrate the both potential field interpretations and examine their coherence or otherwise. This approach proved to be reasonably successful in the Irish setting.

A "training set" for the analysis is the population of 14 ore bodies contained in the district. It should be noted that the spatial analysis presented here takes no account of age or orientation of worm edge, nor its nature (eg. fault or intrusive contact), and is essentially a raw "Nearest and Deepest" analysis. Thus, within a radius of 20km from each deposit, values (in km) for Distance A (to nearest worm line) and Distance B (nearest worm intersection) were calculated, and attributed according to Apparent Depth (in m) of the worm feature. This provides an indication of the relationship of deposits to possible controlling edges, and provides a buffer or filter for subsequent regional scale area selection. Results for each deposit are contained in Appendix 3, as a series of distance/depth line plots. The combined data (Fig. 10) shows that the deposits are never very far from shallow worms or their intersections. More importantly, the deeper values are skewed towards the ore body locations rather than being randomly dispersed.

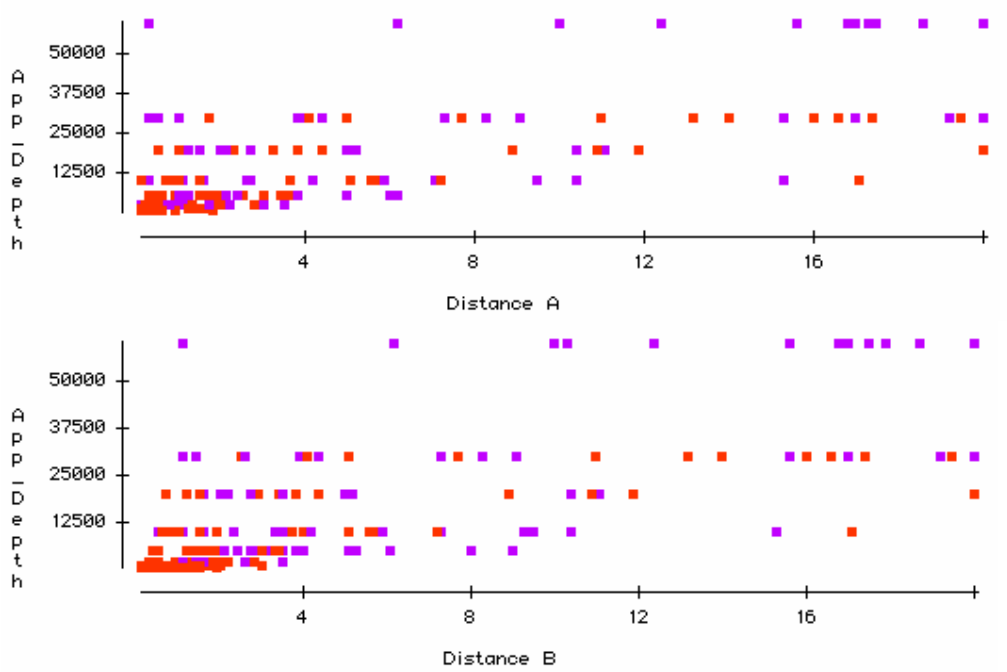

Figure 10: Deposit proximity vs Depth weighted worm features (A) and worm intersections (B) for 14 ore systems in the region. Red - Magnetics, Purple – Gravity.

These relationships suggest that, for a majority of these ore systems, their proximity to a deeper penetrating worm feature provides a useful filter for regional area selection. Within a 2km buffer, deposits that are captured in relation to proximal edge depths are:

Z Level (km)	Distance A	Distance B
60	Eloise	Eloise
30	Mt Elliot, Cannington, Gunpowder, Tick Hill	Mt Elliot, Gunpowder
20	Ernest Henry, Selwyn, Hilton, George Fisher	Ernest Henry, Hilton
10	Osborne, Lady Loretta	Selwyn, Lady Loretta
5	Mt Isa, Dugald, Mary K.	Tick Hill, George Fisher, Osborne, Dugald, Mt Isa, Mary K.

For individual ore systems (see Appendix 3), the following interpretations are drawn:

- **Dugald River**: Gravity and magnetic worm features with edges of around 30km occur at a distance of 3 to 4km from the deposit.
- **Gunpowder**: Virtually "on-structure", with gravity and magnetic worm features of around 30km present within 2km of the deposit.
- **Lady Loretta**: Gravity worm features with apparent depths of around 10km present 2km from the deposit. Magnetic interpretation not yet undertaken.
- **George Fisher**: Gravity and magnetic worm features of 10km within 1km of the deposit, with 20 to 30km features at 3 to 4km distance.
- **Hilton**: Gravity and magnetic worm features of around 10 to 20km within 2km, and a 30km gravity response about 4km from the deposit.
- **Mt Isa**: Not obviously "on-structure". Gravity and magnetic worm features of around 10km at a distance of 3 to 4km from the deposit. Nearest 30km point is about 8km away. Signature of Mt Isa is a region of deep worm dislocation, without itself being located to an obviously deep worm. This is somewhat surprising given the strong geological expression of the Mt Isa Fault – it may be that the Isa "worm" expression is "swamped" by edge effects in and around the Sybella Batholith.
- **Mary Kathleen**: Magnetic worm feature with apparent depth of around 30km present 4km from the deposit, with several shallower intercepts proximal to the deposit.
- **Ernest Henry**: Clustering of 20km magnetic and gravity responses within 2km of the deposit.
- **Eloise**: Essentially "on-structure", in relation to a 60km gravity worm, and a 10km magnetic response.
- **Mt Elliot**: Practically "on-structure", in relation to 30km gravity worm and 10km magnetic response.
- **Selwyn**: Clustering of 20km magnetic and gravity responses within 2km of the deposit.
- **Cannington**: Virtually "on-structure", in relation to 30km gravity worm.
- **Osborne**: Clustering of 10km magnetic responses within 2km of deposit, and 60km gravity response at 6km distance.
- **Tick Hill**: Cluster of 30km gravity and 20km magnetic responses within 2km of deposit.

3.2 W Distributions

The W values show a spectrum of distributions within each data set and outline a number of coherent spatial domains (Appendix 1). The geological context of these signatures is not evaluated here, but is an important aspect to be addressed in further studies of the data. However, there are discrete areas highlighted in the most elevated or anomalous W values that may have exploration significance. Such anomalous regions are assessed "at face value" against the locations of the worms that contain them, and in relation to the existing deposits and mineral occurrences, to determine what correlations might exist.

3.2.1 Aeromagnetics

This aspect of the interpretation remains confidential to MIM.

3.2.2 Gravity

- For the gravity data, anomalous W regions are plotted for MAX (Fig. 11) and EFVD (Fig.12) respectively. There is generally little correlation between their respective spatial distributions and they are treated separately here.
- The anomalous W_MAX regions are closely associated with deep worm lines (60km). The most significant of these is a curvilinear feature along the eastern margin of the Proterozoic outcrop, north of Cloncurry, with a core of intense values rimmed by progressively lower values. The nature and significance of this feature is unclear, but is interpreted as a major fault dislocation separating low density rocks to the east from higher density rock to the west. It seems likely that this feature has a strong bearing on the tectonic framework of the Mt Isa region. Its exploration significance is also unknown and is effectively masked by deep cover sediments. There are only 7 copper occurrences spatially associated with anomalous W_MAX regions in the Proterozoic outcrop area (Appendix 4), and suggests this variable may have little influence on ore location.
- The anomalous W_EVFD values in the gravity (Fig. 12) show correlations with 30, 20 and 10km upward migrated features. There are 39 mineral occurrences spatially associated with these regions, mostly copper, but with some lead and zinc (Appendix 4). The latter occurrences are almost entirely contained in a narrow region in the Lawn Hill platform, derived from the pmd*CRC gravity worms (Fig. 12). This region includes the Century deposit. This surprising result from the W_EVFD values needs to be evaluated further, especially in the context of the structural framework of the worms in this region (Z distribution). This work is planned under the auspices of the current pmd*CRC I1 project.

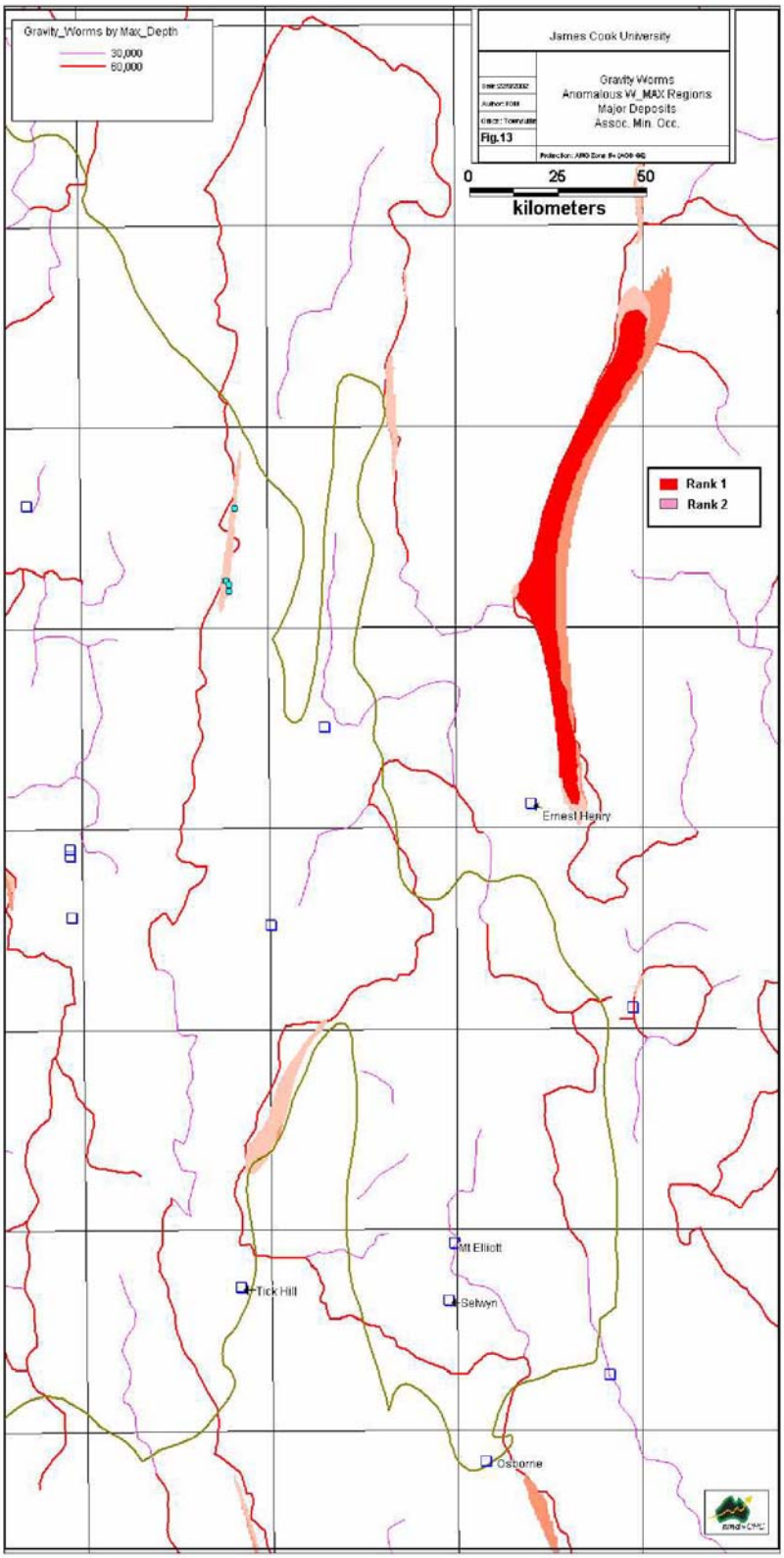

Figure 11: Anomalous W regions in Gravity_MAX data

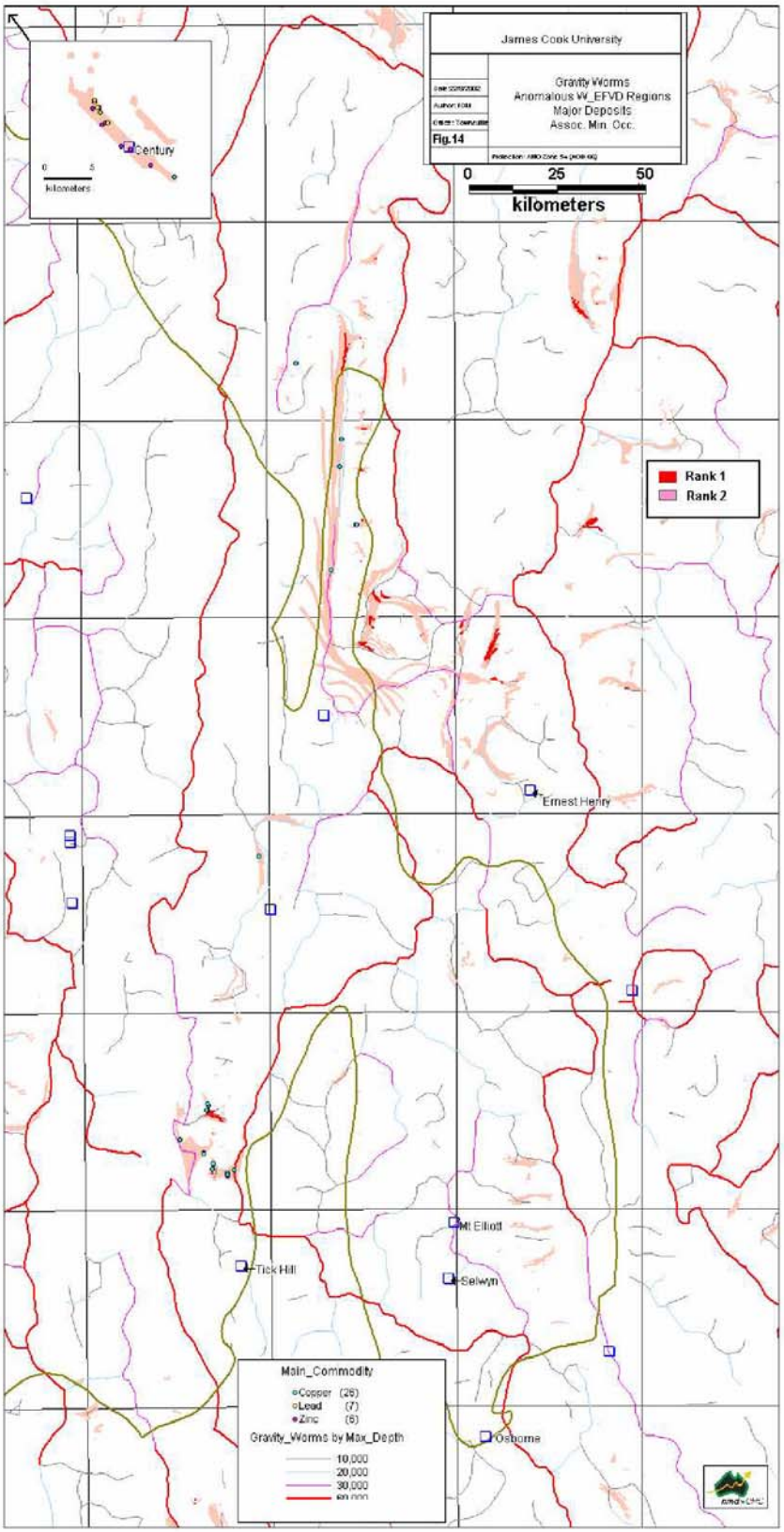

Figure 12: Anomalous W regions in Gravity_EFVD data

4. Target Area Analysis

The depth migrated magnetic and gravity worm line data (Figs. 7 & 8) have been image processed, and statistically manipulated, to derive regional structural relationships that may be applied to target generation. The two types of output from the Z line data are: 1) "Edge_Penetration" images - based on values of apparent penetration depths of interpreted worm *lines* and 2) "Edge_Intersection" images - based on depth weighted values of worm line *intersections*. The results are shown in Appendix 5, and are illustrated here for magnetic data (Fig. 13; Map 9), gravity (Fig. 14), and to a combined magnetic/gravity data set (Fig. 15; Map 10).

With criteria derived from the "nearest and deepest" analysis (Appendix 4), it is apparent that proximity to edges and intersections that migrate to 20km (*ca*. 10km deep) has a part to play in their location. Area intersection indices have been calculated and targets have been derived from this relationship using a series of buffers applied to the aeromagnetic interpretation. This aspect is confidential to MIM.

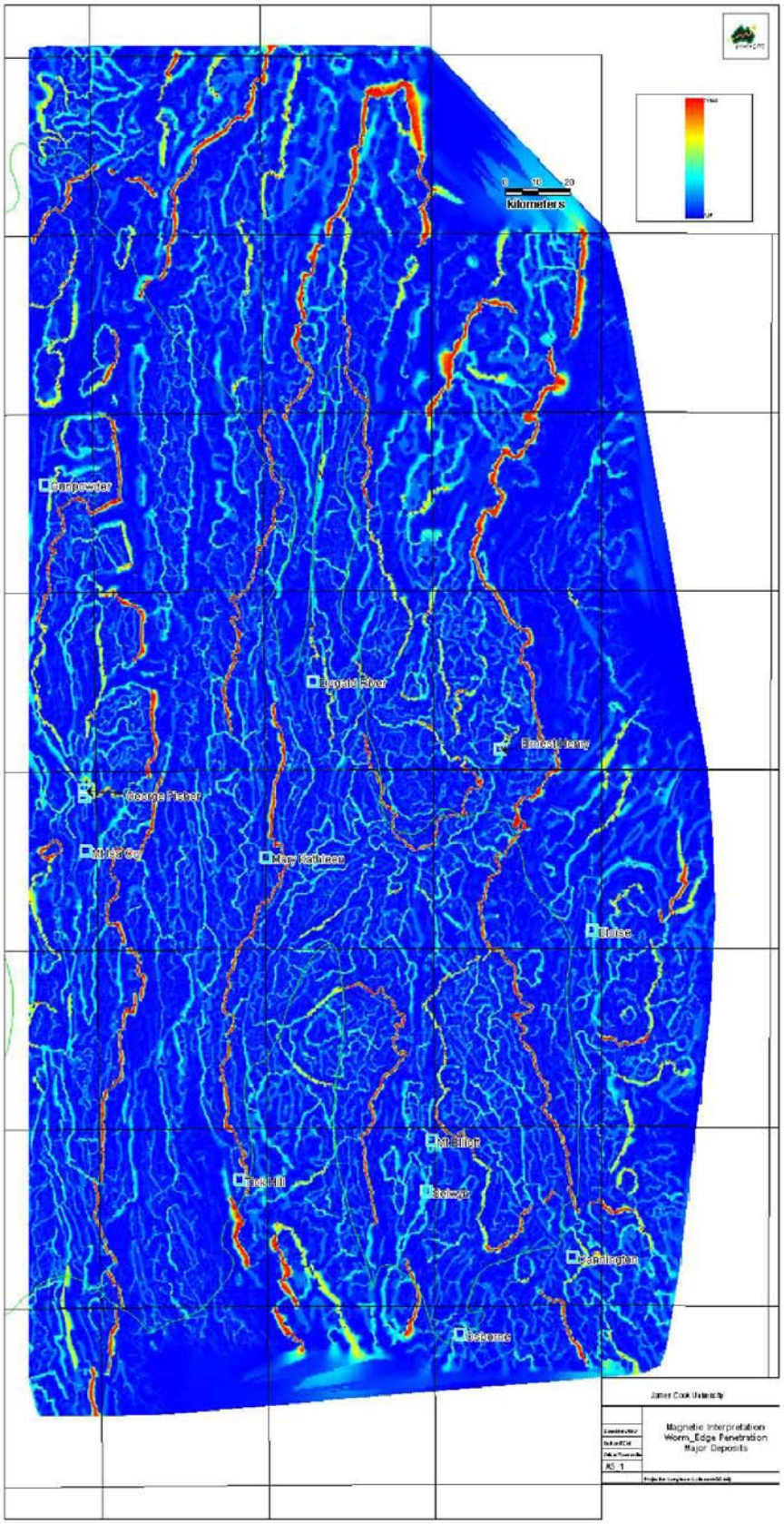

Figure 13: Aeromagnetic edge penetration image

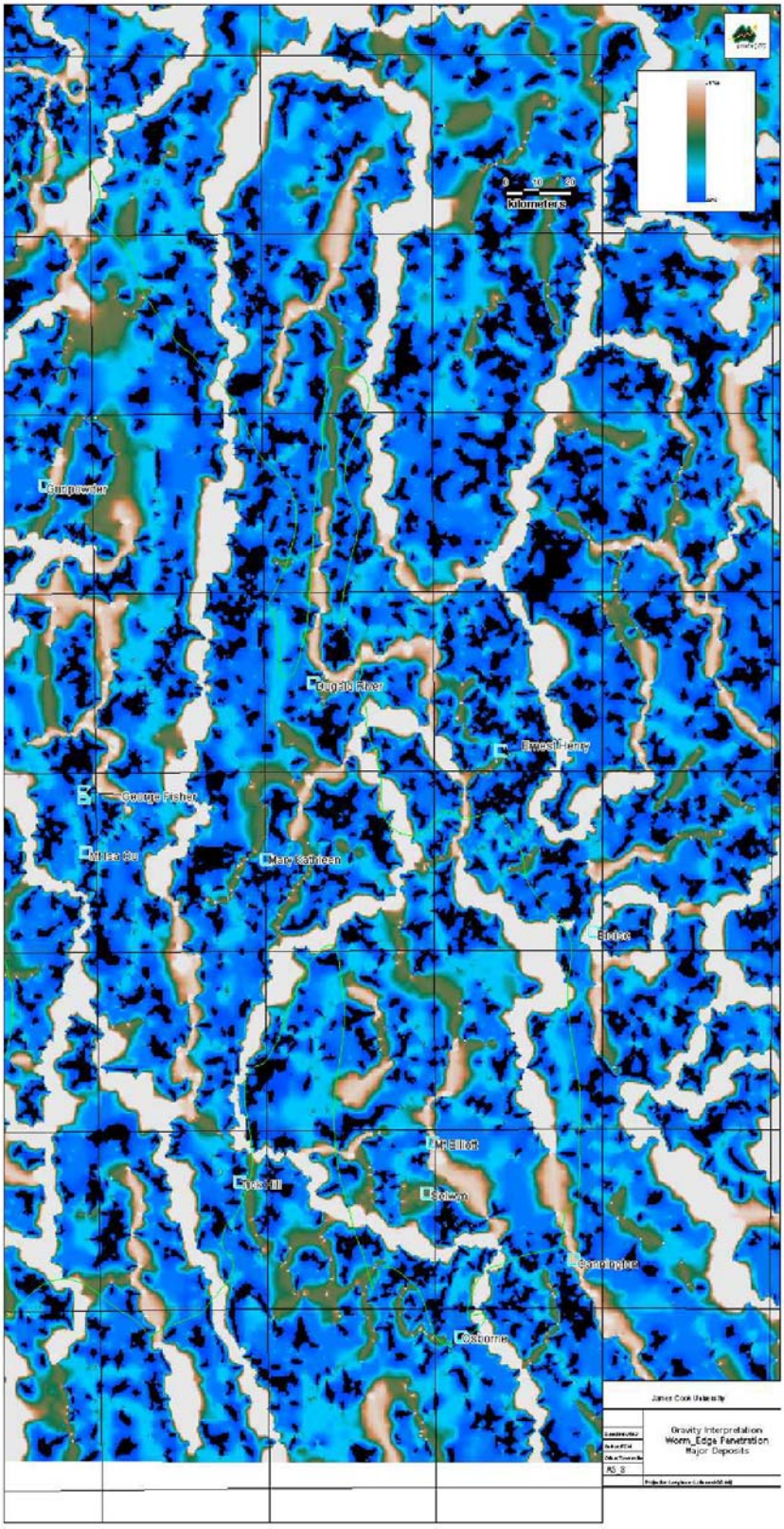

Figure 14: Gravity edge penetration image

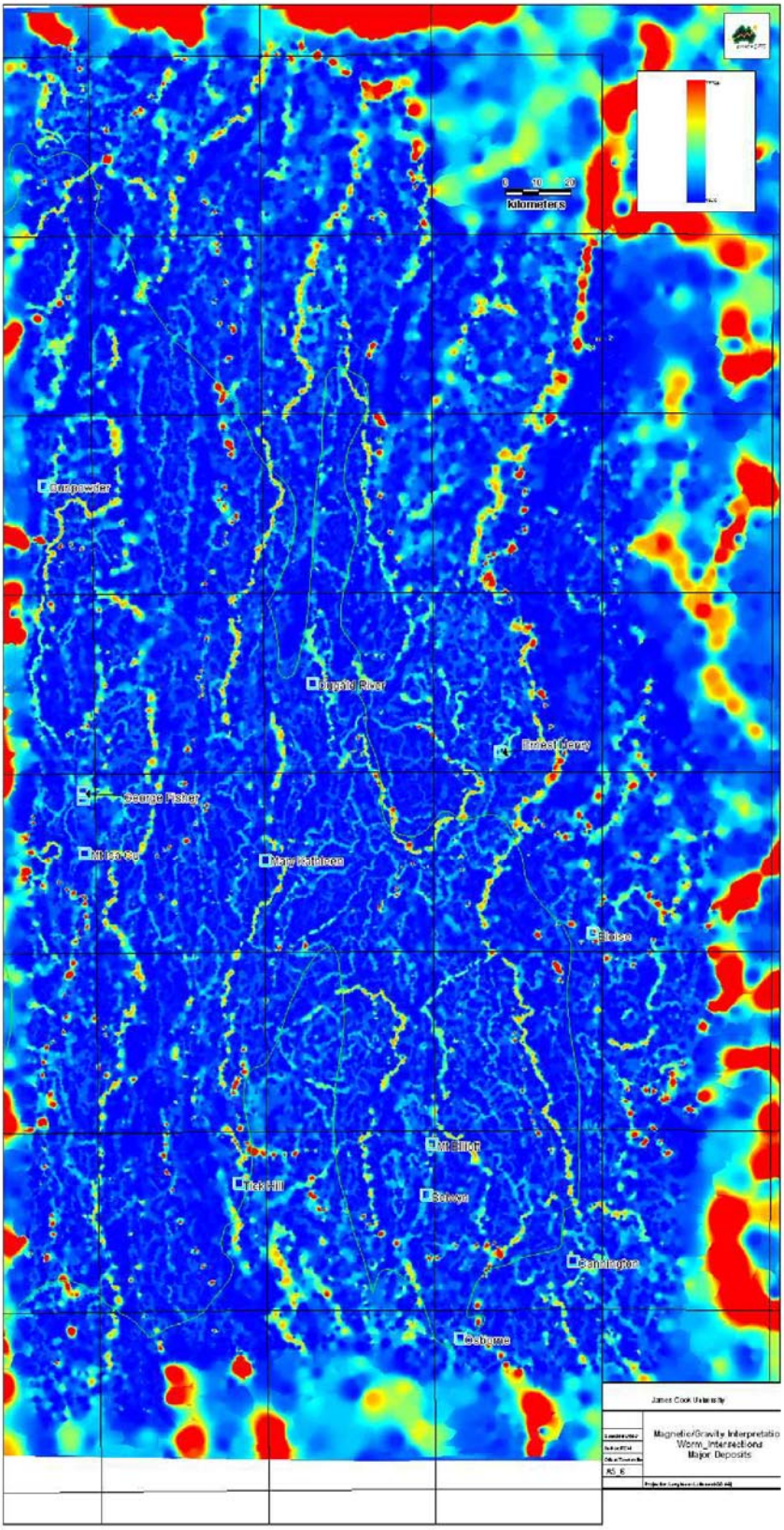

Figure 15: Combined aeromagnetic and gravity edge intersection image

5. Conclusions and Recommendations

The application of multiscale wavelet edges from potential field data to defining the structural framework and targeting ore systems in the Mt Isa region has real promise. The structural architecture derived from migration of worm sheets to a near surface environment shows good correlations with mapped fault and intrusive edges, and gives confidence to interpretation of those edges under cover.

Proximity of deposits to worm edges (the "Z factor") goes some way to defining regions that are considered more permissive for mineralization. The "W factor" has been used to outline anomalous regions, some of which offer tangible exploration targets. A combination with the "permissive" Z regions that overlap with these areas provides a useful area selection filter.

While work to date has focussed on the "where" - in relation to positioning of worm edges, much more work in needed in determining the "what" – in relation to the geological feature being represented, and the "when" – in terms of superposition of edges. Further specific work is envisaged to:

- classifying worm edges with respect to mapped geology, derive dip directions, and map domains of coherent W values
- compare with existing seismics
- construct a 3D framework for visualization and integration of the worms and geological interpretations
- undertake quantitative target area analysis of the gravity worm interpretation
- combine the Western Mt Isa district in the context of the worm interpretations presented here using newly acquired aeromagnetic worms. Because of the relative lack of superposed deformation, this region may offer good scope for targeting ore systems using proximity to edges (Z) as a criterion, and may be particularly instructive in combination with the W data (e.g. targeting the Century deposit).

6. References

Archibald, N., Gow, P. and Boschetti, F. 1999. Multiscale edge analysis of potential field data. Exploration Geophysisc, 30, 38-44.

Archibald, N., Holden, D., Mason, D., Power, B., Boschetti, F. Horowitz, F. and Hornby, P. 2001. "There's a Worm in my soup": Wavelet based analysis for interpretation of crustal scale Potential Field datasets and implications for identification of Giant Hydrothermal Ore systems. A Hydrothermal Odyssey: James Cook University

House. M. 2002. Multiscale Wavelet Edge Analysis of Gravity and Aeromahnetic Data over the Mt Isa Region, Queensland. Memorandum to MIM Exploration.

Hobbs, B. E., Ord, A., Archibald, N. J., Walshe, J. L., Zhang, Y., Brown, M., and Zhao, C. 2000. Geodynamic Modelling as an Exploration Tool. After 200 – The Future of Mining, Sydney Conference.

NWQMPR. 2000. Northwest Queensland Mineral Province Report. Taylor Wall & Assoc.

Large, R., Bull, S., Selley, D., Yang, J., Cooke, D., Garven, G. and McGoldrick, D. 2002. Controls on the formation of giant stratiform sediment-hosted Zn-Pb-Ag deposits: with particular reference to the north Australain Proterozoic. In *Giant Ore Deposits: Characteristics, genesis and exploration.* Eds. D. Cook & J. Pongratz Codes Special Publication, 4. pp 107-149.

Haynes, D. W. 2002. Giant iron oxide-copper-gold deposits: Are they in distinctive geological settings? In *Giant Ore Deposits: Characteristics, genesis and exploration.* Eds. D. Cook & J. Pongratz Codes Special Publication, 4. pp 57-77.

O'Driscoll, E.S.T., 1990, Lineament Tectonics of Australian Ore Deposits, in *Geology of the Mineral Deposits of Australia and Papua New Guinea*. Ed. F. E. Hughes, pp 33-41, The Australian Institute of Mining and Metallurgy: Melbourne.

Appendix 1: Statistical analysis of Worm data sets

XY Scatter plots of Z and W values per MAX and EFVD processing of Gravity and Magnetics, showing Normal Probability plots of each population.

A1: MIM Magnetics_MAX_Z
A2: MIM Magnetics_MAX_W
A3: MIM Magnetics_EFVD_Z
A4: MIM Magnetics_EFVD_W
A5: MIM Gravity_MAX_Z
A6: MIM Gravity_MAX_W
A7: MIM Gravity_EFVD_Z
A8: MIM Gravity_EFVD_W
A9: pmd_ Gravity_MAX_Z
A10: pmd_ Gravity_MAX_W
A11: pmd_ Gravity_EFVD_Z
A12: pmd_ Gravity_EFVD_W

Location template

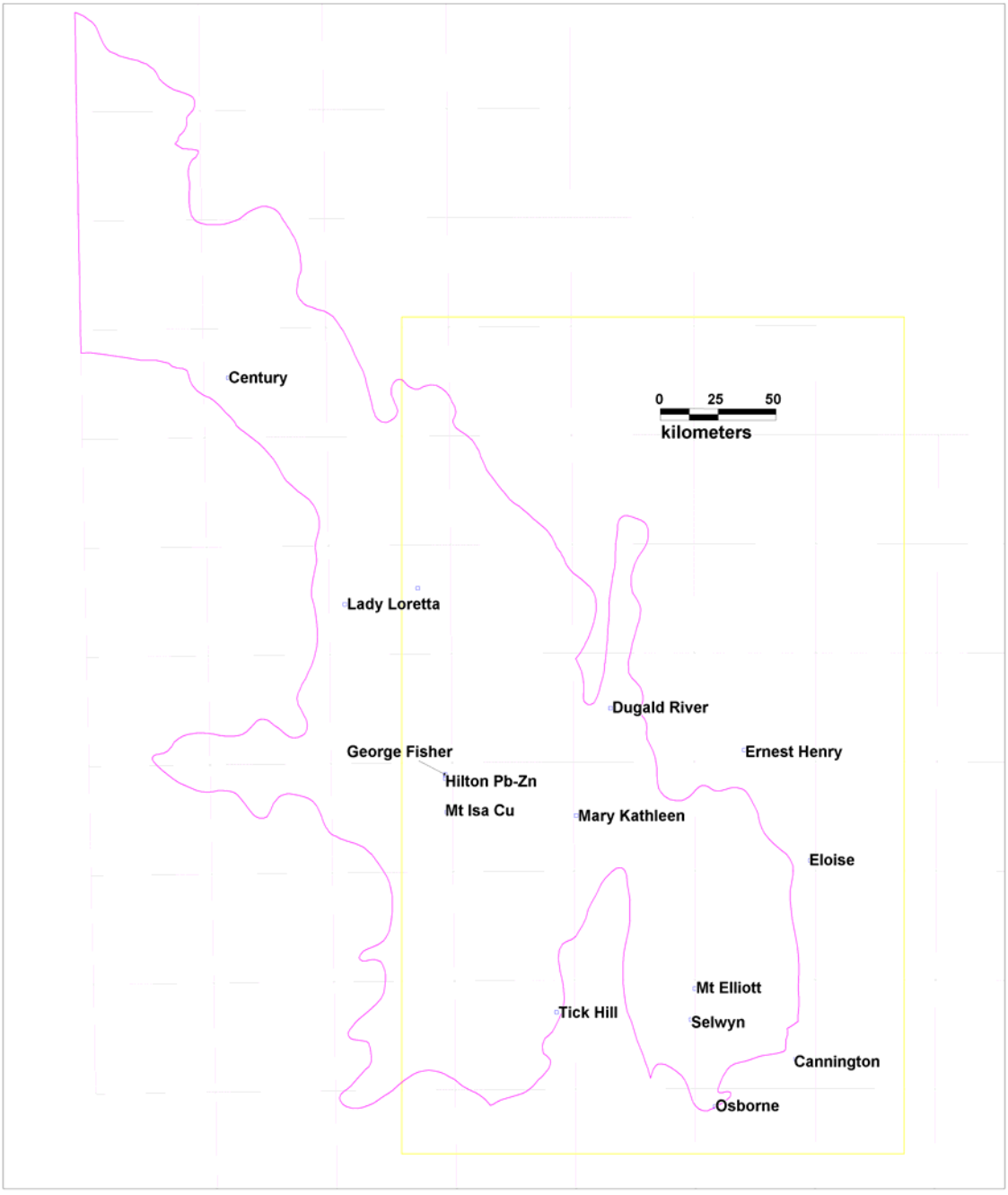

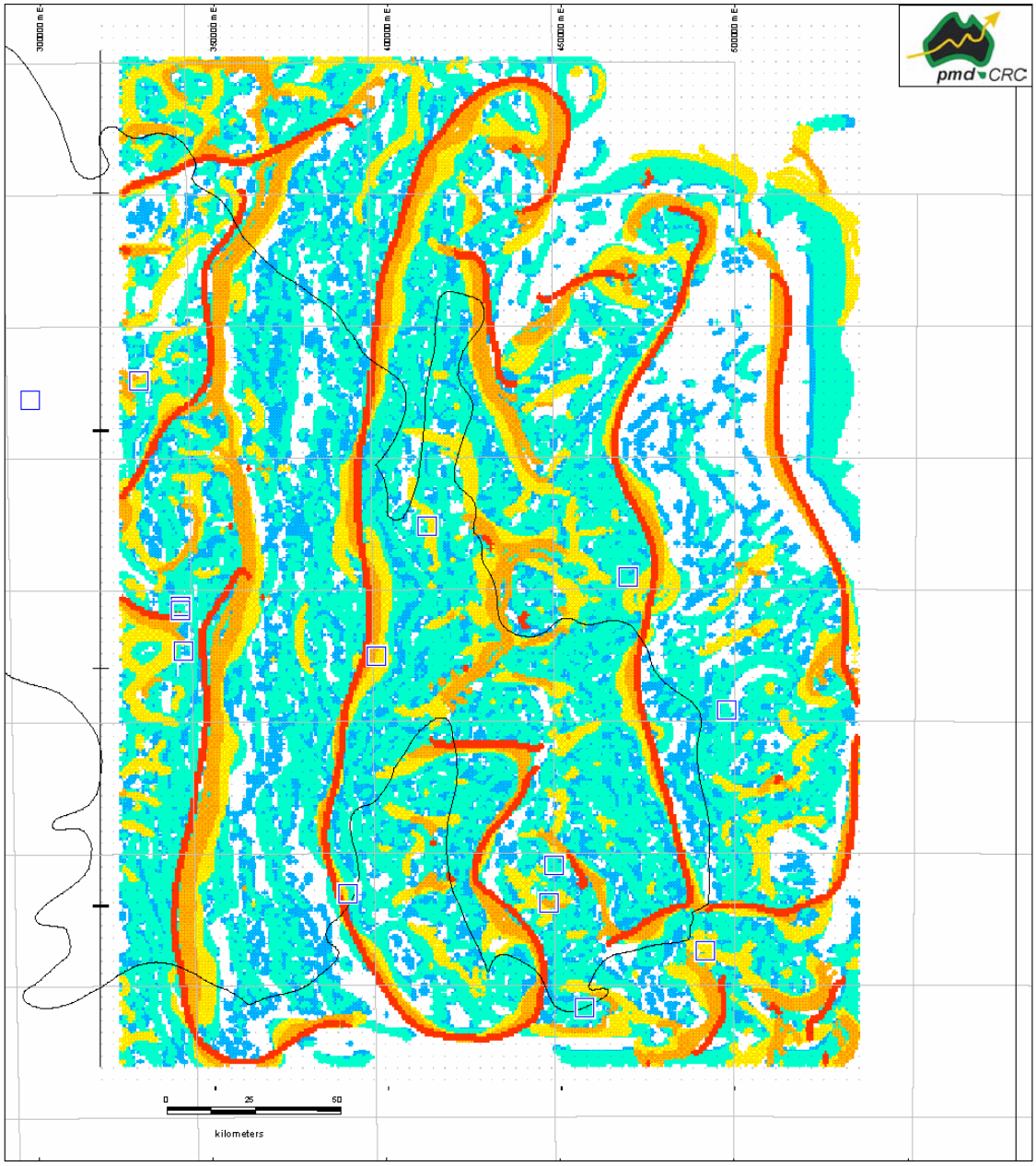

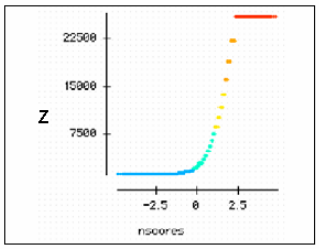

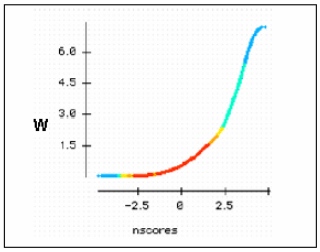

James Cook University

MIM_Magnetics
MAX_Z Values
Major Ore Deposits
100k Sheet Boundaries

Date: 23/8/2002
Author: PCM
Office: Townsville

Fig: A1

Projection: AMG Zone 54 (AGD 66)

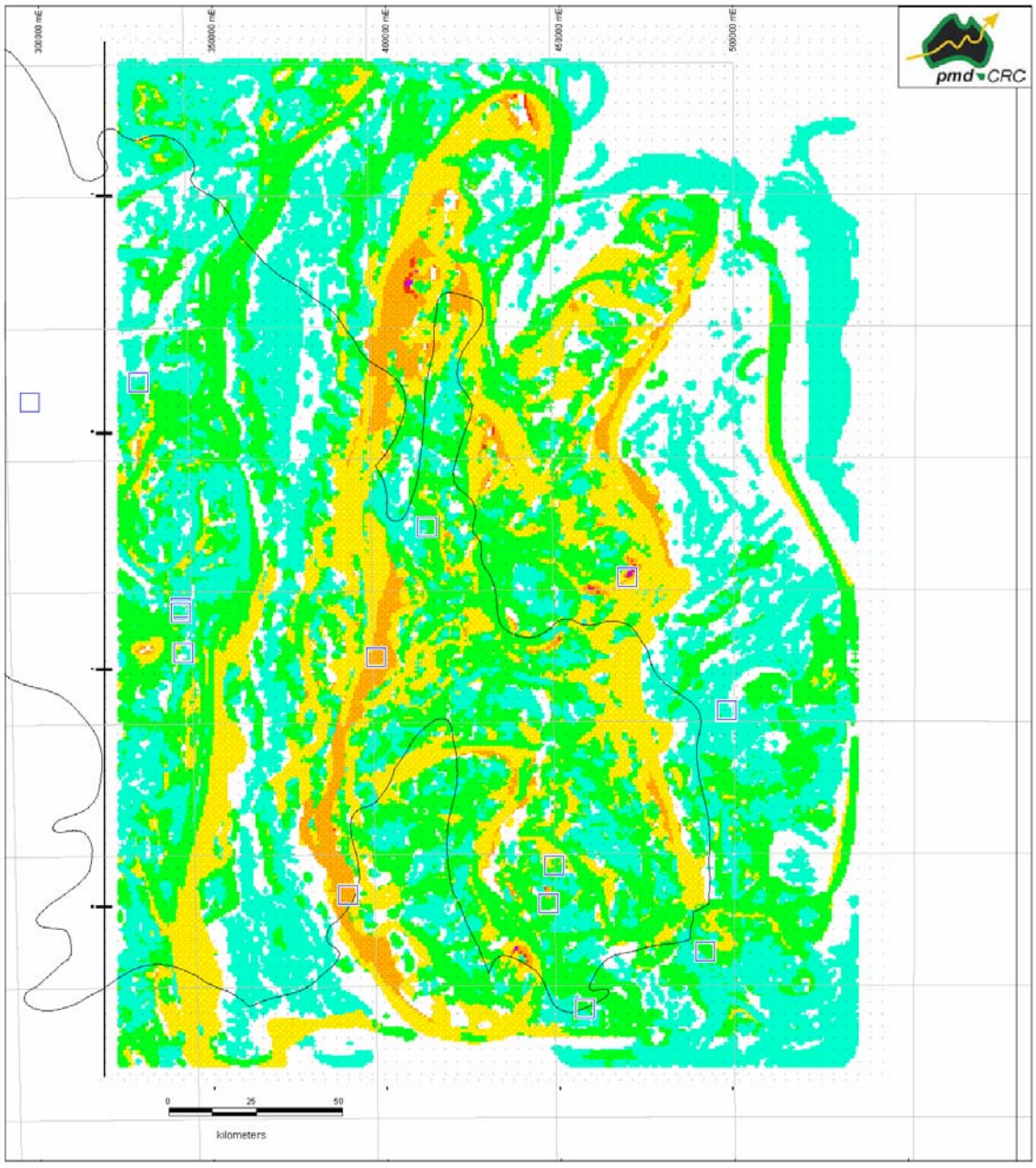

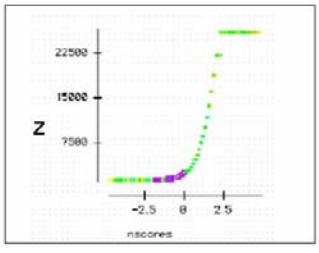

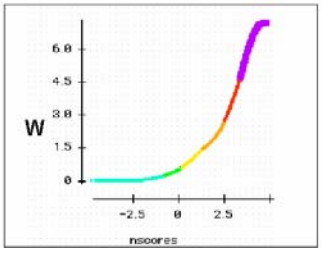

James Cook University	
Date:2/9/2002	MIM_Magnetics MAX_W Values Major Ore Deposits 100k Sheet Boundaries
Author: FCM	
Office: Townsville	
Fig: A2	
	Projection: AMG Zone 54 (AGD 66)

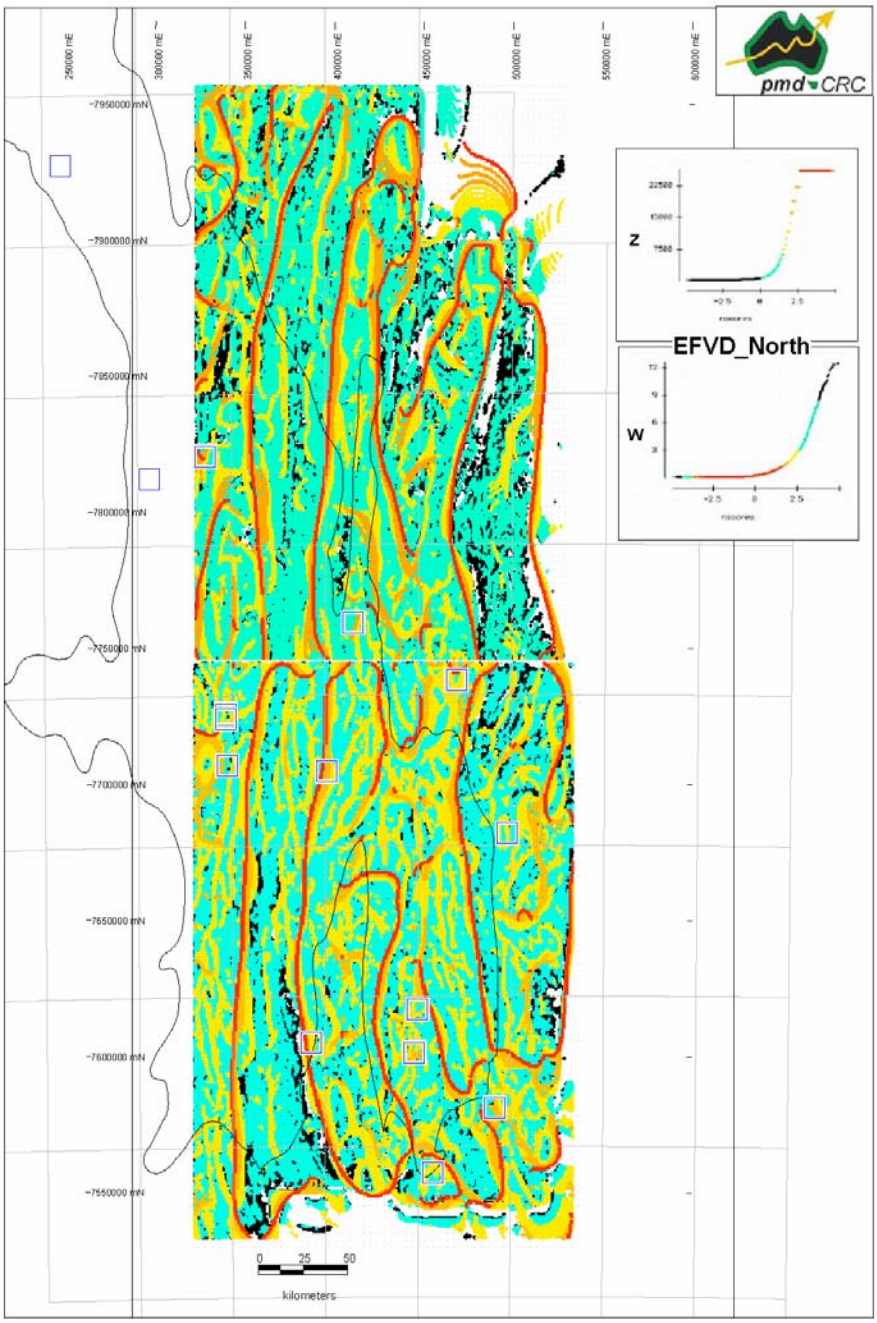

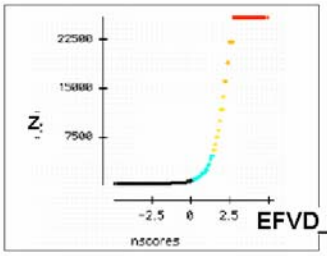

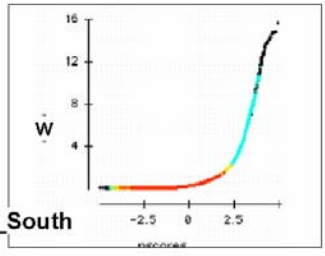

James Cook University	
Date:23/8/2002 Author: FCM Office: Townsville **Fig: A3**	**MIM_Magnetics** **EFVD_Z Values** **Major Ore Deposits** **100k Sheet Boundaries**
	Projection: AMG Zone 54 (AGD 66)

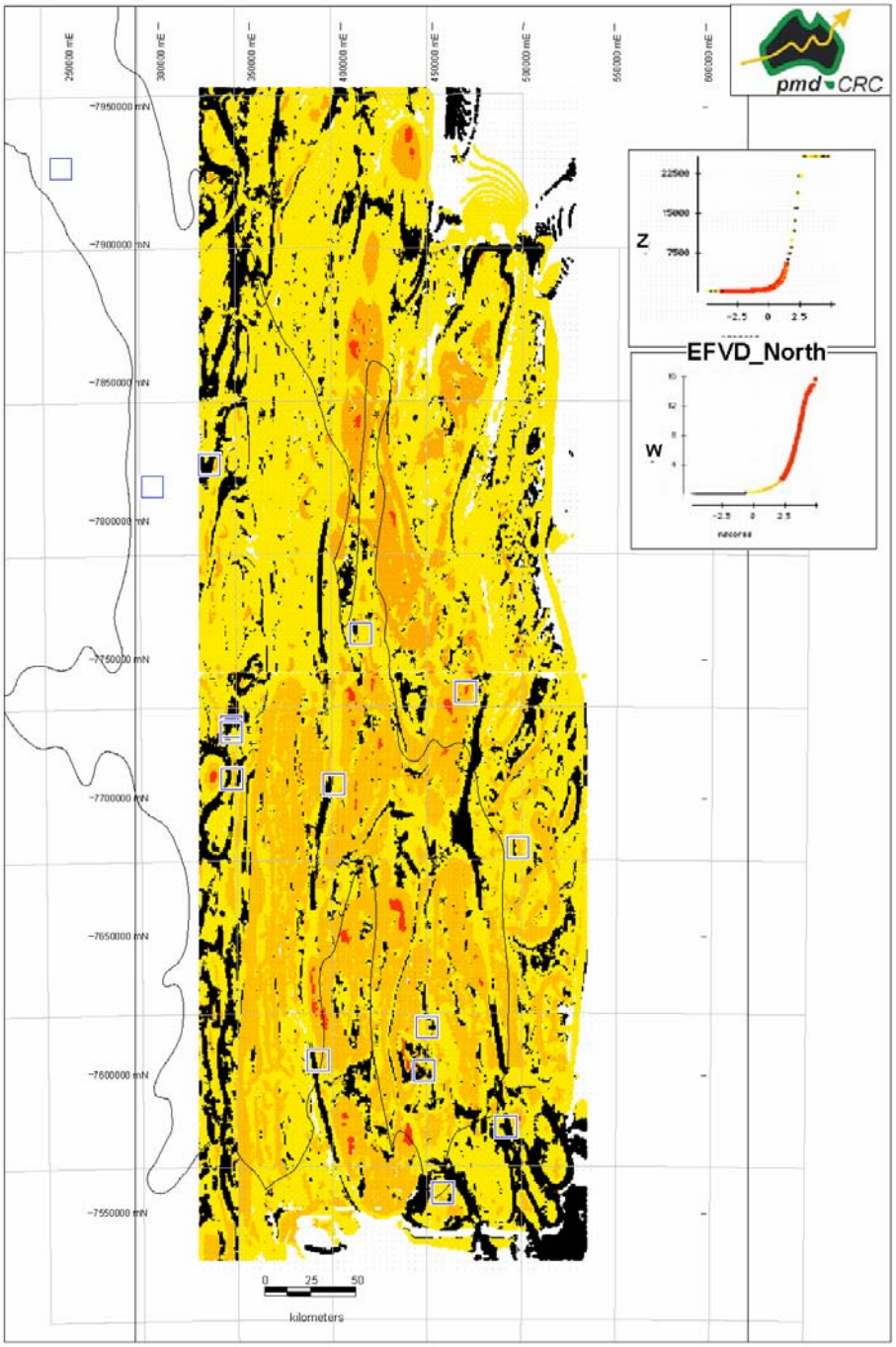

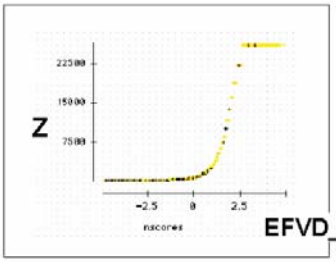

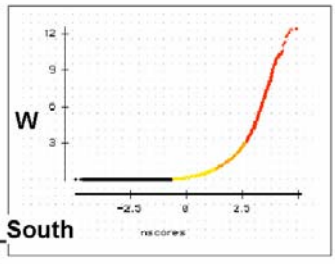

James Cook University

MIM_Magnetics
EFVD_W Values
Major Ore Deposits
100k Sheet Boundaries

Date: 23/8/2002
Author: FCM
Office: Townsville
Fig: A4

Projection: AMG Zone 54 (AGD 66)

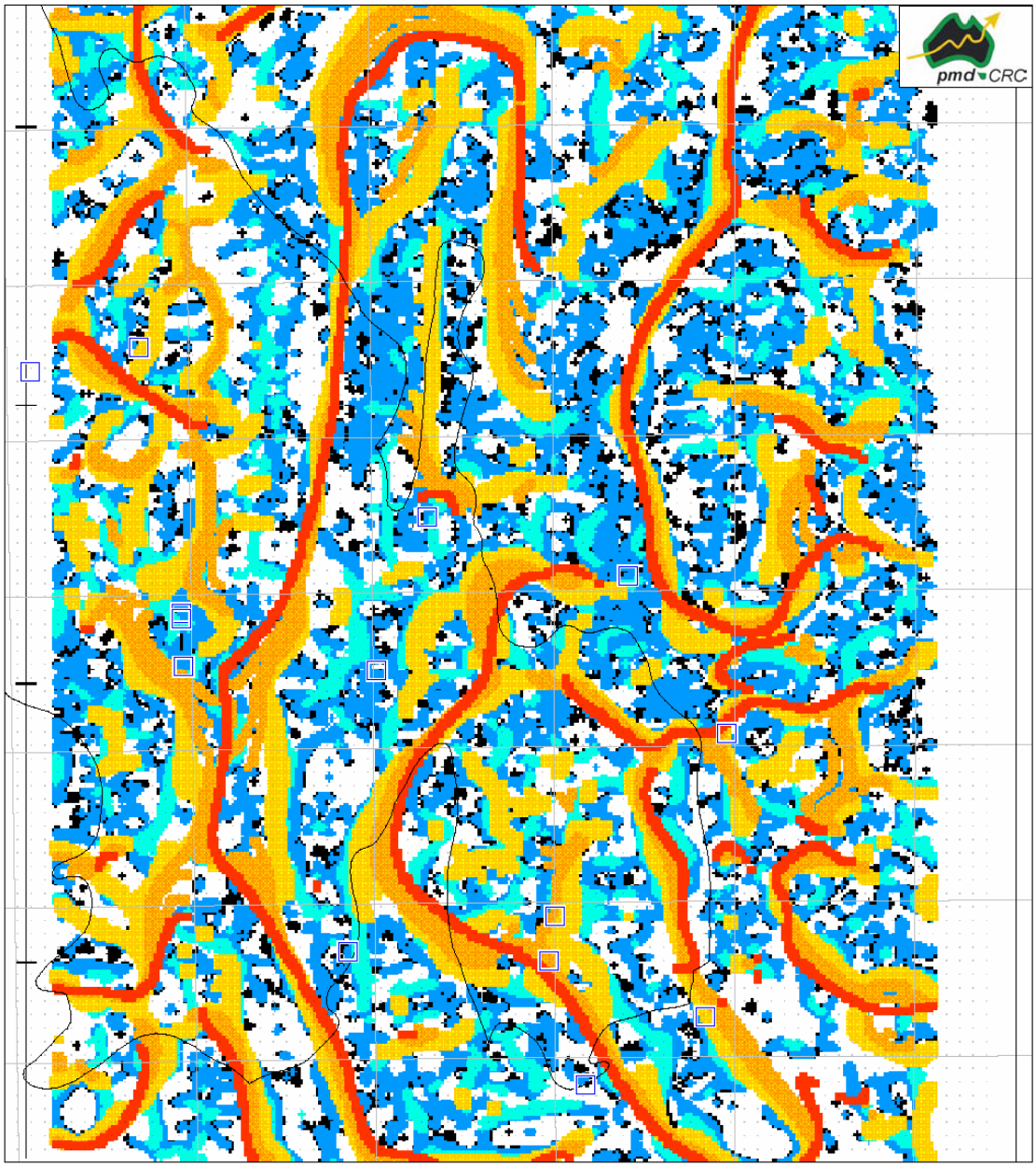

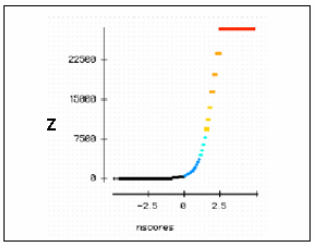

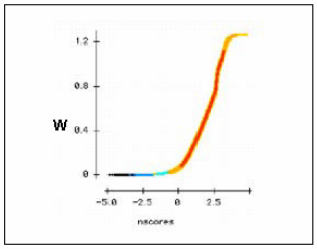

James Cook University

MIM_Gravity
MAX_Z Values
Major Ore Deposits
100k Sheet Boundaries

Date: 23/8/2002

Author: PCM

Office: Townsville

Fig: A5

Projection: AMG Zone 54 (AGD 66)

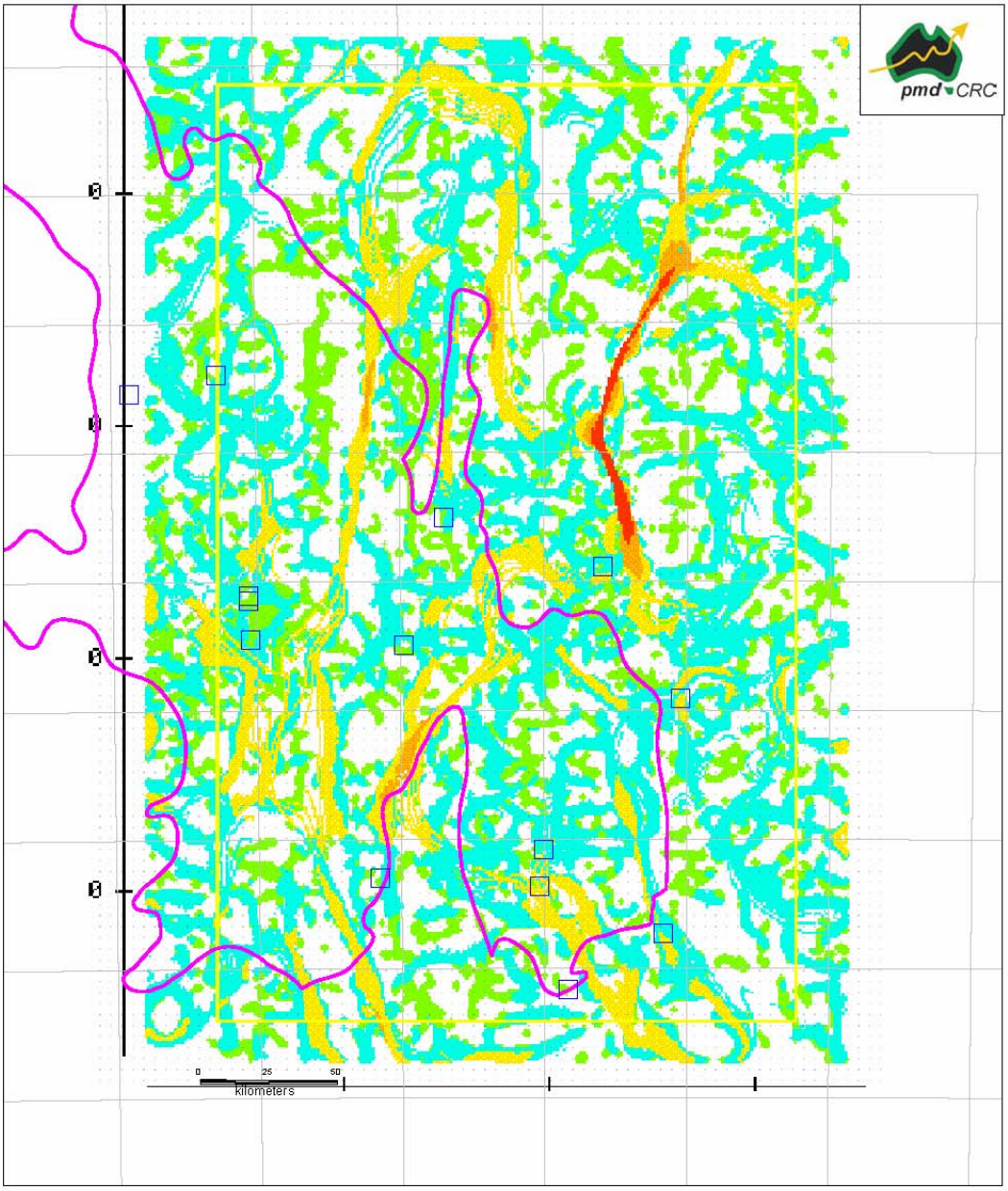

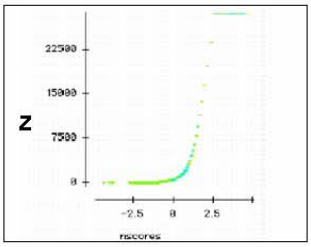

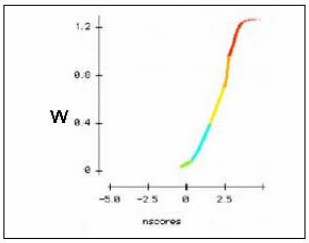

James Cook University

MIM_Gravity
MAX_W Values
Major Ore Deposits
100k Sheet Boundaries

Fig: A6

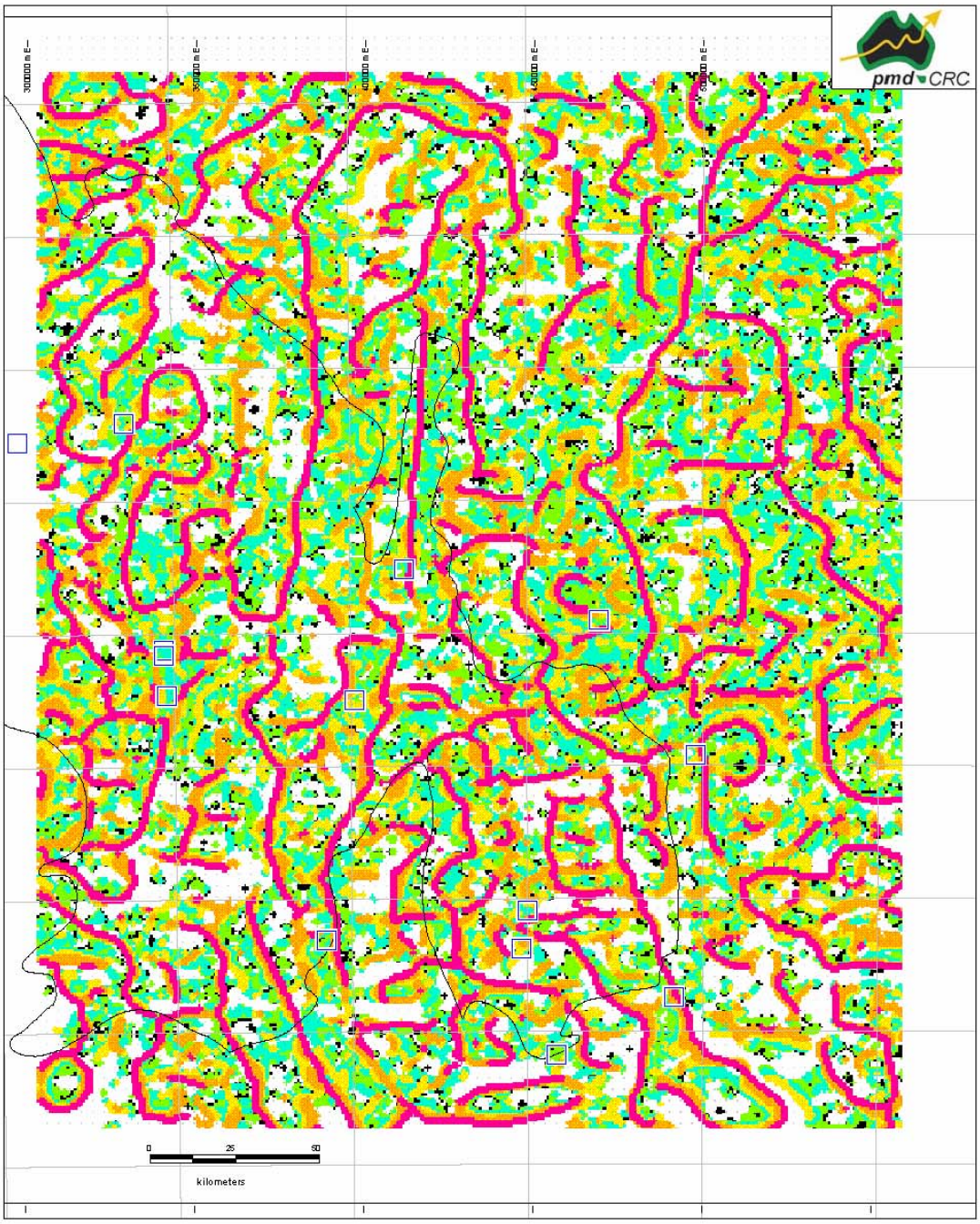

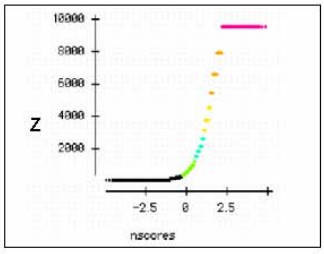

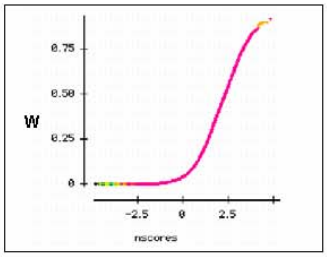

James Cook University

MIM_Gravity
EDVD_Z Values
Major Ore Deposits
100k Sheet Boundaries

Date: 23/8/2002
Author: FCM
Office: Townsville

Fig: A7

Projection: AMG Zone 54 (AGD 66)

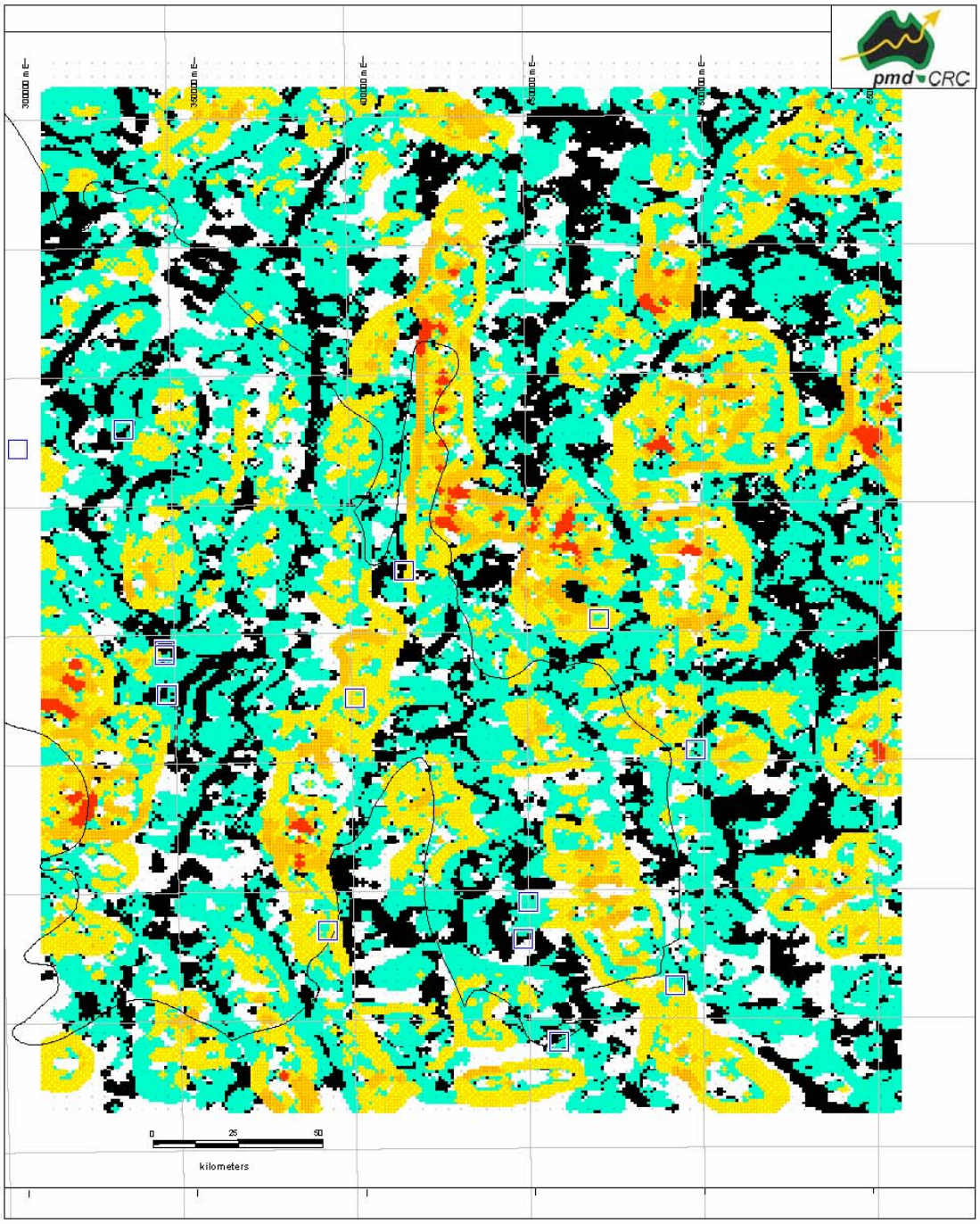

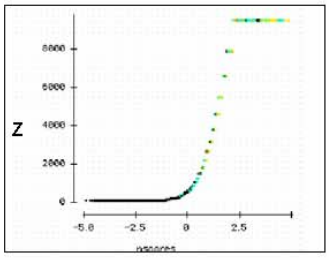

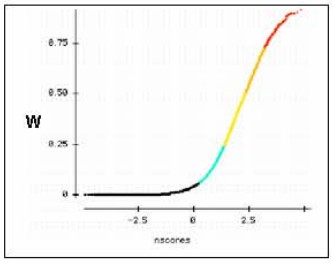

James Cook University

Date: 23/9/2002	MIM_Gravity EDVD_W Values Major Ore Deposits 100k Sheet Boundaries
Author: FCM	
Office : Townsville	
Fig: A8	
	Projection : AMG Zone 54 (AGD 66)

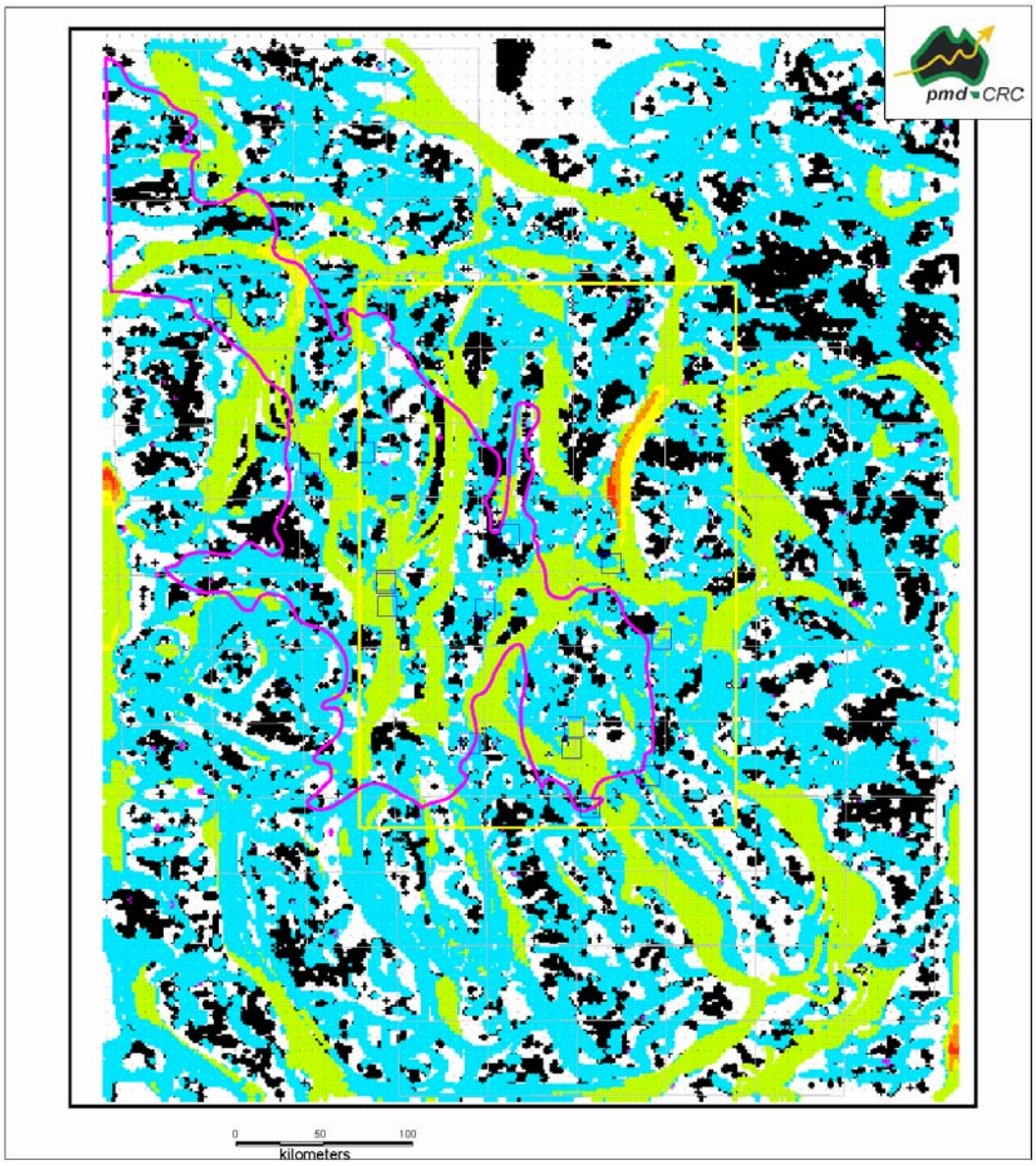

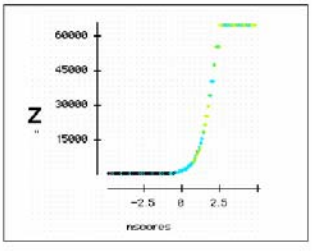

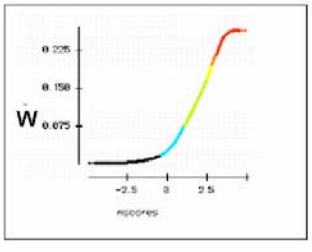

James Cook University	
	pmdCRC_Gravity MAX_W Values Major Ore Deposits 100k Sheet Boundaries
Date: 23/8/2002	
Author: FCM	
Office: Townsville	
Fig: A10	
	Projection: AMG Zone 54 (AGD 66)

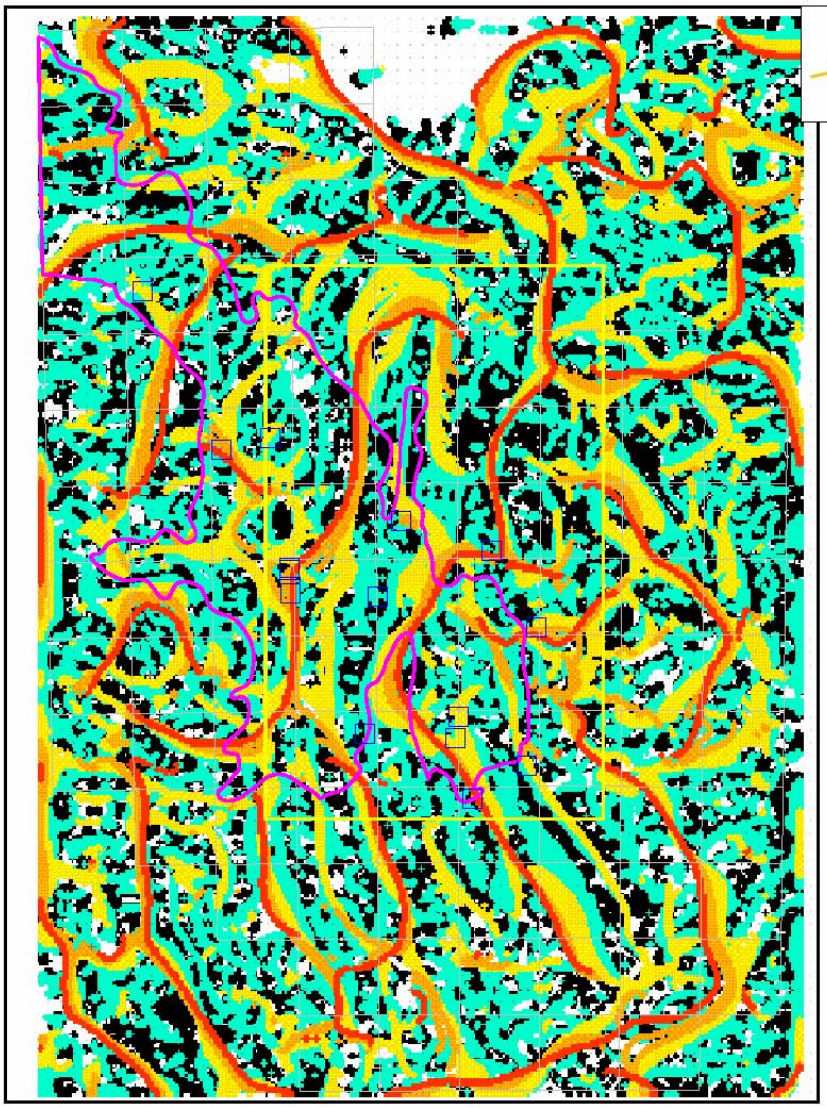

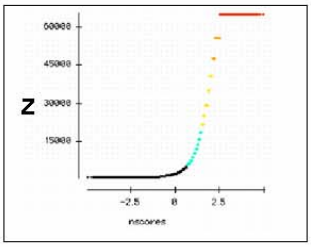

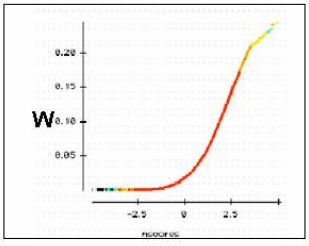

James Cook University

pmdCRC_Gravity
EFVD_Z Values
Major Ore Deposits
100k Sheet Boundaries

Date: 23/9/2002

Author: PCM

Office: Townsville

Fig: A11

Projection: AMG Zone 54 (AGD 66)

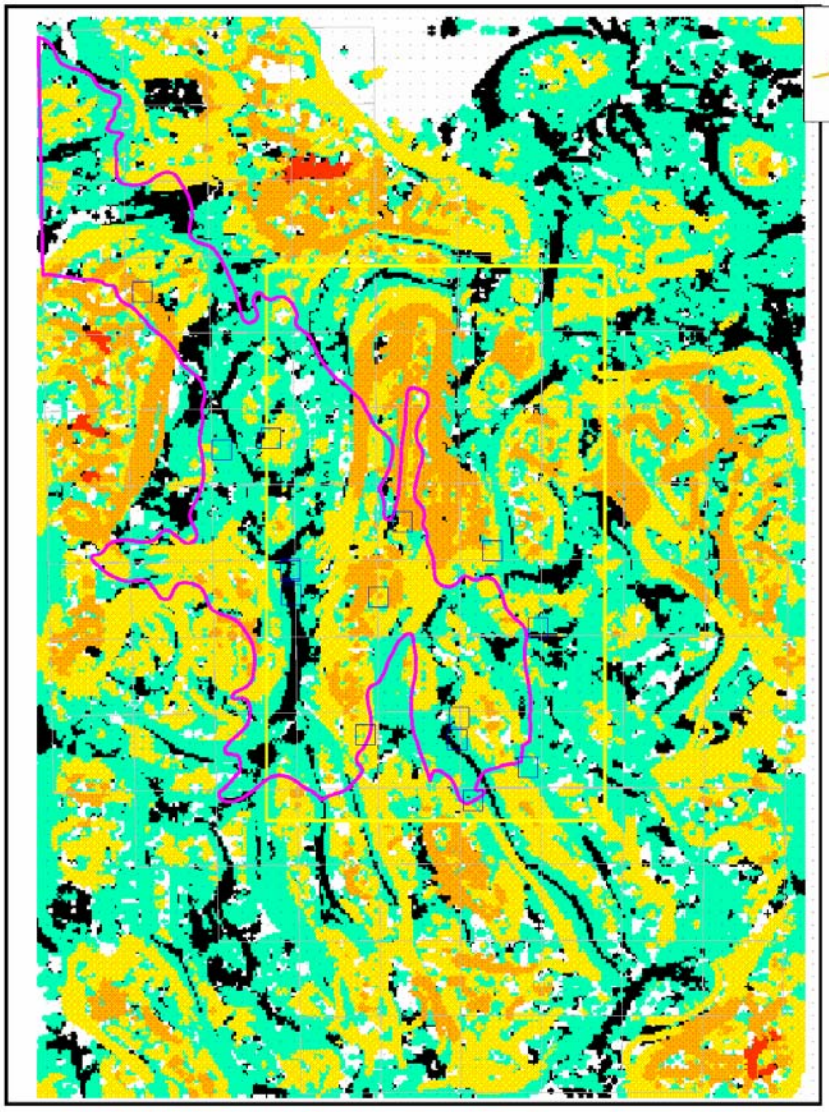

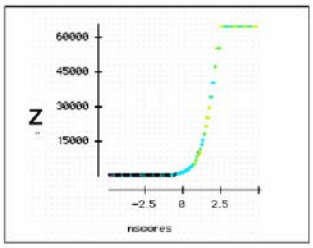

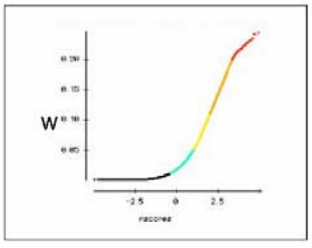

James Cook University

pmdCRC_Gravity
EFVD_W Values
Major Ore Deposits
100k Sheet Boundaries

Fig: A12

Appendix 2: Outline Methodology for up-dip migration of Z values to a Near Surface Environment

In the analysis used here, the manual and semi-automated methods of interpolating Z from 3D into 2D space involve constructing a structural architecture, *via* line tracing the interpreted surface projection of worms. Both methods were trialed over "test" areas in the Eastern Succession and produced very similar results. Examples are shown here for the Malbon 1:100,000 sheet (Fig. A2_1). Advantages of the semi-automated routine are substantially less "hands-on" interpretation, better repeatability, and a >50% time/cost saving. Nevertheless, the analysis still requires a line tracing interpretation step that is reasonably demanding of time and introduces ambiguity through the pen of the interpreter. This interpretation methodology has been applied fairly robustly over the entire Mt Isa region, for both gravity and magnetic data. For the magnetic worms, the scale of interpretation was 1:150,000, and this was largely done on a 1:100,000 sheet area basis. For the gravity worms, the scale of interpretation was 1:500,000. The steps involve:

- Based on initial manipulation of the data in Datadesk, a series of amalgamated Z intervals (from the original 27 levels) are derived for plotting as dot maps in MapInfo (Fig.A2_2). Each "depth interval" reflects a population or range of Z values, up to a maximum level of upward continuation, with 8 levels used in the magnetic interpretation (from 200m to 30000m) and 7 levels for the gravity data (from1000m to 60000m). It is important to note that, in this analysis, the MAX and EFVD Z values were used in a combined interpretation of the data, rather than individually, as they are complimentary of each other and together provide a greater continuity to the worm sheets.
- In the manual method, the migration of Z levels to their near surface expression is through visual inspection of worm "dot maps". Based on the coherence of points in map view, a line is traced and is attributed according to the maximum down dip extent of the worm sheet.
- The semi-automated routine utilizes the same initial dot maps but in this instance depth sliced Z intervals are saved as bitmaps (Fig. A2_3) and exported to an image processing package (Scion Image, freeware) that is used to convert the chains of dots into line images (Fig. A2_4). The line images are in turn vectorised and imported into MapInfo. A new line is then manually traced - based on the vectorised line depth slices - and this line is attributed according to the maximum down dip extent of the worm sheet. The process involves far less visual interpolation, and is inherently more reliable, repeatable and time saving. The optimum scale of interpretation is important to determine in order to derive a meaningful result. If the scale is too large, then the coherence of worm points is lost, while if the scale is too small the density of data becomes too great to extract features of interest. The Scion Image process is sensitive to initial point size and their distribution density.
- Using the series of depth levels, the structural features interpreted from the worms are through an assessment of truncations, coherent geometries and linear alignments. The interpretation is constructed on an overlay that is subsequently colour scanned and vectorised in MapInfo (Fig. A2_5).
- The new vector lines in MapInfo are populated with additional nodes along their length in order to derive a near equi-spaced population of points, and this makes for a uniform data set, thereby diminishing any bias that may arise in the

digitizing process. Each node along a line is attributed with the relevant maximum penetration depth (based in Z intervals).

- A critical aspect to the line interpretation lies in mapping the intersections of features in the derived architecture. Each line intersection point (node) is attributed according to the count and sum of the intersecting line values. In this way, the intersection points are weighted for subsequent imaging. It is important in this regard that the nodes of intersecting lines are "snapped" to each other.

There are a number of caveats to the worm interpretation presented here. These relate both to primary aspects of the data and to aspects of the mapping methods employed:

- Determinations of the maximum level of upward continuation can be erroneous where the MAX and EFVD values "crossover" at a particular Z value (N. Archibald pers. comm. 2002). Crossovers were not evaluated in this analysis.
- The level of upward continuation is only a broad measure of actual penetration depth of edges, and is more reliably correlated to edges derived from gravity than to those from aeromagnetics.
- Low frequency / long wavelength responses are typically attributed to deeper sources, but this does not hold true universally (N. Archibald pers. comm. 2002). The impact of this on the current analysis has not been determined, but the implication is that some apparently deep responses may be due to shallow sources. This should have minimal impact for regional analysis of large strike length features (faults).
- High frequency/short wavelength responses typically reflect lithological signals (eg. amphibolites in a layered sequence), minor faults and shears, and "noise" effects. These have not been attributed as such in the analysis, but are "filtered out" in the broader structural interpretation of the region.
- Low frequency/long wavelength responses (ie. deep features) mostly appear to have some near surface expression. Those that don't have obvious connectivity to the surface have, in most cases, been projected into the 2D representation, but have not been identified separately here. To identify such regions, one needs to consult the original worm maps.
- Deriving the wrong "picks" from 2D analysis of 3D data. The direction of dip of worm sheets are, typically, reasonably consistent but dip magnitude can vary significantly, eg. listric geometries. As a result, shallow dipping features can cause confusion in determining the up dip projection to the surface. This is a significant issue in regions of complex worms, particularly intersecting features that have significant apparent depth penetration. The determination of the surface projections of worms in such regions is more difficult, and would be optimized by 3D visualization, especially as these are, potentially, the regions of exploration interest.
- A significant proportion of the worm sheets fall short of making intersections and such regions require interpolation of lines, eg. zones of worm disruption, corner effects of intersecting edges.
- Dip directions, as seen in the worm dot maps, have not been incorporated in the 2D interpretation, and must be in further work on the project.

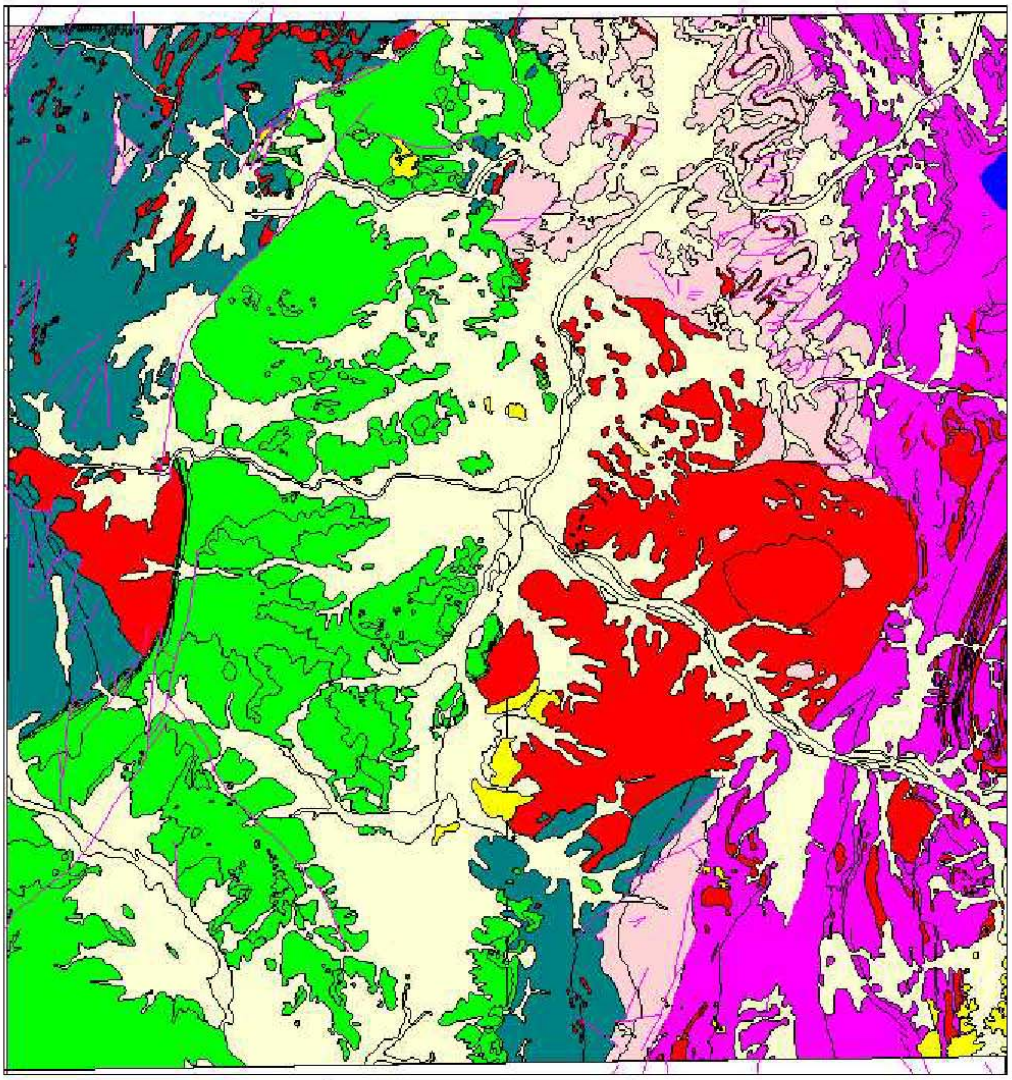


pmd*CRC


Malbon_geolp by GROUP
Cainozoic
Cambrian
Malbon Group
Mary Kathleen Group
Mesozoic
Mount Albert Group
Quaternary
Soldiers Cap Group
Tertiary
Tertiary-Quarternary
Tewinga Group
Williams Batholith

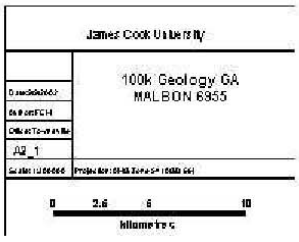
James Cook University
100k Geology GA
MALBON 6955
A2_1
0
2.5
5
10
kilometres

22212_25989
11853_18985
05406_10131
02107_4621
01124_1801
00600_961
00320_513
00200_273

James Cook University

Magnetic Worms_EFVD
All Levels_Dot Map
MALBON 6955
GA Faults

A2_2

0 2.5 5 10
kilometres

James Cook University

Magnetic Worms MAX
MALBON 8855
600-961m Level
Dot Map
GA Faults

A2_3

0 2.5 5 10
kilometres

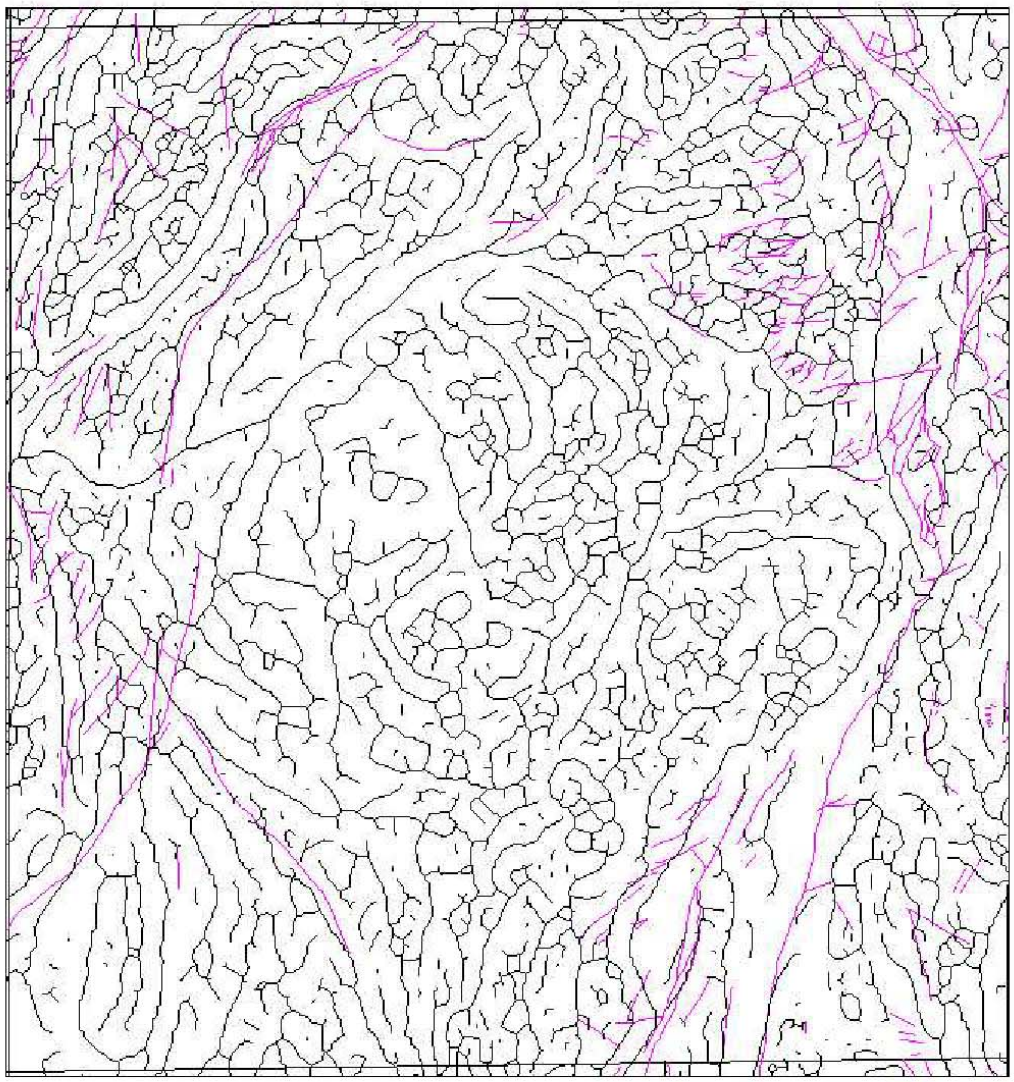

James Cook University

Magnetic Worms MAX/BFVD
MALBON 6955
600-981m Level
Binary Image Line Map
GA Faults

A2_4

0 2.5 5 10
kilometres

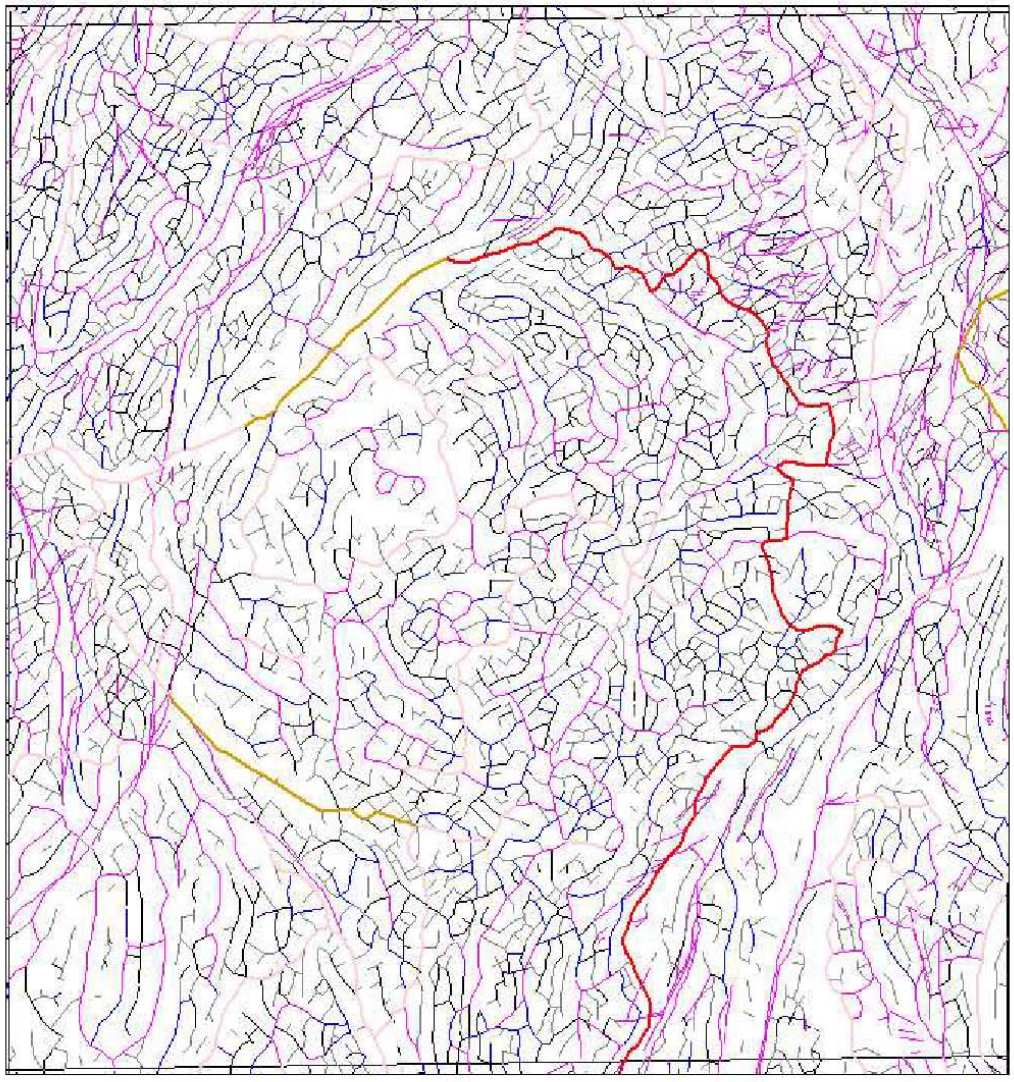


pmd CRC

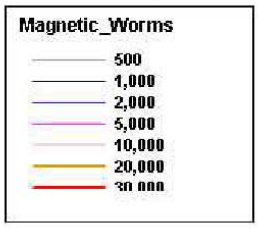
Magnetic_Worms
500
1,000
2,000
5,000
10,000
20,000
30,000

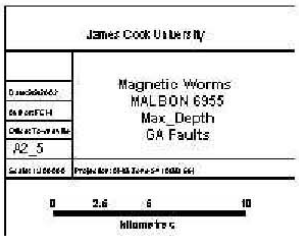
James Cook University
Magnetic Worms
MALBON 6955
Max_Depth
GA Faults
A2_S
0
2.5
5
10
kilometres

Appendix 3: Proximity analysis of Major Deposits in relation to Worm Line interpretations

Each deposit shown with 20km radius of influence with respect to magnetic and gravity worm lines.

XY plots of Distance vs Apparent Edge Depth for:

A: Deposit distance from Worm Line

B: Deposit distance from Worm Intersection

(Red - Magnetics; Purple – Gravity)

Deposits:

Ernest Henry
Selwyn
Mt Elliott
Osborne
Eloise
Cannington
Gunpowder
George Fisher
Hilton
Mt Isa
Dugald River
Lady Loretta
Mary Kathleen
Tick Hill

Location_Template

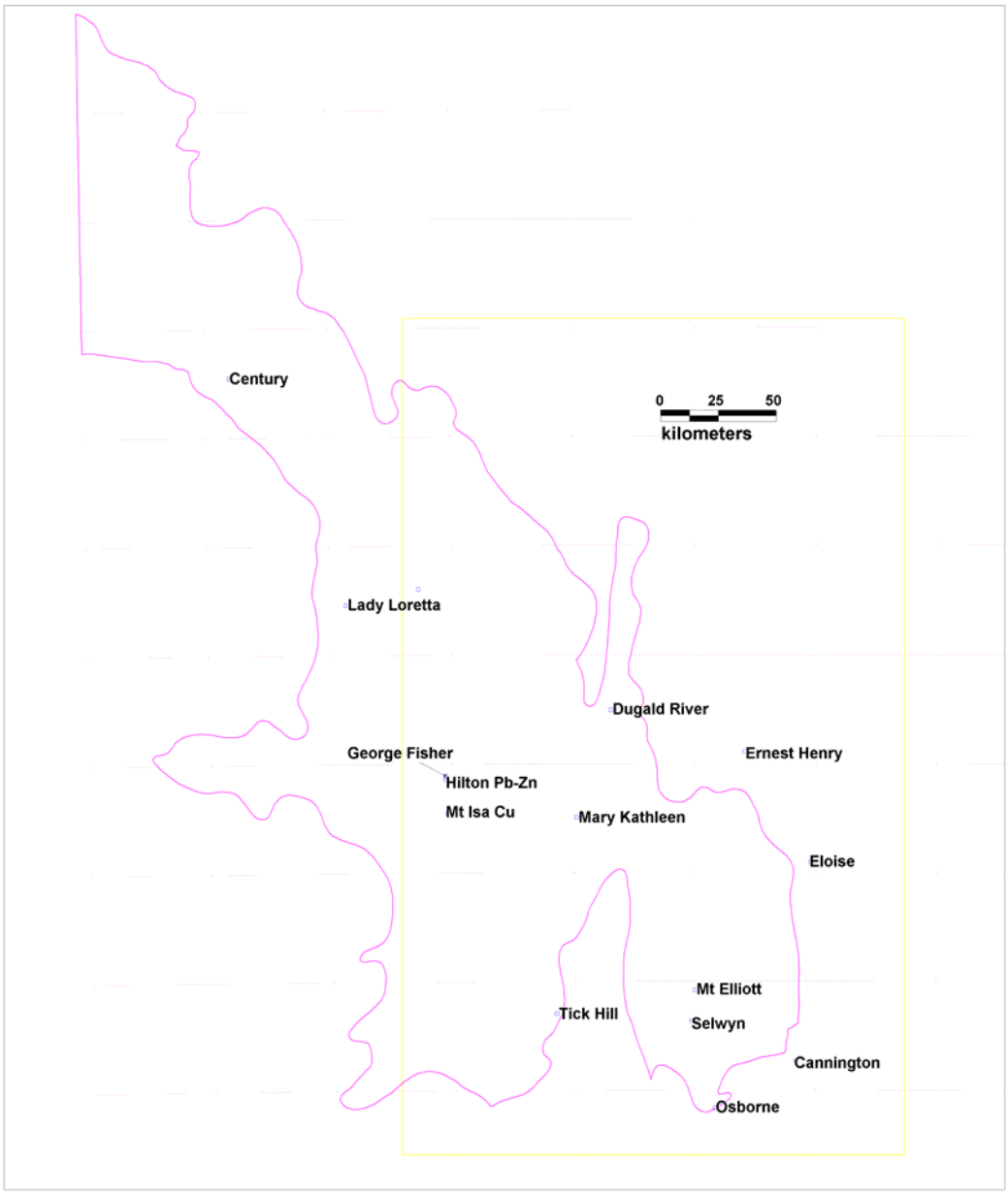

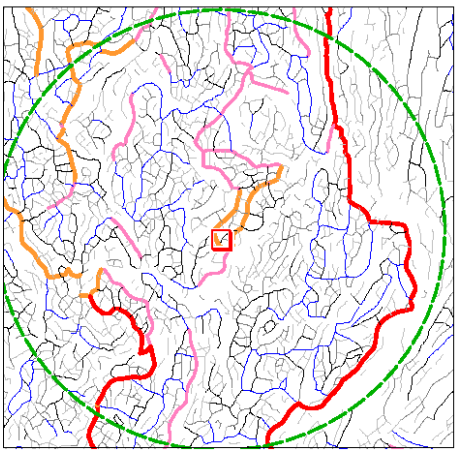

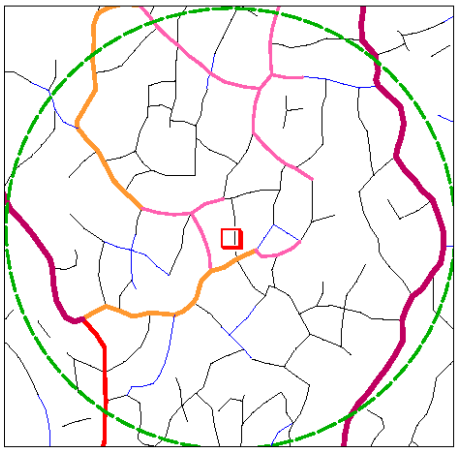

Magnetic_Worms_ by Max_Depth

500
1,000
2,000
5,000
10,000
20,000
30,000

Ernest Henry

0 5 10

kilometers

Gravity_Worms by Max_Depth

2,000
5,000
10,000
20,000
30,000
60,000

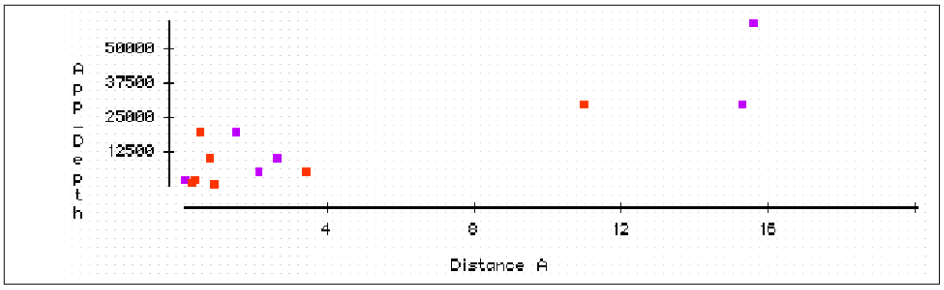

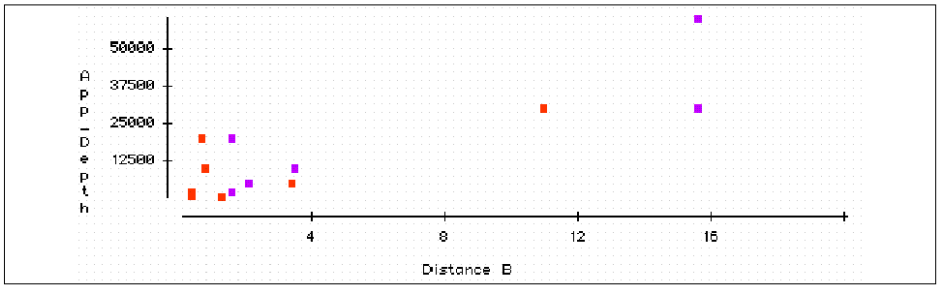

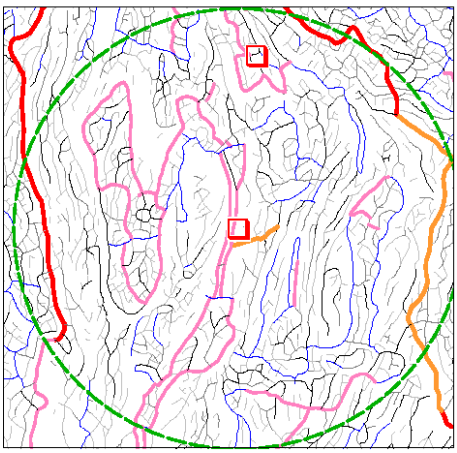

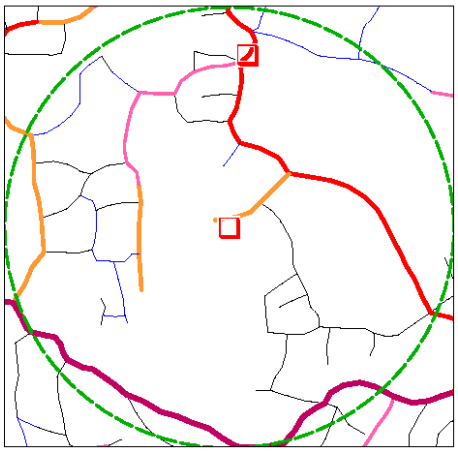

Magnetic_Worms_ by Max_Depth

500
1,000
2,000
5,000
10,000
20,000
30,000

Selwyn

0 5 10

kilometers

Gravity_Worms by Max_Depth

2,000
5,000
10,000
20,000
30,000
60,000

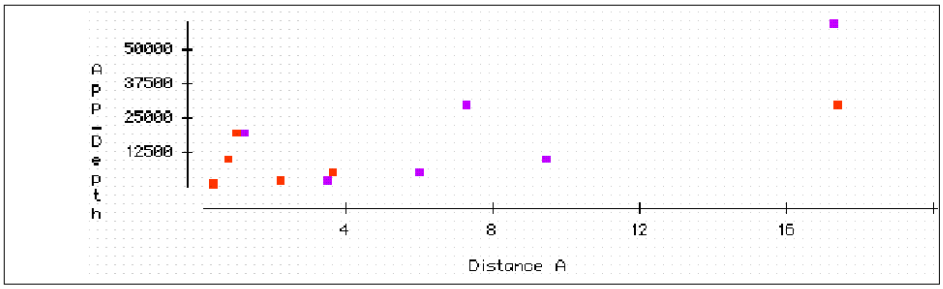

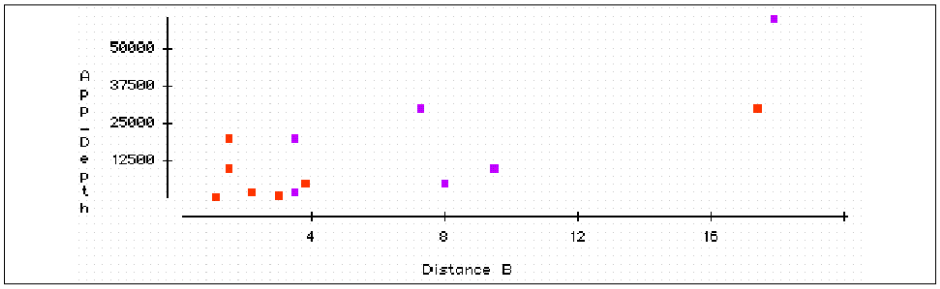

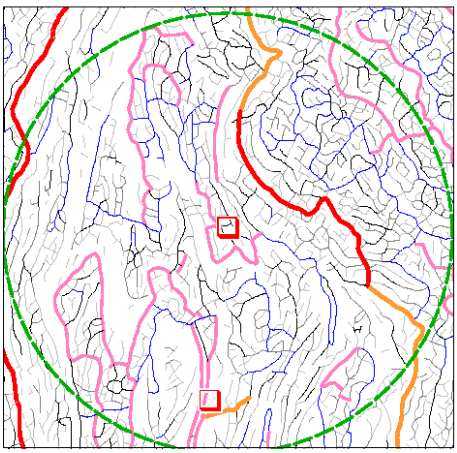

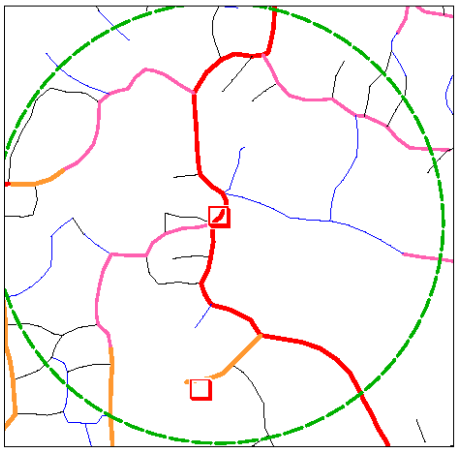

Magnetic_Worms_ by Max_Depth

500
1,000
2,000
5,000
10,000
20,000
30,000

Mt Elliott

0 5 10

kilometers

Gravity_Worms by Max_Depth

2,000
5,000
10,000
20,000
30,000
60,000

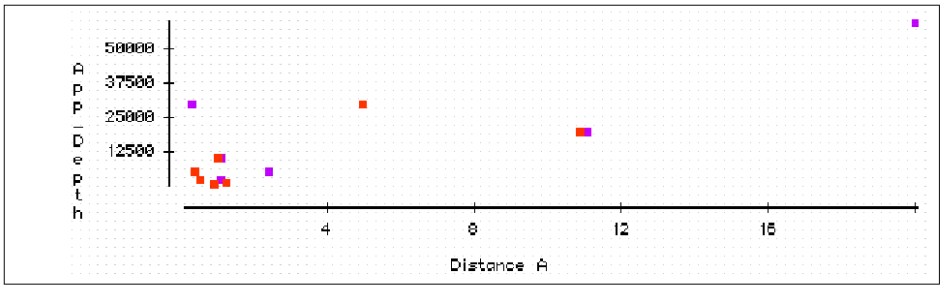

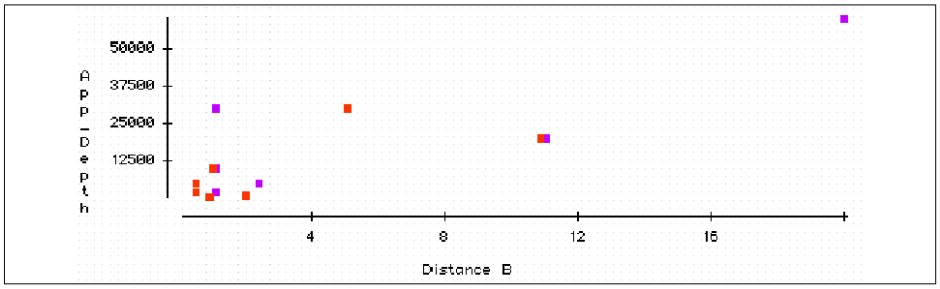

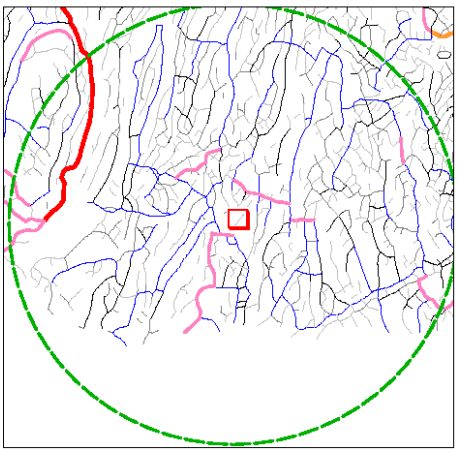

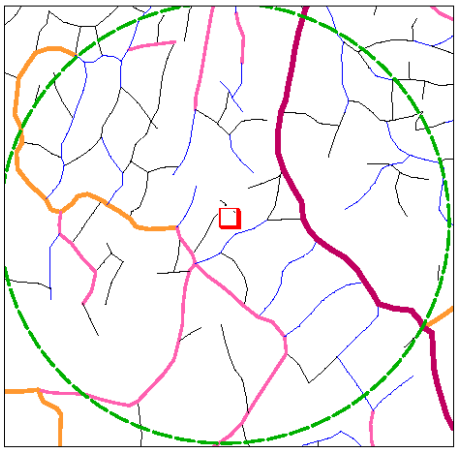

Magnetic_Worms_ by Max_Depth

500
1,000
2,000
5,000
10,000
20,000
30,000

Osborne

0 5 10

kilometers

Gravity_Worms by Max_Depth

2,000
5,000
10,000
20,000
30,000
60,000

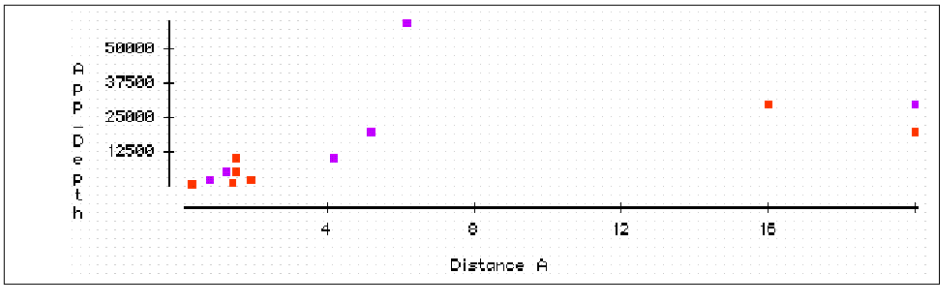

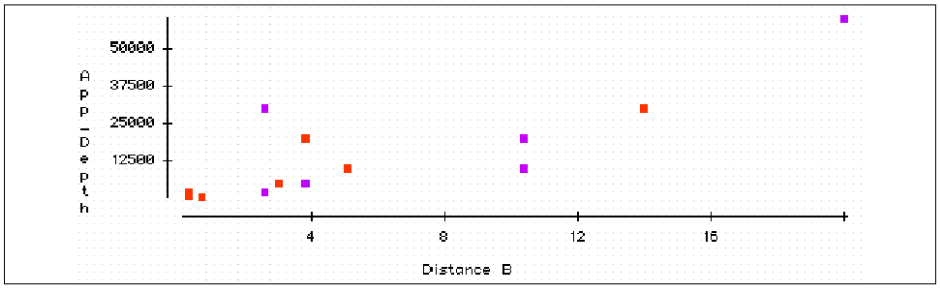

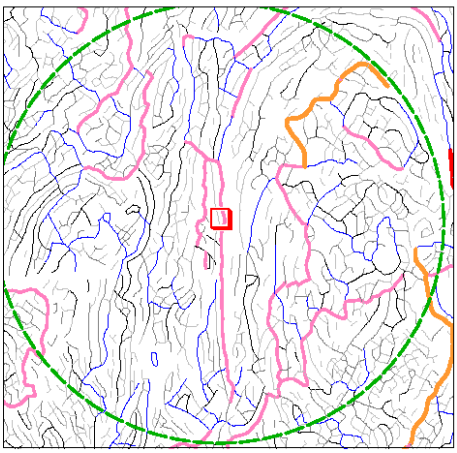

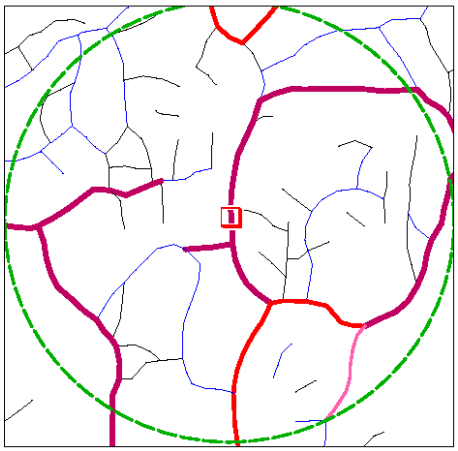

Magnetic_Worms_ by Max_Depth

500
1,000
2,000
5,000
10,000
20,000
30,000

Eloise

0 5 10

kilometers

Gravity_Worms by Max_Depth

2,000
5,000
10,000
20,000
30,000
60,000

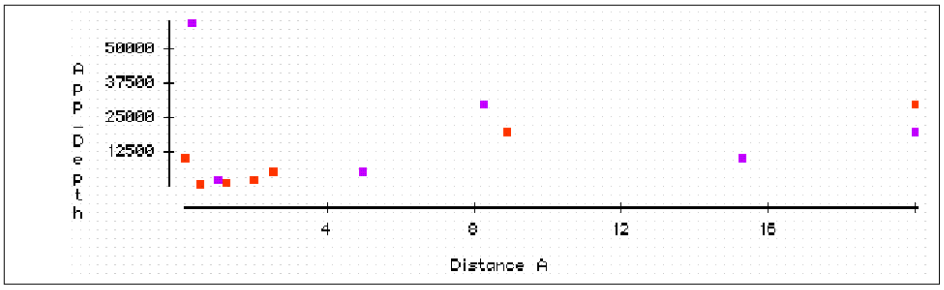

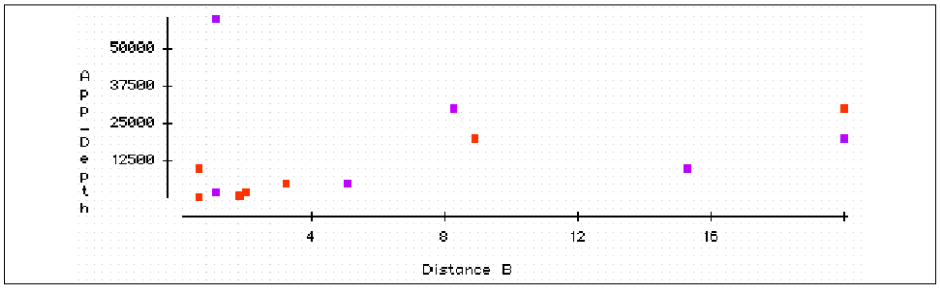

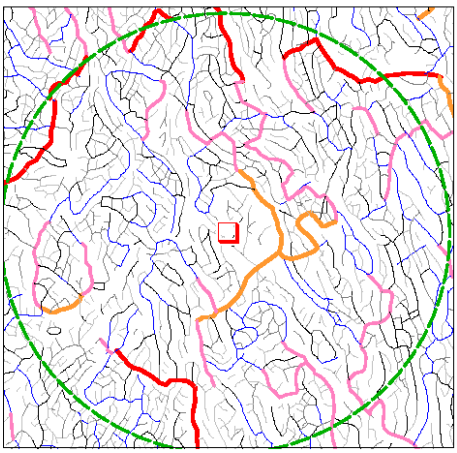

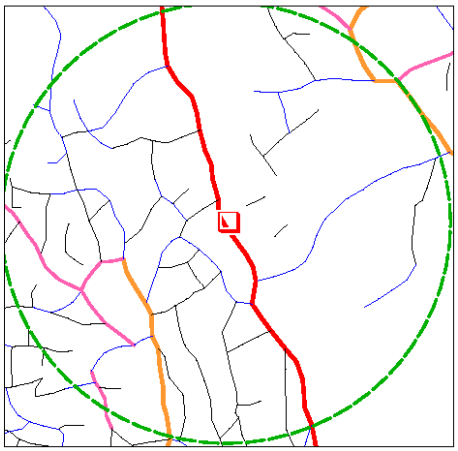

Magnetic_Worms_ by Max_Depth

500
1,000
2,000
5,000
10,000
20,000
30,000

Cannington

0 5 10

kilometers

Gravity_Worms by Max_Depth

2,000
5,000
10,000
20,000
30,000
60,000

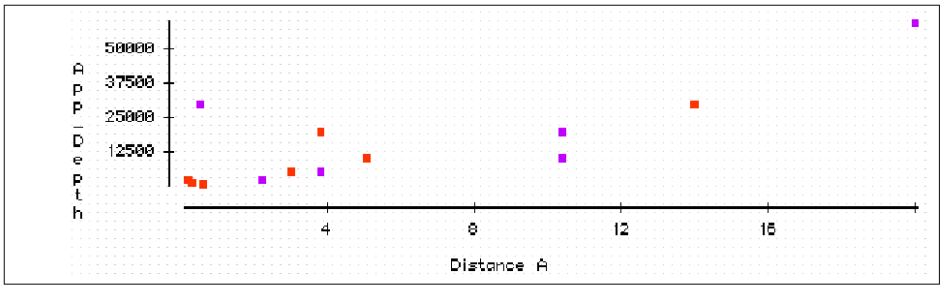

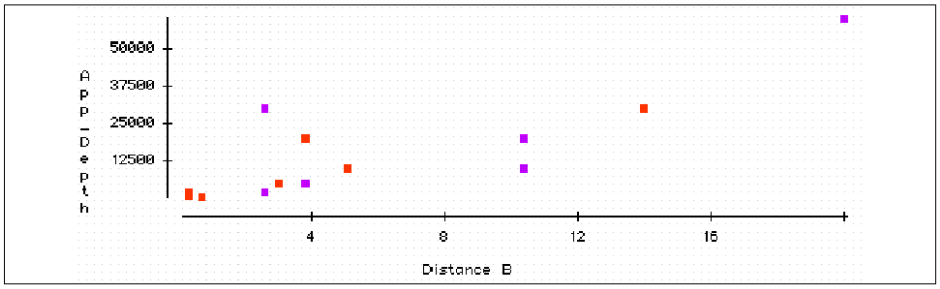

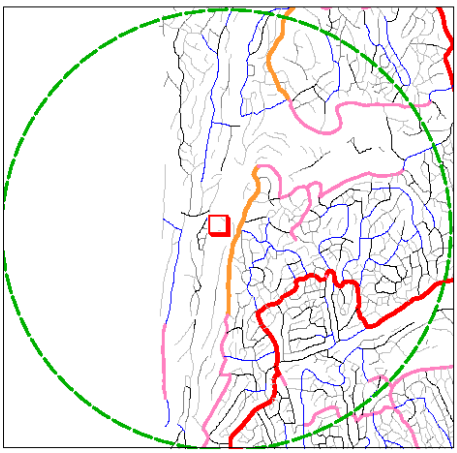

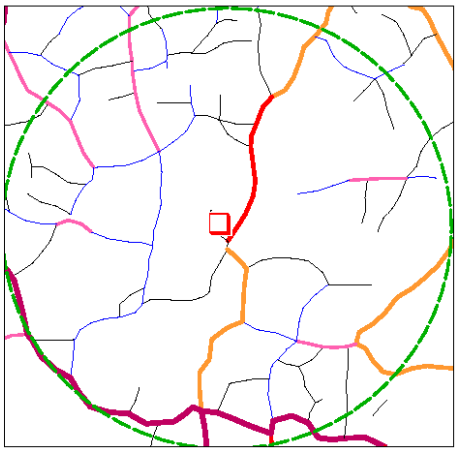

Magnetic_Worms_ by Max_Depth

500
1,000
2,000
5,000
10,000
20,000
30,000

Gunpowder

0 5 10

kilometers

Gravity_Worms by Max_Depth

2,000
5,000
10,000
20,000
30,000
60,000

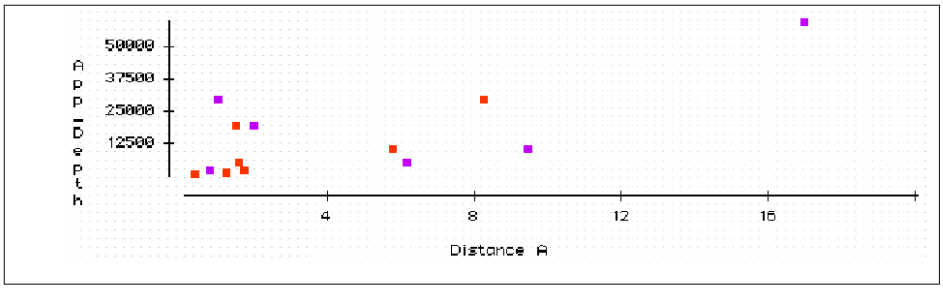

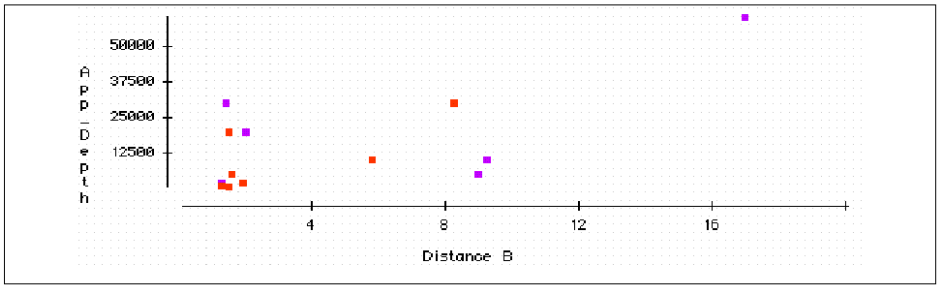

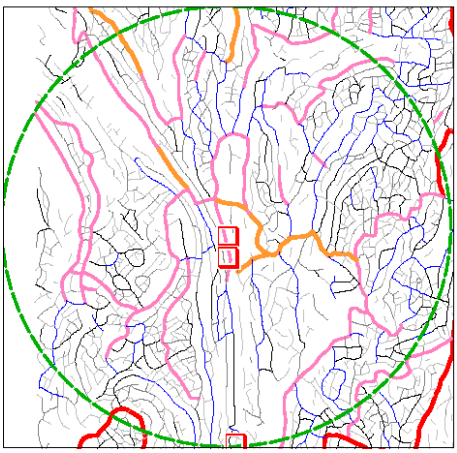

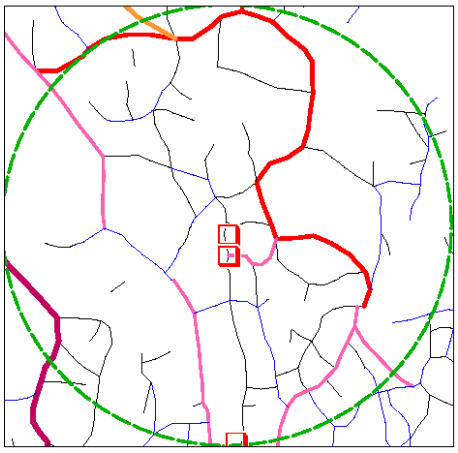

Magnetic_Worms_ by Max_Depth

- 500
- 1,000
- 2,000
- 5,000
- 10,000
- 20,000
- 30,000

George Fisher

0 5 10

kilometers

Gravity_Worms by Max_Depth

- 2,000
- 5,000
- 10,000
- 20,000
- 30,000
- 60,000

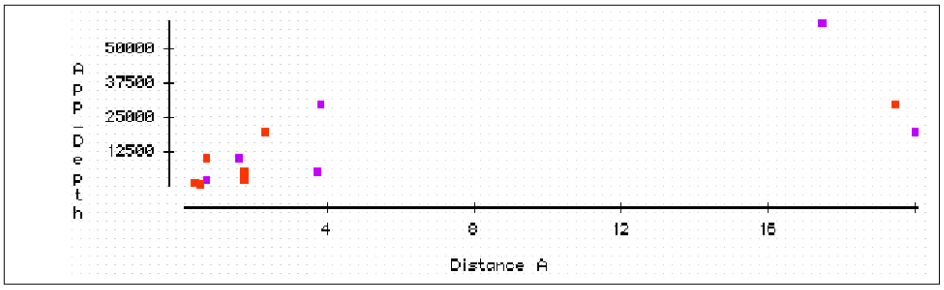

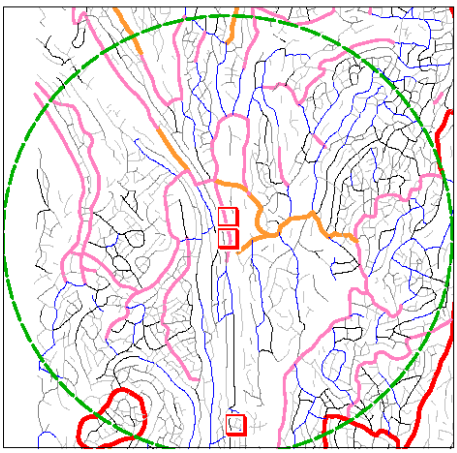

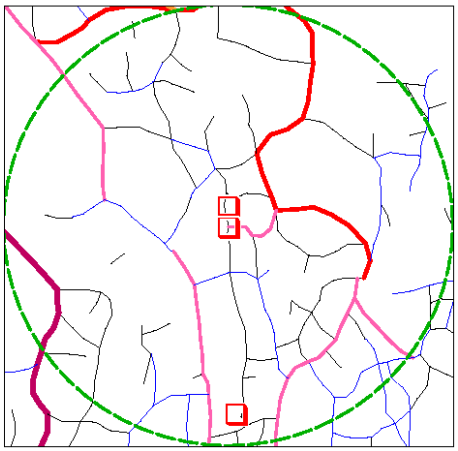

Magnetic_Worms_ by Max_Depth

- 500
- 1,000
- 2,000
- 5,000
- 10,000
- 20,000
- 30,000

Hilton

0 5 10

kilometers

Gravity_Worms by Max_Depth

- 2,000
- 5,000
- 10,000
- 20,000
- 30,000
- 60,000

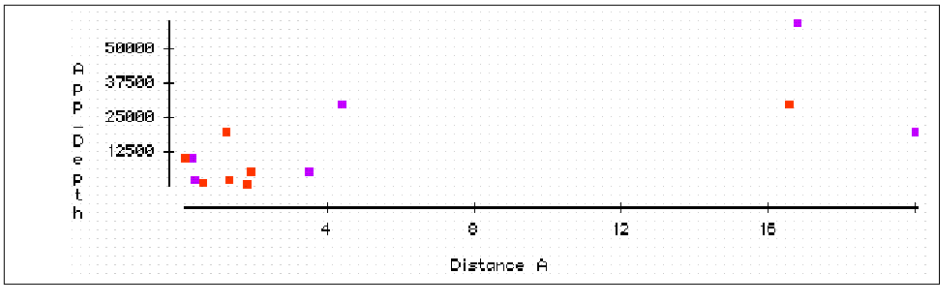

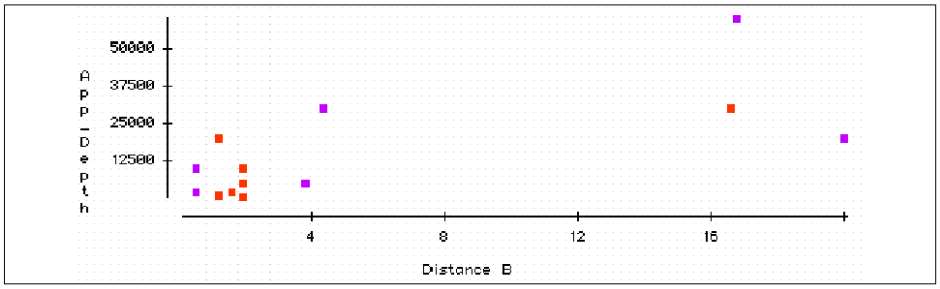

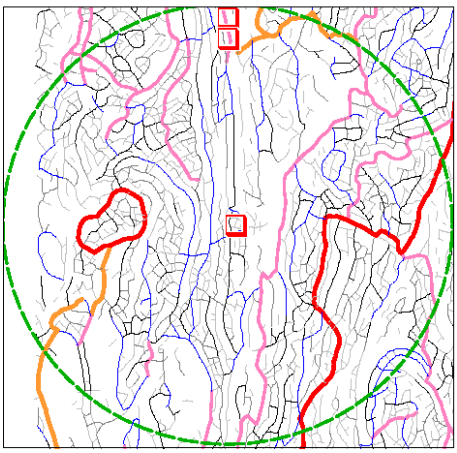

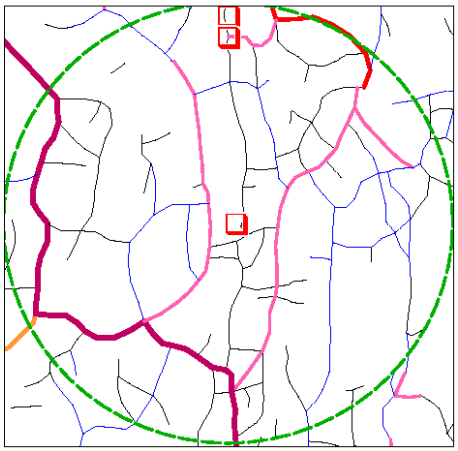

Magnetic_Worms_ by Max_Depth

500
1,000
2,000
5,000
10,000
20,000
30,000

Mt Isa

0 5 10

kilometers

Gravity_Worms by Max_Depth

2,000
5,000
10,000
20,000
30,000
60,000

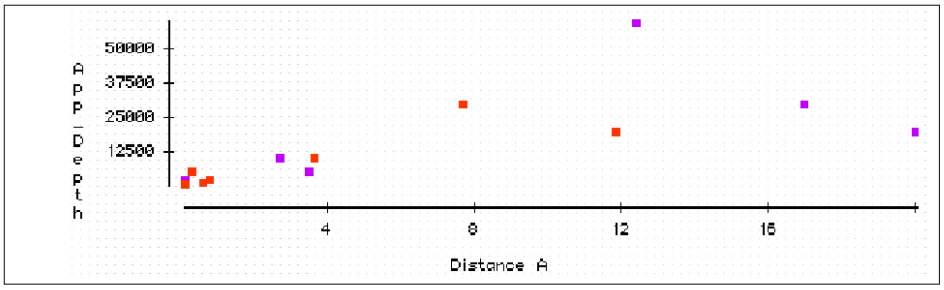

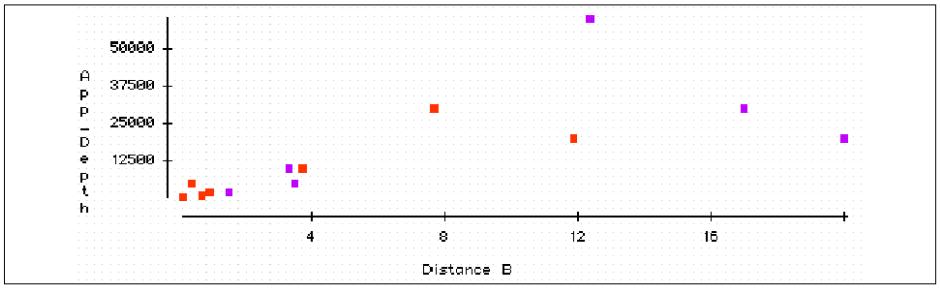

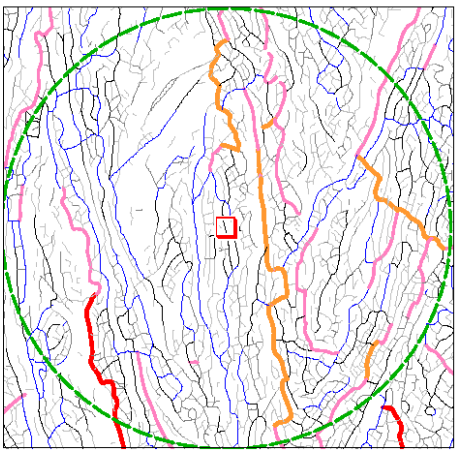

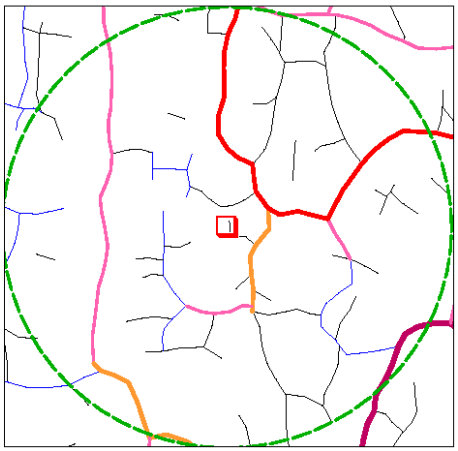

Magnetic_Worms_ by Max_Depth

500
1,000
2,000
5,000
10,000
20,000
30,000

Dugald River

0 5 10

kilometers

Gravity_Worms by Max_Depth

2,000
5,000
10,000
20,000
30,000
60,000

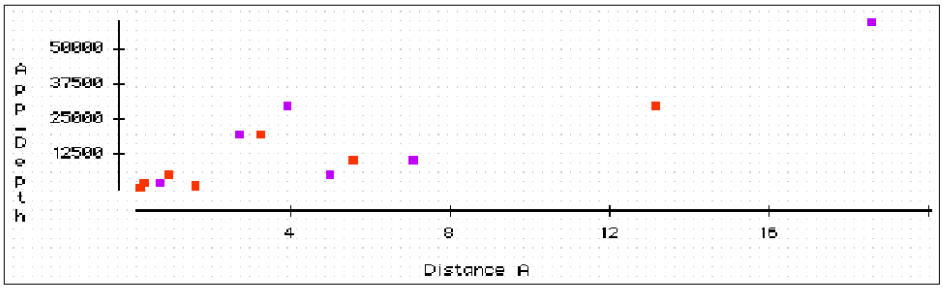

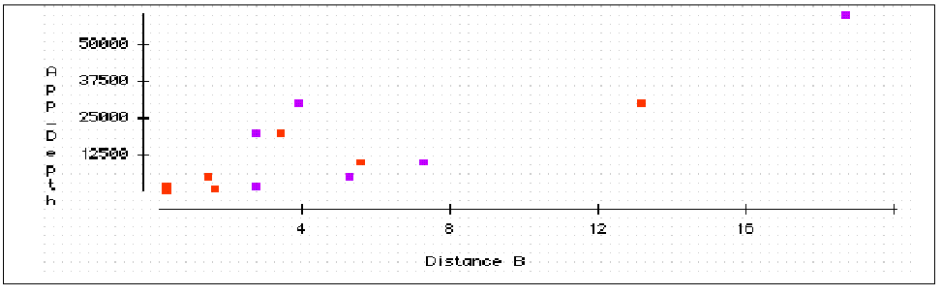

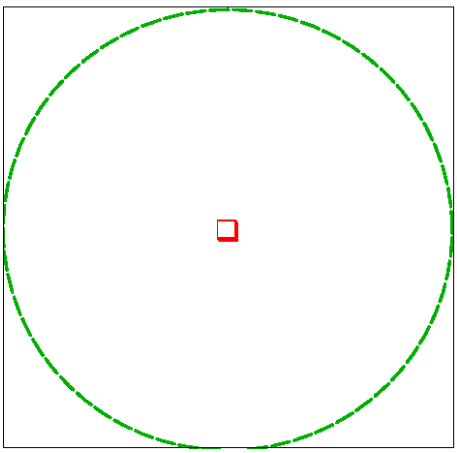

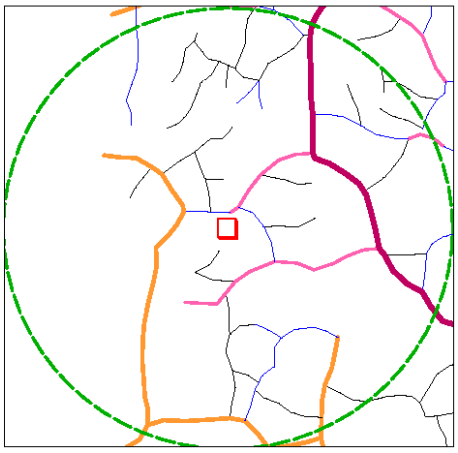

Magnetic_Worms_ by Max_Depth

500
1,000
2,000
5,000
10,000
20,000
30,000

Lady Loretta

0 5 10

kilometers

Gravity_Worms by Max_Depth

2,000
5,000
10,000
20,000
30,000
60,000

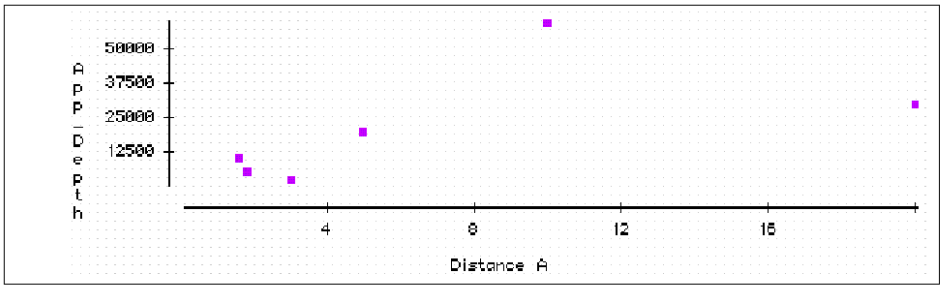

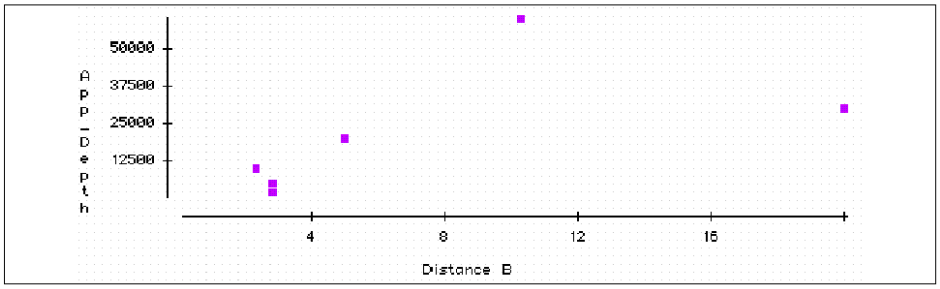

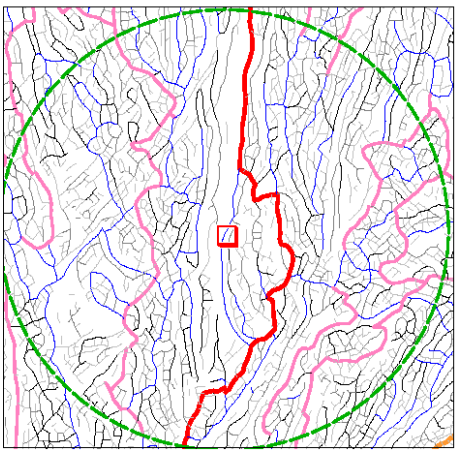

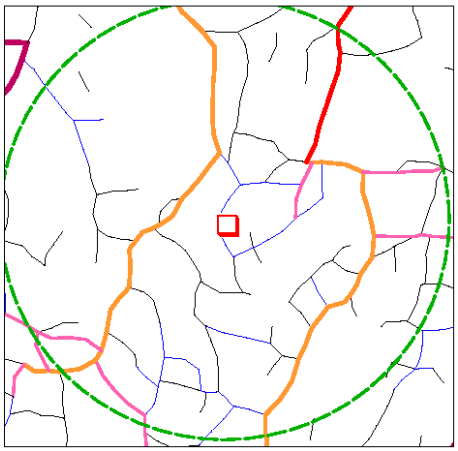

Magnetic_Worms_ by Max_Depth

500
1,000
2,000
5,000
10,000
20,000
30,000

Mary Kathleen

0 5 10

kilometers

Gravity_Worms by Max_Depth

2,000
5,000
10,000
20,000
30,000
60,000

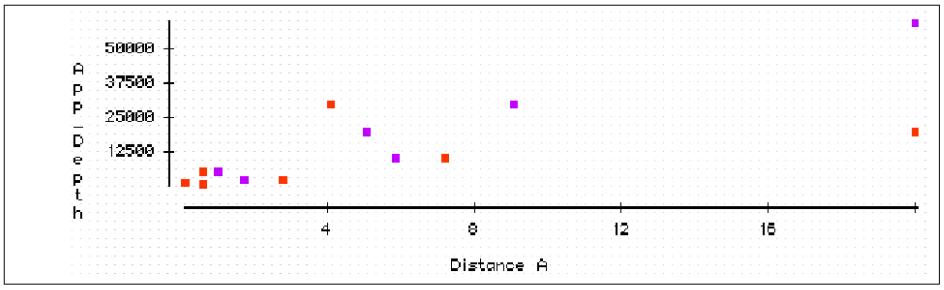

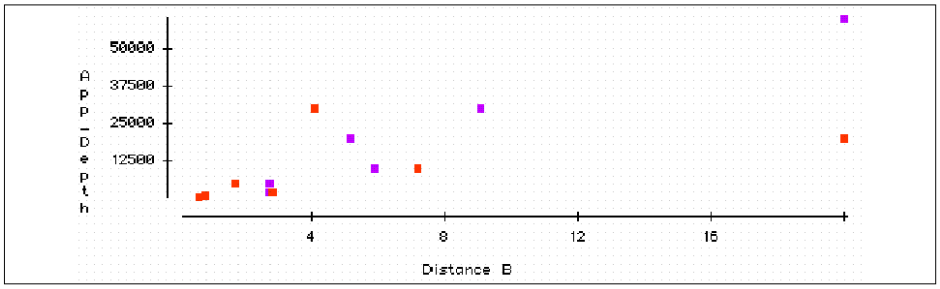

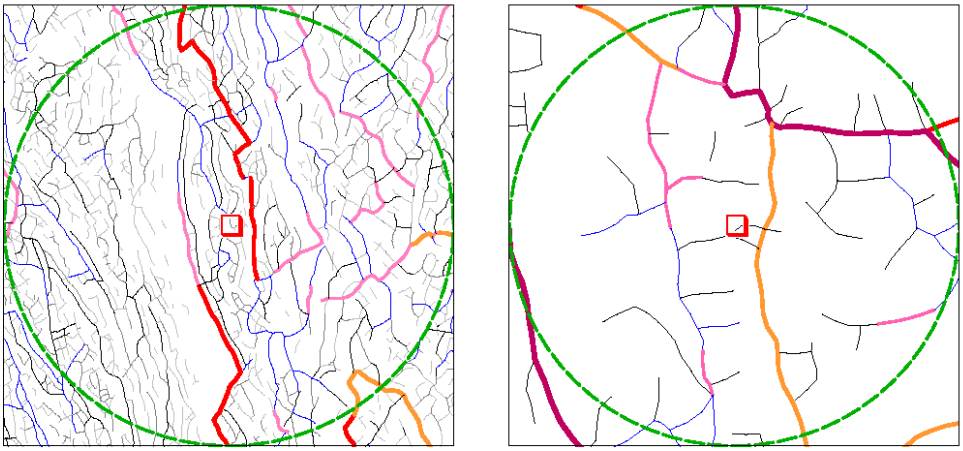
Magnetic_Worms_ by Max_Depth
500
1,000
2,000
5,000
10,000
20,000
30,000
Tick Hill
0
5
10
kilometers
Gravity_Worms by Max_Depth
2,000
5,000
10,000
20,000
30,000
60,000

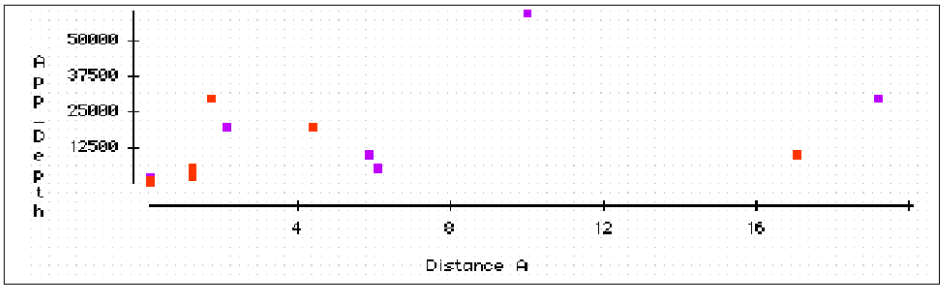
App_Depth
50000
37500
25000
12500
4
8
12
16
Distance A

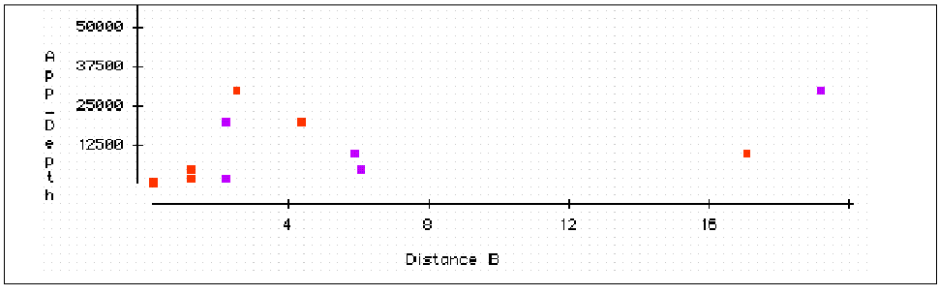
App_Depth
50000
37500
25000
12500
4
8
12
16
Distance B

APPENDIX 4: Mineral Occurrences associated with Anomalous W Regions (Gravity)

SITE_NO	*Mine_Name*	*W_Worm_Assoc*	*Deposit_Size*	*Map_Name*	*Main_Com*	*All_Com*
Gravity_MAX						
494883	Warwick Castle	MIM_Grav_MAX	Small	Alsace	Copper	CU AU SIL
503277	Goatskin Creek Prospect	MIM_Grav_MAX	Very Small	Alsace	Copper	CU
503328	Pamela	MIM_Grav_MAX	Very Small	Alsace	Copper	CU
503336	Ruby	MIM_Grav_MAX	Very Small	Alsace	Copper	CU
490909	Unnamed 873217	MIM_Grav_MAX	Very Small	Lawn Hill	Copper	CU
494193	Unnamed 866211	MIM_Grav_MAX	Very Small	Lawn Hill	Copper	CU
494194	Unnamed 860206	MIM_Grav_MAX	Very Small	Lawn Hill	Copper	CU
503277	Goatskin Creek Prospect	MIM_Grav_MAX	Very Small	Alsace	Copper	CU
Gravity_EFVD						
43622	Little Beauty	MIM_Grav_EFVD	Small	Mary Kathleen	Copper	CU
494858	Saint Andrews	MIM_Grav_EFVD	Very Small	Duchess	Copper	CU
502938	Daltons Bore	MIM_Grav_EFVD	Small	Coolullah	Copper	CU
503286	Kamileroi Anomaly	MIM_Grav_EFVD	Very Small	Kamileroi	Copper	CU
503331	Quail	MIM_Grav_EFVD	Very Small	Coolullah	Copper	CU AU
503363	Unnamed 200143	MIM_Grav_EFVD	Very Small	Coolullah	Copper	CU
503365	Unnamed 202143	MIM_Grav_EFVD	Very Small	Coolullah	Copper	CU
506103	Ardath	MIM_Grav_EFVD	Very Small	Duchess	Copper	CU
506112	Edgarda	MIM_Grav_EFVD	Very Small	Duchess	Copper	CU
506128	Empress	MIM_Grav_EFVD	Small	Duchess	Copper	CU
506129	Fource	MIM_Grav_EFVD	Very Small	Duchess	Copper	CU
506130	Freckle	MIM_Grav_EFVD	Very Small	Duchess	Copper	CU
506131	Galilee	MIM_Grav_EFVD	Very Small	Duchess	Copper	CU
506171	Napoleon?	MIM_Grav_EFVD	Very Small	Duchess	Copper	CU LST
506199	Sling Shot	MIM_Grav_EFVD	Very Small	Duchess	Copper	CU
506237	Unnamed 784501	MIM_Grav_EFVD	Very Small	Duchess	Copper	CU
506239	Pilgrim	MIM_Grav_EFVD	Very Small	Duchess	Copper	CU
506254	Unnamed 708417	MIM_Grav_EFVD	Very Small	Duchess	Copper	CU
506285	Unnamed 775378	MIM_Grav_EFVD	Very Small	Duchess	Copper	CU LST
506400	Unnamed 841325	MIM_Grav_EFVD	Very Small	Duchess	Copper	CU
506401	Unnamed 842318	MIM_Grav_EFVD	Very Small	Duchess	Copper	CU
506402	Unnamed 842319	MIM_Grav_EFVD	Very Small	Duchess	Copper	CU
43493	Totts Creek	pmd_Grav_EFVD	Very Small	Camooweal	Lead	PB
493635	Century	pmd_Grav_EFVD	Giant	Lawn Hill	Zinc	ZN PB AG
494110	Axis	pmd_Grav_EFVD	Very Small	Lawn Hill	Lead	PB AG ZN
494120	Black Snake	pmd_Grav_EFVD	Very Small	Lawn Hill	Zinc	ZN PB AG
494123	Burke Copper Mine	pmd_Grav_EFVD	Very Small	Lawn Hill	Copper	CU
494127	Dorothy	pmd_Grav_EFVD	Very Small	Lawn Hill	Lead	PB AG ZN
494137	Little Banner	pmd_Grav_EFVD	Very Small	Lawn Hill	Lead	PB AG CU
494138	Little Banner	pmd_Grav_EFVD	Very Small	Lawn Hill	Lead	PB AG
494152	Silver Queen	pmd_Grav_EFVD	Very Small	Lawn Hill	Lead	PB AG ZN
494156	Star Spangled Banner	pmd_Grav_EFVD	Very Small	Lawn Hill	Zinc	ZN CU AG PB
494163	Tunnel Hill	pmd_Grav_EFVD	Very Small	Lawn Hill	Zinc	ZN PB AG
494185	Unnamed 435321	pmd_Grav_EFVD	Very Small	Lawn Hill	Lead	PB AG
494908	Century West	pmd_Grav_EFVD	Very Small	Lawn Hill	Zinc	ZN PB CU
494920	Zinc Hills	pmd_Grav_EFVD	Very Small	Lawn Hill	Zinc	ZN PB CU
503276	Galion	pmd_Grav_EFVD	Very Small	Coolullah	Copper	CU
506171	Napoleon?	pmd_Grav_EFVD	Very Small	Duchess	Copper	CU LST
506187	Pilgrim Extended?	pmd_Grav_EFVD	Very Small	Duchess	Copper	CU LST

Appendix 5: Worm Edge Penetration and Intersection Images in relation to Major Deposits

A1: Edge Penetration Image of Magnetic Worms
A2: Edge Intersection Image of Magnetic Worms
A3: Edge Penetration Image of Gravity Worms
A4: Edge Intersection Image of Gravity Worms
A5: Edge Penetration Image of Total Mag/Grav Worms
A6: Edge Intersection Image of Total Mag/Grav Worms

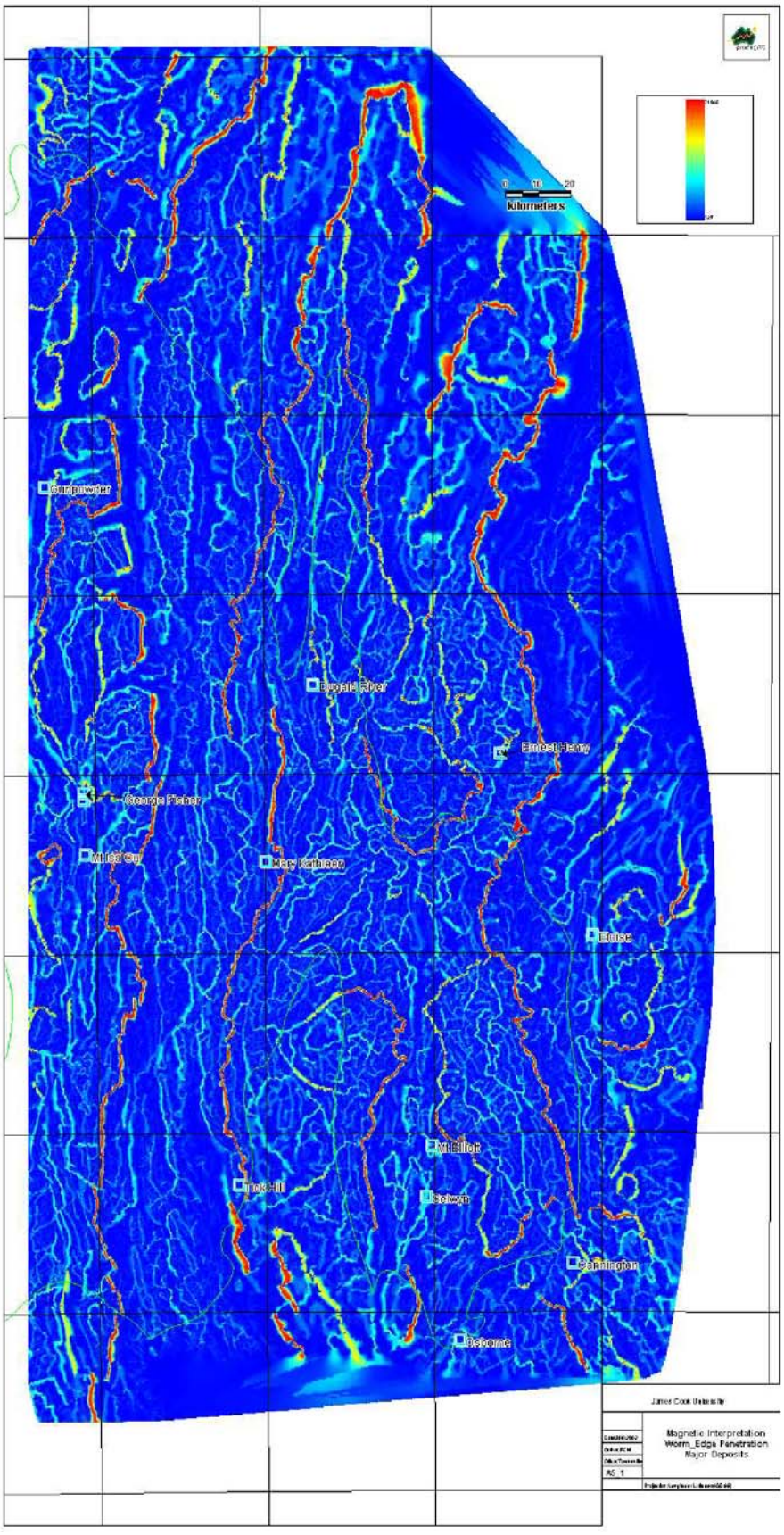
0 10 20
kilometers
Duchess
Ernest Henry
George Fisher
Mary Kathleen
Elaine
Mt Elliot
Lochinvar
Cannington
Osborne
James Cook University
Magnetic Interpretation
Worm_Edge Penetration
Major Deposits

A1

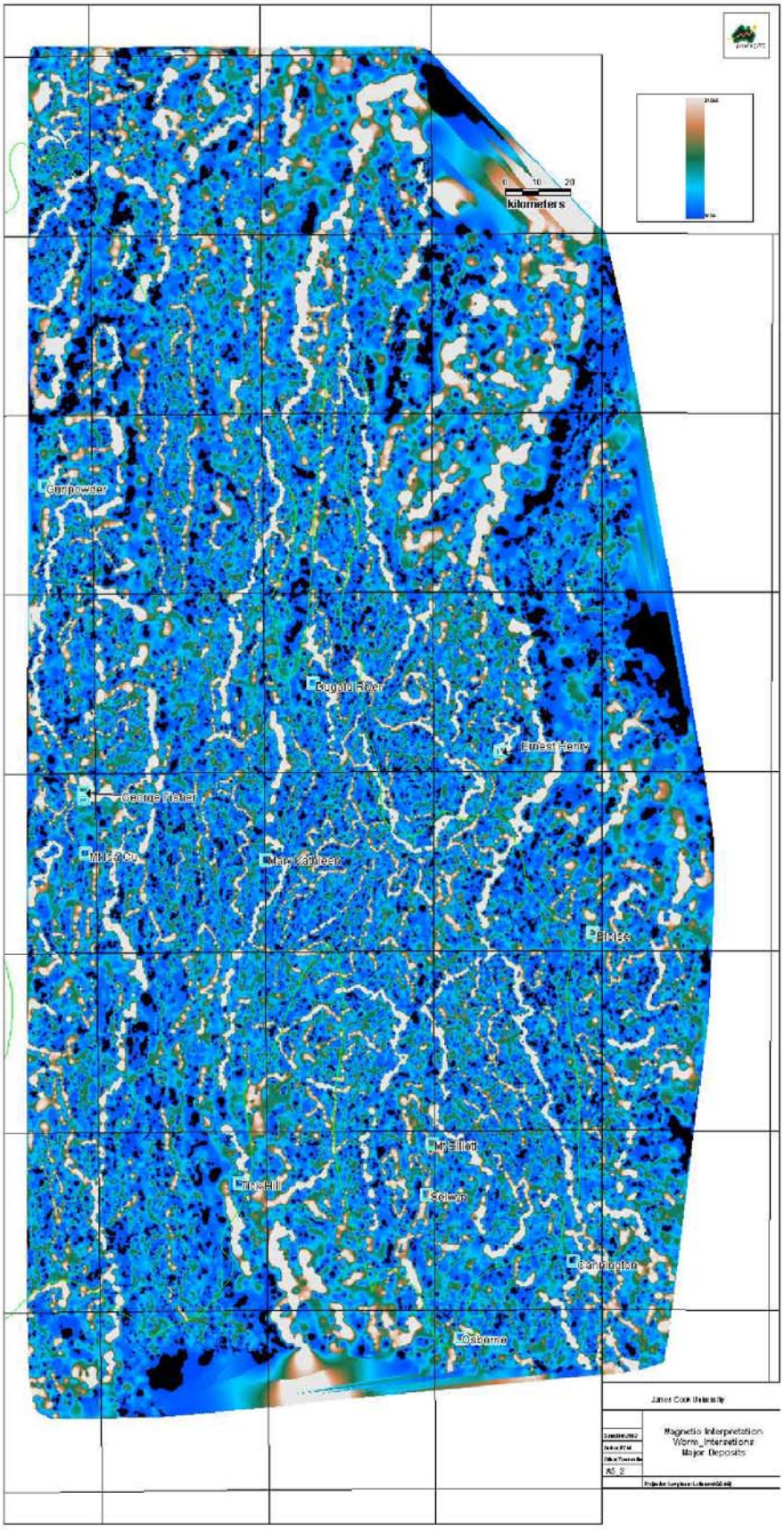
0 10 20
kilometers
Gunpowder
Dugald River
Ernest Henry
Osborne Fisher
Mica Creek
Mary Kathleen
Eloise
Mt Elliot
Tick Hill
Selwyn
Barrington
Osborne
James Cook University
Magnetic Interpretation
Worm_Interpretions
Major Deposits

A2

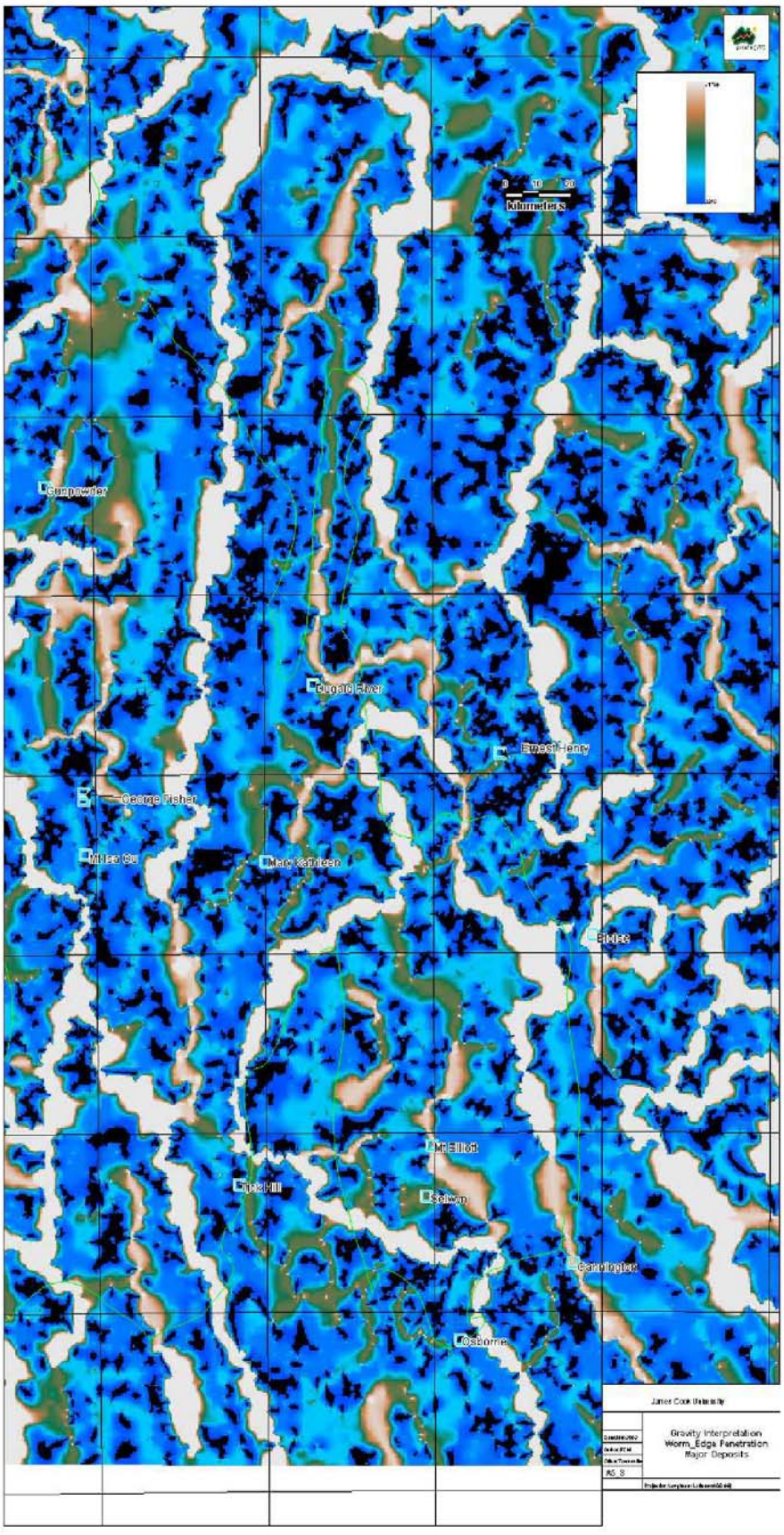
Kilometers
Gunpowder
Eloise
Ernest Henry
George Fisher
Mt Isa Cu
Mary Kathleen
Mt Elliott
Cannington
Osborne
James Cook University
Gravity Interpretation
Worm_Edge Penetration
Major Deposits

A3

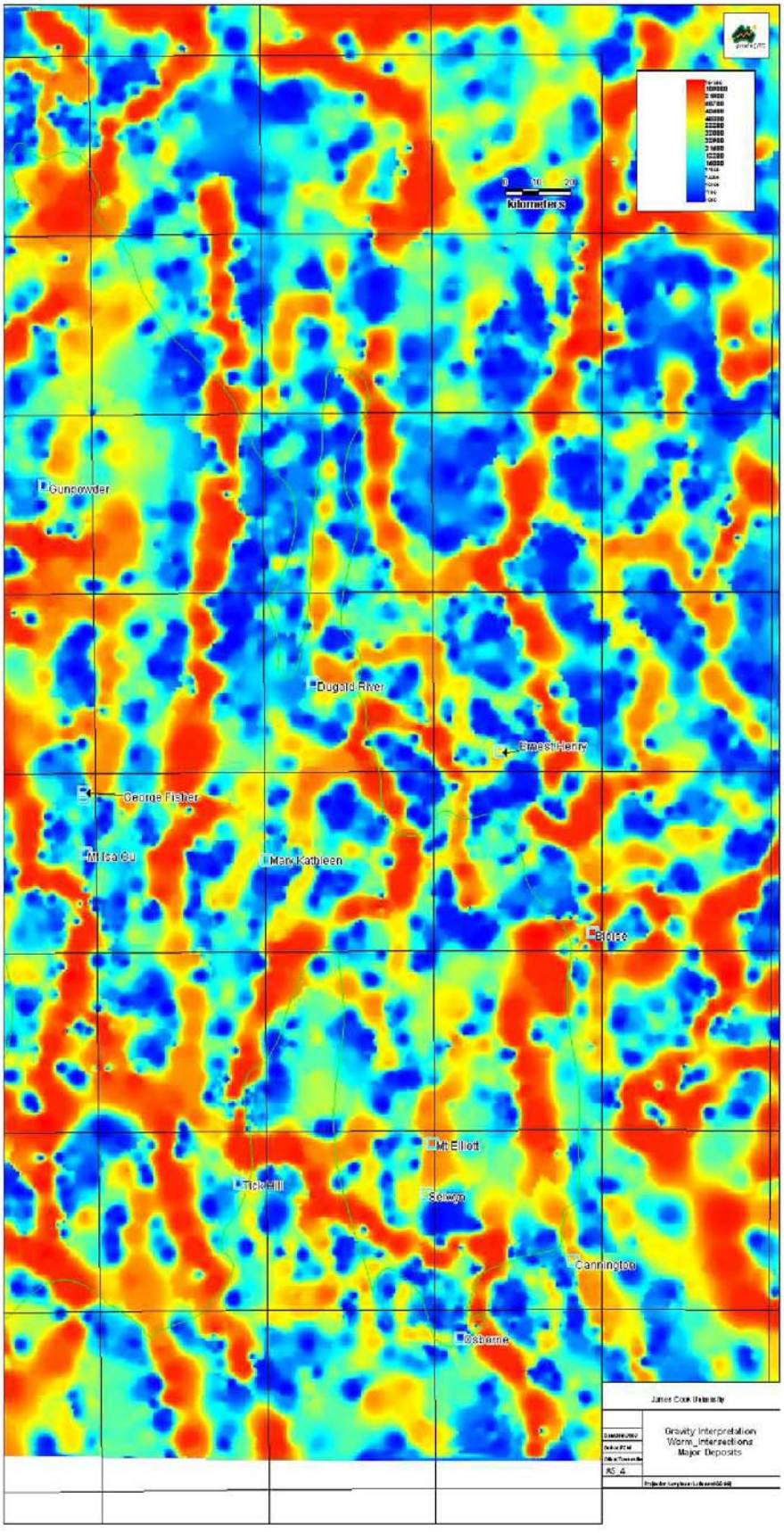
0 10 20
Kilometers
Gunpowder
Dugald River
Ernest Henry
George Fisher
Mt Isa Cu
Mary Kathleen
Biotee
Mt Elliott
Tick Hill
Selwyn
Cannington
Osborne
James Cook University
Gravity Interpretation
Worm_Intersections
Major Deposits
A5 4

A4

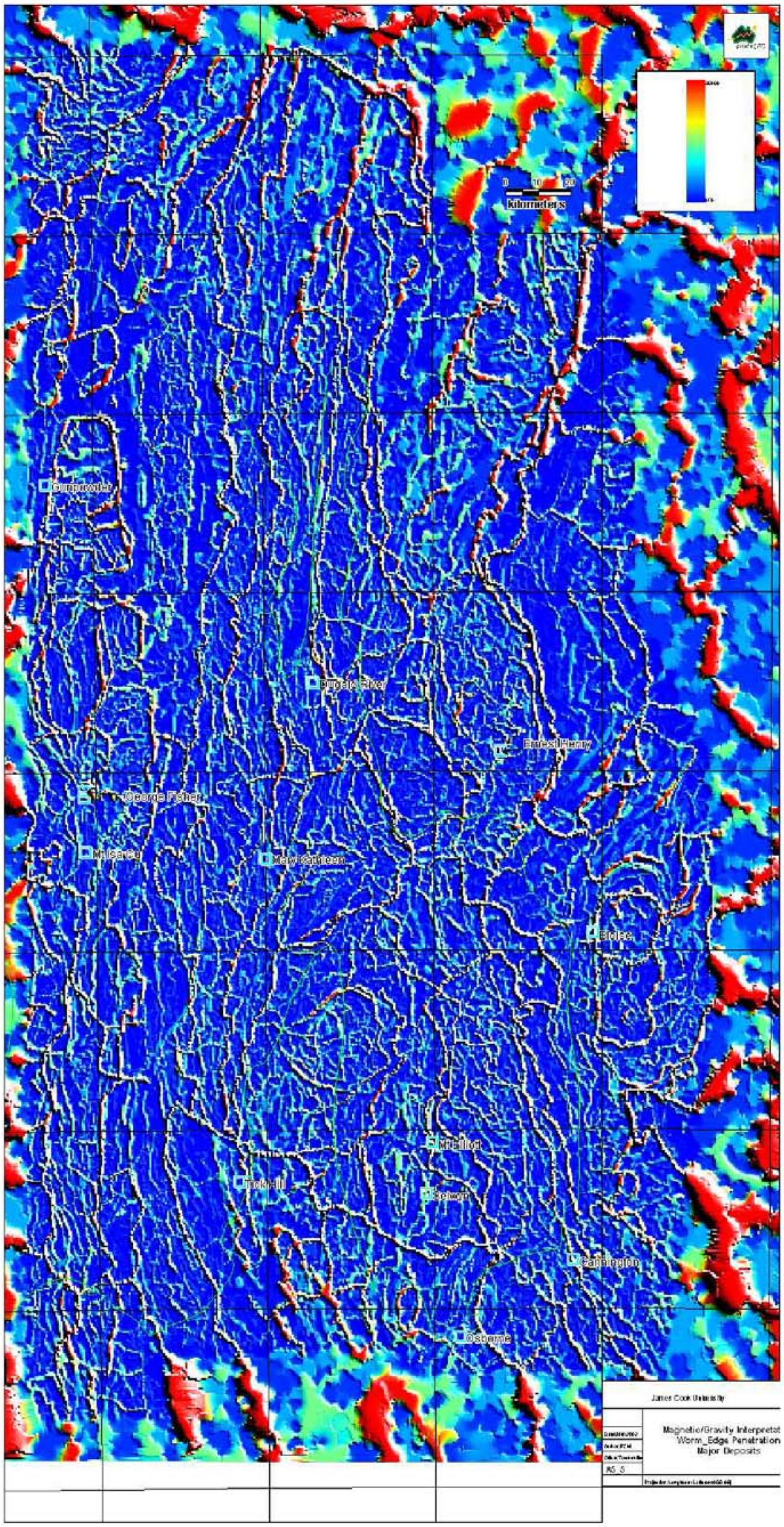
Kilometers
Gunpowder
Ernest Henry
Mary Kathleen
Eloise
Osborne
James Cook University
Magnetic/Gravity Interpretat
Worm_Edge Penetration
Major Deposits
A5_5

A5

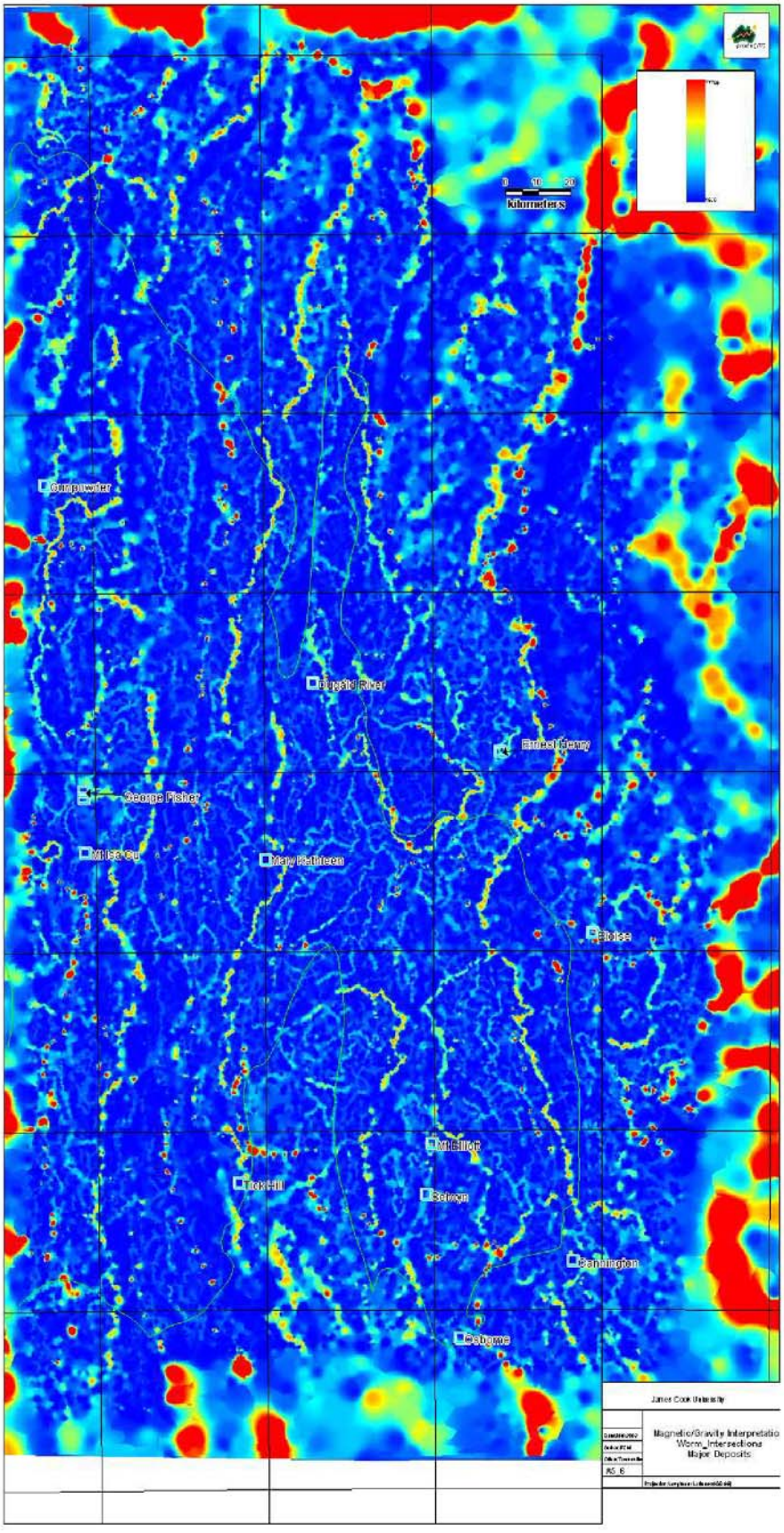
kilometers
Gumpewhite
Donald River
Ernest Henry
George Fisher
Mt Isa
Mary Kathleen
Biloela
Mt Elliott
Rocklea
Selwyn
Canarvon
Selwyn
James Cook University
Magnetic/Gravity Interpretatio
Worm_Intersections
Major Deposits

A6